PEOPLE'S DEMOCRATIC REPUBLIC OF ALGERIA
MINISTRY OF HIGHER EDUCATION
AND SCIENTIFIC RESEARCH

SAAD DAHLAB UNIVERSITY OF BLIDA 1

Physics Department

Final Year Project Thesis

Submitted in Partial Fulfillment of the Requirements for the Master's Degree in Radiation Physics

---

Application of Nuclear Techniques in Food Safety Assessment: Case Studies From the Algerian Market

---

BY
BENNEFISSA Nada & ROUAKI Leila Rym

Presented and publicly defended on (29/06/2025) before the members of the jury :

CHEKIRINE Mamoun	Professor	Saad Dahleb Blida 1 University	President
SILHADI Hana	Principal Researcher	CRNA - Algiers	Examiner
BENAROUS Samiha	Principal Researcher	CRNA - Algiers	Supervisor
KHELIFI Rachid	Professor	Saad Dahleb Blida 1 University	Co-Supervisor

2024/2025

Abstract

This study was conducted to evaluate the levels of natural radioactivity and toxic elemental contamination in commonly consumed food products in Algeria. Seven representative food items, including dates, green tea, baby formula, wheat, fish feed, broth cubes, and bread were collected from various regions and analyzed using high-purity germanium (HPGe) gamma-ray spectrometry and energy dispersive X-ray fluorescence (EDXRF).

Elemental analysis by EDXRF revealed notable aluminium contamination across several samples and slight exceedances of toxic metals, particularly mercury and lead with the highest concern observed in baby formula. While most samples remained within international safety limits, the presence of these elements in infant-targeted products warrants further monitoring.

Gamma spectrometry was employed to measure activity concentrations of naturally occurring radionuclides, including Uranium-235 (^{235}U), Thorium-232 (^{232}Th), Radium-226 (^{226}Ra) and Potassium-40 (^{40}K), as well as the artificial radionuclide Cesium-137 (^{137}Cs). Comparative analysis with international data indicated general conformity, though certain food types showed elevated levels.

Keywords: food safety, Algeria, gamma spectrometry, EDXRF, HPGe detector, heavy metals, natural radioactivity, NORM, infant exposure, contamination assessment.

Résumé

Cette étude visait à évaluer les niveaux de radioactivité naturelle et la contamination par des éléments toxiques dans des produits alimentaires couramment consommés en Algérie. Sept produits ont été analysés : les dattes, le thé vert, le lait infantile, le blé, l'aliment pour poissons, les cubes de bouillon et le pain. Ces échantillons ont été prélevés dans différentes régions du pays et analysés à l'aide de la spectrométrie gamma avec détecteur à germanium haute pureté (HPGe) et de la fluorescence X à dispersion d'énergie (EDXRF).

L'analyse élémentaire par EDXRF a révélé une contamination notable en aluminium dans plusieurs échantillons, ainsi que des niveaux modérés de métaux toxiques, principalement le mercure et le plomb. Ces dépassements sont particulièrement préoccupants dans le lait infantile. Bien que la majorité des échantillons respectent les limites de sécurité internationales, la présence de ces contaminants dans des produits destinés aux nourrissons justifie la mise en place d'une surveillance renforcée.

La spectrométrie gamma a permis de quantifier les concentrations des radionucléides naturellement présents, notamment l'Uranium-235 (^{235}U), Thorium-232 (^{232}Th), Radium-226 (^{226}Ra) et le Potassium-40 (^{40}K), ainsi que du césium-137 (^{137}Cs), un radionucléide artificiel. L'analyse comparative avec les données internationales a indiqué une conformité générale, bien que certains types d'aliments aient présenté des niveaux élevés.

Mots-clés : sécurité alimentaire, Algérie, spectrométrie gamma, EDXRF, détecteur HPGe, métaux lourds, radioactivité naturelle, NORM, exposition infantile, évaluation de la contamination.

ملخص

تم إجراء هذه الدراسة بهدف تقييم مستويات النشاط الإشعاعي الطبيعي ،و التلوث بالمعادن السامة في بعض المنتجات الغذائية شائعة الإستهلاك في الجزائر. تم جمع سبعة أصناف غذائية من الأسواق الجزائرية تشمل التمر، الشاي الأخضر، حليب الرضع، القمح ،مغذيات الأسماك، مكعبات المرق، والخبز من مناطق مختلفة، وتم تحليلها باستخدام التحليل الطيفي لأشعة غاما بجهاز جرمانيوم عالي النقاء، و الفلورة بالأشعة السينية المشتتة للطاقة.

كشفت التحاليل العنصرية باستخدام تقنية الأشعة السينية عن تلوث ملحوظ بعنصر الألمنيوم في عدة عينات، إلى جانب تجاوزات طفيفة في تركيزات بعض المعادن السامة خاصة الزئبق والرصاص وكانت أعلى مستويات التركيز مرتبطة بحليب الرضع. وعلى الرغم من أن معظم العينات كانت ضمن الحدود الآمنة المعترف بها دوليًا، فإن وجود هذه العناصر في منتجات مخصصة للرضع يتطلب مراقبة مستمرة.

تم استخدام مطيافية أشعة غاما لقياس تراكيز النشاط الإشعاعي للنظائر المشعة الطبيعية، بما في ذلك الراديوم 226، والثوريوم 232، والبوتاسيوم 40، واليورانيوم 235، بالإضافة إلى النظير المشع الصناعي السيزيوم 137. أشارت التحليلات المقارنة مع البيانات الدولية إلى توافق عام، رغم أن بعض أنواع الأطعمة أظهرت مستويات مرتفعة.

الكلمات المفتاحية: السلامة الغذائية، الجزائر، مطيافية أشعة غاما، كاشف الجرمانيوم عالي النقاء، المعادن الثقيلة، النشاط الإشعاعي الطبيعي، النويدات المشعة الطبيعية، تقييم التلوث.

Acknowledgments

We would like to express our sincere gratitude to all those who contributed to the successful completion of this study.

First and foremost, our sincere appreciation goes to Mr. A. Guittoum, Director General of the Nuclear Research Center of Algiers (CRNA), for welcoming us into the center and allowing us to carry out this internship.

We extend our deepest thanks to Mrs. Samiha Benarous, researcher at the Nuclear Research Center of Algiers (CRNA), for her invaluable supervision, insightful guidance, and continuous support throughout our internship. Her expertise greatly enriched the quality of our work.

We are also grateful to Mr. Azeddine Arabi, specialized engineer at CRNA, for his essential assistance with the gamma spectrometry and ED-XRF analyses.

We would also like to acknowledge the staff of the CRNA laboratories for providing the equipment and environment necessary to complete this work.

We thank our academic department for the knowledge imparted over the years and for helping us define our research topic.

Finally, we express our warm thanks to Professor CHEKIRINE Mamoun, who honored us by presiding over the defense jury, as well as Dr. SILHADI Hana for acting as examiner, and Professor KHELIFI Rachid for supervising us throughout our work. We are grateful for the time they dedicated to reviewing our work and for their constructive feedback.

To all those who contributed, directly or indirectly, to the completion of this research, thank you.

Contents

List of Figures

List of Tables

List of Acronyms

- **ADC** : Analogique Digital Convertisseur
- **AED** : Annual Committed Effective Dose
- **AXIL** : Analysis of X-ray Spectra by Iterative Least Squares
- **Bq** : Becquerel
- **CAC** : Codex Alimentarius Commission
- **CF** : Contamination Factor
- **CRMs** : Certified Reference Materials
- **EDXRF** : Energy Dispersive X-Ray Fluorescence
- **EDI** : Estimated Daily Intake
- **EFSA** : European Food Safety Authority
- **ELCR** : Excess Lifetime Cancer Risk
- **EPA** : Environmental Protection Agency
- **EWI** : Estimated Weekly Intake
- **FAO** : Food and Agriculture Organization
- **FP** : Fundamental Parameters
- **GL** : Guideline Level
- **HI** : Hazard Index
- **Hin** : Internal Hazard Index
- **HQ** : Hazard Quotient
- **HPGe** : High Purity Germanium
- **HV** : High Voltage
- **IAEA** : International Atomic Energy Agency
- **ICRP** : International Commission on Radiological Protection
- **IR** : Ingestion Rate
- **LOD** : Limit of Detection

- **MCA** : Multi-Channel Analyzer
- **MPI** : Metal Pollution Index
- **MPL** : Maximum Permissible Limit
- **NORM** : Naturally Occurring Radioactive Material
- **PLI** : Pollution Load Index
- **PTWI** : Provisional Tolerable Weekly Intake
- **RfD** : Reference Dose
- **SA** : Saudi Arabia
- **SD** : Standard Deviation
- **SDD** : Silicon Drift Detector
- **SV** : Sievert
- **TDS** : Total Diet Study
- **UAE** : United Arab Emirates
- **UK** : United Kingdom
- **UNSCEAR** : United Nations Scientific Committee on the Effects of Atomic Radiation
- **USEPA** : United States Environmental Protection Agency
- **WHO** : World Health Organization
- **WDXRF** : Wavelength Dispersive X-Ray Fluorescence

General Introduction

Food safety is an essential pillar of public health, particularly in regions where agricultural production intersects with environmental and industrial pressures [3]. In Algeria a country with a diverse food landscape, expanding urbanization, and evolving consumption patterns, the potential contamination of food products by toxic heavy metals and naturally occurring radioactive materials (NORMs) presents a growing concern. Chronic exposure to such contaminants, even at low doses, can lead to long-term health effects, especially in vulnerable populations such as infants and children. Despite this, scientific data on the contamination levels in Algerian food products remain limited and fragmented.

In recent decades, nuclear analytical techniques have proven invaluable in environmental and food quality monitoring due to their sensitivity, precision, and non-destructive nature. Among these, gamma-ray spectrometry using High-Purity Germanium (HPGe) detectors enables the identification and quantification of radionuclides such as Uranium-235 (^{235}U) Radium-226 (^{226}Ra), Thorium-232 (^{232}Th), Potassium-40 (^{40}K), and Cesium-137 (^{137}Cs). Similarly, Energy Dispersive X-Ray Fluorescence (EDXRF) spectroscopy offers a rapid and effective approach for detecting a wide range of metallic and non-metallic elements in complex matrices. The integration of these methods in food monitoring allows for a comprehensive assessment of both radiological and toxicological hazards.

The present thesis investigates the levels of natural radioactivity and toxic metals in a selection of food items commonly consumed in Algeria, including both plant-based and animal-derived products. By employing EDXRF and HPGe gamma spectrometry, the study aims to generate baseline data on elemental and radionuclide concentrations in foods sourced from local markets. The results are interpreted in light of international regulatory standards, such as those set by the Codex Alimentarius, WHO, IAEA, and UNSCEAR.

This work is structured as follows:
Chapter 1 introduces the major pathways of food contamination, including the origins of heavy metals and radionuclides in the food chain, and reviews international safety thresholds and exposure guidelines. Chapter 2 outlines the theoretical principles of the analytical methods used, with emphasis on electron and photon interactions, detector systems, matrix effects, and calibration protocols.

Chapters 3 and 4 present the experimental design, sample preparation procedures, and the main results. The concentrations measured were compared against Maximum Permissible Limits (MPLs) and used to estimate exposure and health risks through indices such as the Estimated Daily Intake (EDI), Estimated Weekly Intake (EWI), Hazard Quotient (HQ), Hazard Index (HI), Contamination Factor (CF), and Pollution Load Index (PLI). These indicators help quantify the extent of contamination and assess the potential for both chronic and acute health effects.

Finally, the thesis discusses the broader implications of the findings for public health and food regulation in Algeria. It underscores the potential role of nuclear analytical techniques

in supporting national food safety surveillance systems and highlights the need for continued monitoring and interdisciplinary collaboration. Through this integrated approach, the study contributes to strengthening Algeria's capacity for evidence-based food risk assessment and consumer protection.

Chapter 1

Contamination Pathways and Regulatory Framework

1.1 Introduction

This chapter provides an overview of the main contamination pathways involving naturally occurring radioactive materials (NORMs) and heavy metals. It outlines how these substances enter the food chain, the associated health risks, and relevant international safety standards. It also highlights the role of nuclear techniques in food safety monitoring.

1.2 Problem Overview: Food Contamination Risks

Food safety is a fundamental aspect of public health, ensuring that food does not pose risks to consumers when processed and consumed as intended [1]. However, in Algeria, food safety remains a significant challenge due to the presence of naturally occurring radioactive materials (NORMs) and heavy metals in food products. These contaminants, whether of natural origin or influenced by human activities, can accumulate in food and pose serious long-term health risks. The agri-food sector in Algeria is largely dominated by small and medium enterprises (SMEs) many of which lack structured food safety management systems [2]. This regulatory gap raises concerns about the effectiveness of contamination monitoring, particularly for heavy metals and radionuclides, which require advanced analytical techniques for accurate detection. Additionally, the increasing concerns over food safety and security in Algeria align with global trends, as food contamination has become a growing public concern, particularly in relation to chemical and radioactive hazards [3].

From a health perspective, chronic exposure to naturally occurring radionuclides, primarily uranium-238 (^{238}U), thorium-232 (^{232}Th), and potassium-40 (^{40}K), as identified by the UNSCEAR 2000 Report can lead to radiation-induced DNA damage, increased cancer risks, and other biological effects. Ionizing radiation emitted by these radionuclides interacts with biological tissues, potentially causing mutations, oxidative stress, immune suppression, and reproductive toxicity. Long-term exposure may contribute to organ damage, impaired cell function, and increased susceptibility to genetic diseases [4]. Similarly, heavy metals such as lead (Pb), cadmium (Cd), and mercury (Hg) are known to cause neurotoxicity, kidney damage, and metabolic disorders due to their ability to accumulate in organs over time [5]. Their bio accumulative nature further amplifies these risks, making long-term dietary exposure a significant public health concern.

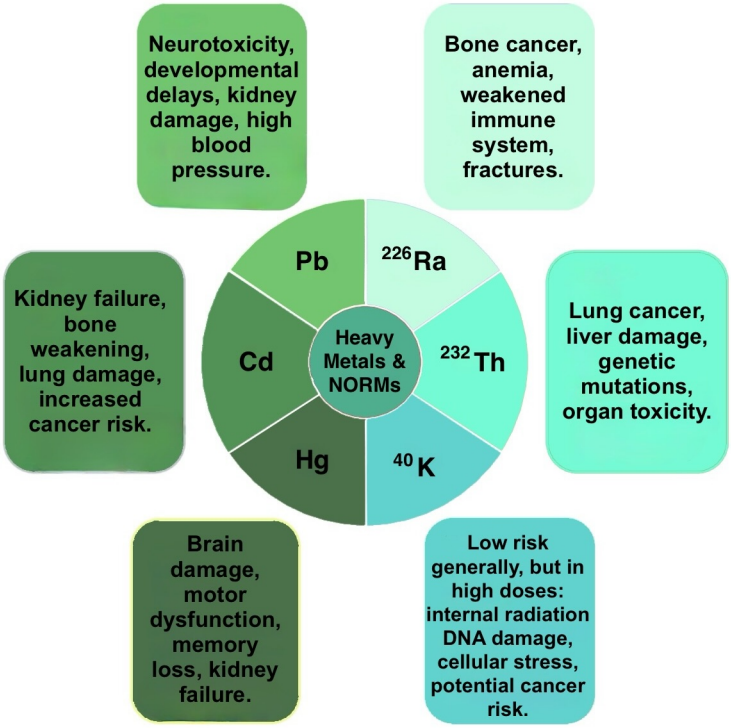

Figure 1.1: Health Impacts of Prolonged Exposure to Heavy Metals & NORMs [4,5].

To assess and mitigate these risks, systematic monitoring and risk assessment are necessary. Given their invisible and persistent nature, advanced detection methods are required. While previous studies have examined the presence of heavy metals and radionuclides in specific regions, there is limited recent data on commonly consumed food products in Algeria [14]. Additionally, conventional techniques such as Atomic Absorption Spectrometry (AAS) and Inductively Coupled Plasma Mass Spectrometry (ICP-MS), though effective, require extensive sample preparation, chemical digestion, and long processing times, making them less practical for routine food safety monitoring [15]. Similarly, radiochemical methods for radionuclide detection often involve complex separation procedures that increase the risk of sample contamination and analytical errors. Moreover, these conventional approaches generally focus on single-element analysis, making them inefficient for detecting multiple contaminants simultaneously [16].

1.3 Food Chain and Possible Contamination Pathways

Food contamination arises when hazardous substances, such as NORMs and heavy metals, accumulate in agricultural products. In Algeria, this risk is amplified by geological conditions, industrial emissions, and certain farming practices. Understanding how these contaminants reach food is crucial for evaluating public health risks and guiding nuclear-based detection strategies.

NORMs originate from the Earth's crust and enter the food supply mainly through soil, water, and air. Plants absorb them via their roots, particularly in contaminated soils or when irrigated with groundwater containing elevated radium levels. Surface water polluted by leaching or industrial runoff can also introduce these radionuclides. Additionally, atmospheric deposition, such as windborne dust, aerosols, and radon decay products, can settle

on crops like lettuce and wheat, further contributing to contamination. These materials then reach humans through direct crop consumption or indirectly through animal products [6, 7].

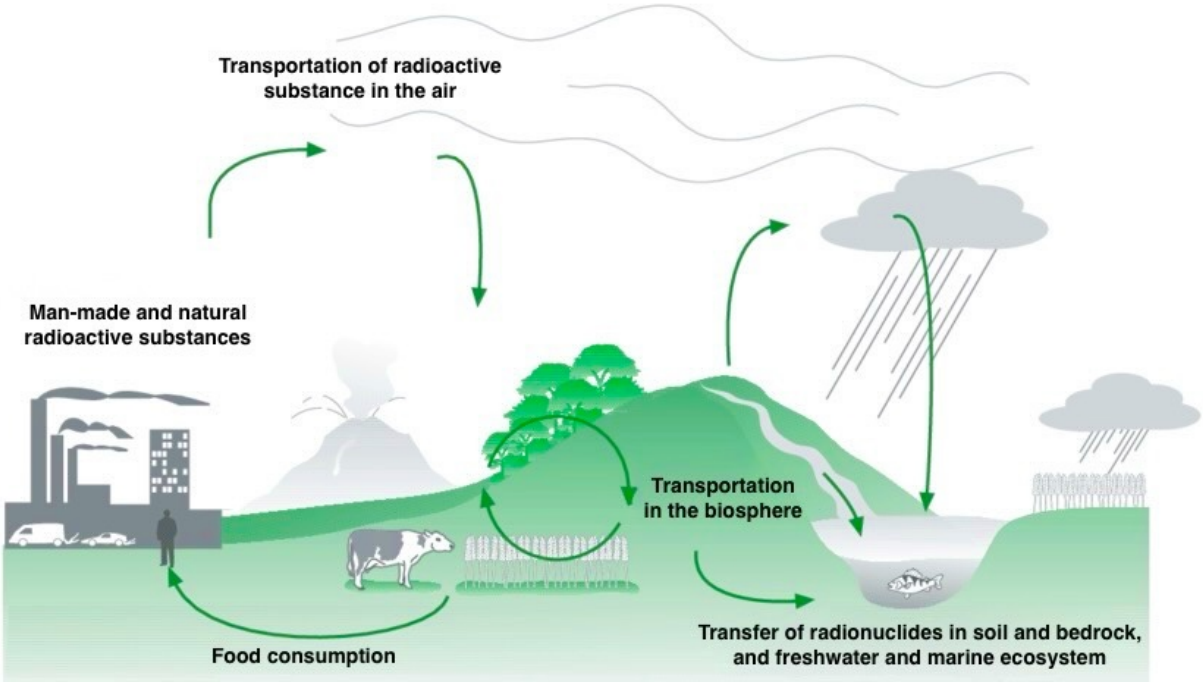

Figure 1.2: Pathways of Radioactive Contaminants in the Environment and Food Chain [7].

Heavy metals such as lead (Pb), cadmium (Cd), and mercury (Hg) are persistent environmental pollutants that pose significant health risks due to their ability to accumulate in the food supply. Unlike radionuclides, they do not decay and can remain in ecosystems indefinitely. These metals enter agricultural systems through industrial emissions, mining waste, contaminated fertilizers, pesticides, and irrigation with polluted water. Once present, they are taken up by crops and may concentrate in edible parts.

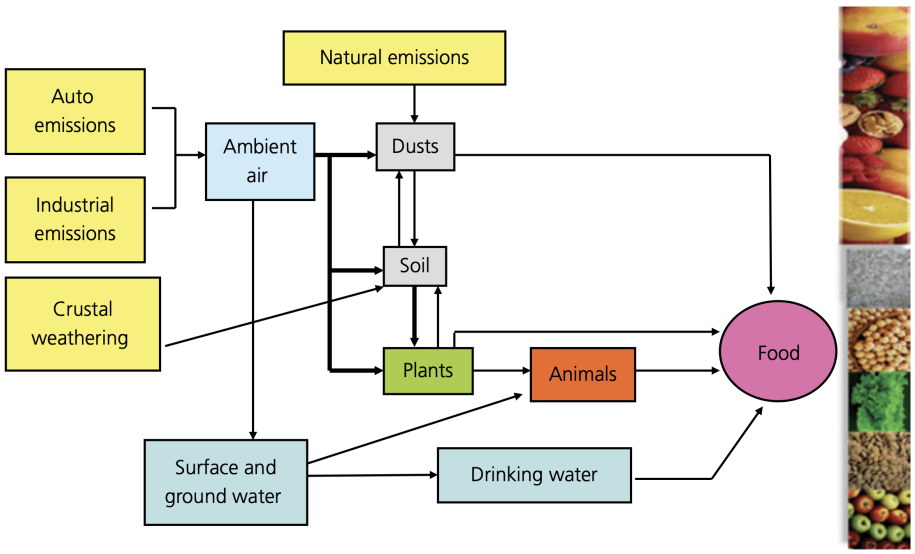

Figure 1.3: Pathways of heavy metals from the environment to food [8].

In aquatic environments, marine pollution contributes to the accumulation of heavy metals in fish and seafood. Commercial and processed foods may also be affected during manufac-

turing, where contamination can occur through additives, preservatives, packaging materials, or metal-based equipment [8, 9].

1.4 Safety Standards and Risk Assessment Factors

Food safety regulations establish limits on contaminants in food to minimize health risks and serve as reference points for assessing contamination levels. International organizations such as the Codex Alimentarius Commission (CAC), managed by the Food and Agriculture Organization (FAO) and the World Health Organization (WHO), provide widely recognized guidelines that define maximum permissible concentrations of hazardous substances in food. The Codex General Standard for Contaminants and Toxins in Food and Feed (Codex STAN 193-1995) sets limits for heavy metals such as lead, cadmium, and mercury [10], while the International Atomic Energy Agency (IAEA) and the United Nations Scientific Committee on the Effects of Atomic Radiation (UNSCEAR) establish reference levels for radionuclides. These regulations provide the framework for evaluating food safety and are essential for interpreting the findings of contamination assessments.

At the national level, regulations vary according to environmental factors and policy frameworks. The European Union (EU) enforces contamination limits through Regulation (EC) No 1881/2006, while Council Regulation (Euratom) 2016/52 defines maximum radionuclide concentrations in food following radiological events. In the United States, the Food and Drug Administration (FDA) and the Environmental Protection Agency (EPA) set permissible levels for heavy metals and radioactive elements in food products. Algeria applies national food safety regulations that align with international standards and conducts monitoring programs to assess contamination risks [11].

In addition to regulatory limits, food contamination risk is evaluated through radiological and toxicological risk assessment factors. For radionuclide exposure, indices such as the Annual Committed Effective Dose (AED) estimates the yearly radiation dose from ingesting radionuclides in food. It reflects short-term exposure, while the Excess Lifetime Cancer Risk (ELCR) provides an estimate of the long-term probability of cancer development due to ingestion of radioactive elements. Other radiological hazard indicators include the Internal Hazard Index (Hin), which assess the overall radiation hazard posed by multiple radionuclides [12].

For heavy metal contamination, risk assessment is based on toxicity thresholds and exposure calculations. The Hazard Index (HI) is commonly used to evaluate non-carcinogenic health risks by comparing metal intake levels to reference doses [13]. These risk assessment methods complement regulatory limits by providing a quantitative estimation of potential health effects, aiding in the interpretation of contamination levels beyond simple compliance with existing standards.

The regulatory thresholds established by international and national authorities will serve as reference values in this study, against which measured concentrations of radionuclides and heavy metals will be compared. Additionally, selected risk assessment factors will be used to further evaluate potential health risks associated with contaminated food. These assessments provide a more comprehensive understanding of contamination beyond concentration limits, integrating both regulatory compliance and health risk estimation.

1.5 Advantages of Nuclear Techniques

Nuclear techniques offer a powerful alternative to chemical and conventional methods due to their non-destructive, multi-elemental, and highly precise analytical capabilities. Gamma Spectrometry, using High-Purity Germanium (HPGe) detectors, allows for direct measurement of gamma-emitting radionuclides without requiring complex chemical separation [17]. It provides accurate quantification of activity concentrations (Bq/kg) in food, enabling compliance with international safety standards set by the IAEA and UNSCEAR. EDXRF, on the other hand, is a rapid and efficient method for detecting heavy metals, requiring minimal sample preparation while allowing for simultaneous analysis of multiple elements [18]. These characteristics make nuclear techniques particularly valuable for high-precision food safety monitoring and regulatory assessments.

By applying Gamma Spectrometry and EDXRF, this study aims to establish a recent contamination database for widely consumed food products in Algeria. Although the research will focus on a limited number of food samples, it will provide high-precision data on their contamination levels, serving as a scientific reference for future studies and food safety policies. Furthermore, these findings will contribute to strengthening national and international efforts to manage food contamination risks, ensuring that consumers are protected from potentially hazardous dietary exposure to radionuclides and toxic metals. The use of nuclear techniques in this study will not only enhance food safety monitoring in Algeria but also provide a scientific foundation for future research and policy development in contamination risk assessment.

Understanding contamination pathways is essential for developing effective monitoring and risk assessment strategies. The integration of regulatory standards with advanced nuclear techniques enables more accurate detection of hazardous substances in food. This foundation sets the stage for the following chapters, which address the theoretical background and practical methods used in the analysis of food contaminants.

Chapter 2

Background Theory

2.1 Introduction

This chapter outlines the theoretical principles necessary for understanding the interaction of radiation with matter and the analytical techniques used in this study. It begins with the fundamental processes of electron and gamma-ray interactions, followed by the operational principles of X-ray fluorescence (XRF) and gamma-ray spectrometry. The chapter also introduces key concepts of radioactivity, which are essential for interpreting the detection and quantification of contaminants in food samples.

2.2 Definition of Radiation

Radiation refers to the transfer of energy through space in the form of electromagnetic waves or particle beams. This energy transfer propagates isotropically, and its trajectory depends on its energy. Radiation is classified into two categories: ionizing and non-ionizing. It is considered ionizing when it has the ability to remove electrons from matter during interaction. Ionizing radiation is produced either by the decay of radionuclides (radioactivity) or by electrical generators such as X-ray machines and particle accelerators. Among these radiations, we find two main types: directly ionizing radiation, which consists of charged particles (α particles, β particles, electrons and protons), and indirectly ionizing radiation, which involves uncharged particles (photons and neutrons) [24].

2.3 Electron-Matter Interactions

When high-energy electrons interact with matter, their energy is progressively lost through a series of electromagnetic processes involving atomic electrons and nuclei. These interactions determine the range, scattering behavior, and radiation output of the incident electrons, which are critical parameters in techniques such as energy-dispersive X-ray fluorescence (EDXRF) [19].

Due to their small mass compared to heavy charged particles (e.g., protons or alpha particles), electrons experience significant angular deflections during collisions, leading to zigzagging trajectories. As a result, the path length of an electron is much longer than its penetration range, complicating their transport modeling in dense media.

The primary mechanisms of energy loss for electrons in matter include ionization, excitation, and radiative losses such as bremsstrahlung. These processes are stochastic in nature but

can be described statistically through the stopping power S, which quantifies the rate of energy loss per unit path-length [20].

2.3.1 Ionization and Excitation

The most probable interaction between a high-energy incident electron and an atom in the absorbing medium is via inelastic Coulomb interactions with atomic electrons. The energy transferred can be sufficient to excite the electron to a higher bound state without ejection. Or ionize the atom by ejecting the electron entirely.

In the ionization process, the incident electron transfers part of its kinetic energy to a tightly bound atomic electron typically from the inner K or L shells, overcoming the binding energy Eb of the electron. This results in the ejection of a secondary electron and the formation of a positive ion. The kinetic energy T of the emitted electron is given by:

$$T = E_i - E_b \tag{2.1}$$

where E_i is the energy of the incident electron.

In contrast, excitation raises an atomic electron to a higher bound energy level. The atom subsequently relaxes by emitting a photon whose energy corresponds to the difference in energy levels. This emitted radiation is often in the UV, visible, or soft X-ray regions, depending on the transition [21].

2.3.2 Auger and Characteristic X-ray Emission

Following the ionization of an inner-shell electron, the atom is left in an excited state. To regain electronic stability, an electron from a higher energy level transitions into the vacant lower-energy orbital, releasing energy equivalent to the difference in binding energies between the two shells. This excess energy can be dissipated through two main mechanisms:

A. Characteristic X-rays: emitted as photons with discrete energies that are specific to the element and the electronic transition involved. The energy of these emitted X-rays is governed by Moseley's law, which relates the square root of the X-ray frequency to the atomic number of the emitting atom minus a screening constant:

$$E_x = RhC(Z - \sigma)^2(\frac{1}{n_1^2} - \frac{1}{n_2^2}) \tag{2.2}$$

where E_x is the photon energy, Z is the atomic number, σ is the screening constant, and n_1 and n_2 are the principal quantum numbers of the involved energy levels. Only transitions that satisfy dipole selection rules (Δ l $= \pm 1$ and Δ J $= 0$ or ± 1) are allowed, thus defining the possible spectral lines [22].

B. Auger electrons: produced when the transition energy is instead transferred to another electron in an outer shell, which is then ejected from the atom without photon emission.

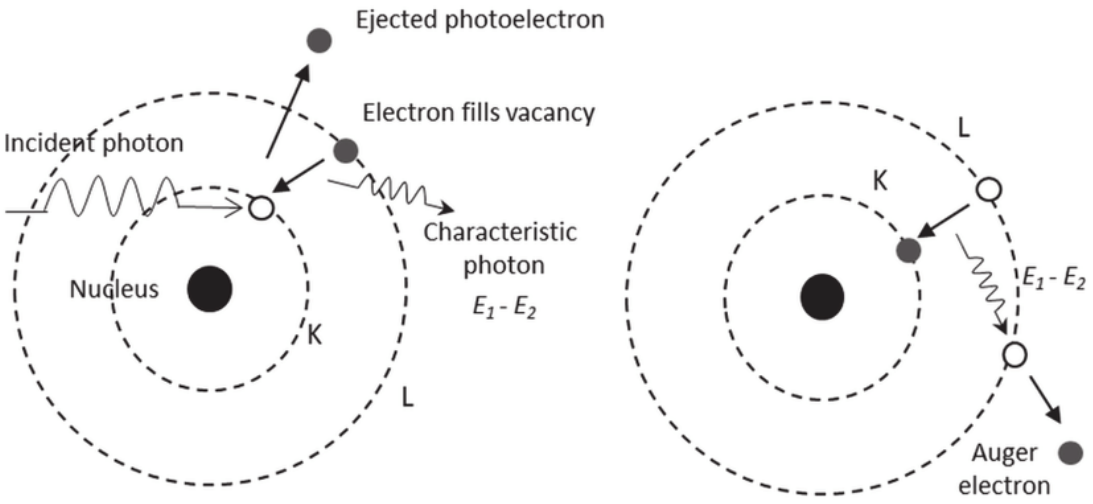

Figure 2.1: Production of Characteristic X-rays and Auger Electrons via Inner-shell Ionization.

The likelihood of characteristic X-ray emission versus Auger emission is described by the fluorescence yield ω, which increases with atomic number. For lighter elements ($Z < 15$), Auger processes dominate due to lower ω values, whereas in heavier elements, X-ray emission becomes the prevailing relaxation mechanism. This trend has critical implications for XRF sensitivity across the periodic table [19].

2.3.3 Bremsstrahlung Radiation

When an electron passes near the nucleus of an atom, it is deflected by the nuclear Coulomb field, causing it to decelerate and emit radiation. This phenomenon, known as bremsstrahlung (German for "braking radiation"), results in the emission of continuous spectrum X-rays.

Unlike characteristic radiation, bremsstrahlung photons can have any energy up to the incident electron energy, and their distribution forms a broad continuum. The total power radiated due to bremsstrahlung is given approximately by [20]:

$$P \propto Z^2.\frac{1}{m^2} \tag{2.3}$$

where Z is the atomic number of the medium, and m is the mass of the incident particle. This implies that bremsstrahlung is:

- More intense for high-Z materials.
- Negligible for heavy charged particles due to their larger mass.
- Especially significant at high electron energies (above $\sim 1MeV$), where radiative losses start to dominate over collisional losses.

2.3.4 Emission Spectrum

The X-ray emission spectrum generated by electron interactions consists of two components:

A. Continuous spectrum from bremsstrahlung forming a smooth background.

B. Line spectrum from characteristic X-ray emissions appearing as sharp peaks at energies corresponding to transitions between specific atomic energy levels.

This dual nature of the spectrum is crucial in EDXRF, where the continuous background provides information about bremsstrahlung contributions and instrumental effects and the sharp characteristic peaks enable qualitative and quantitative elemental analysis.

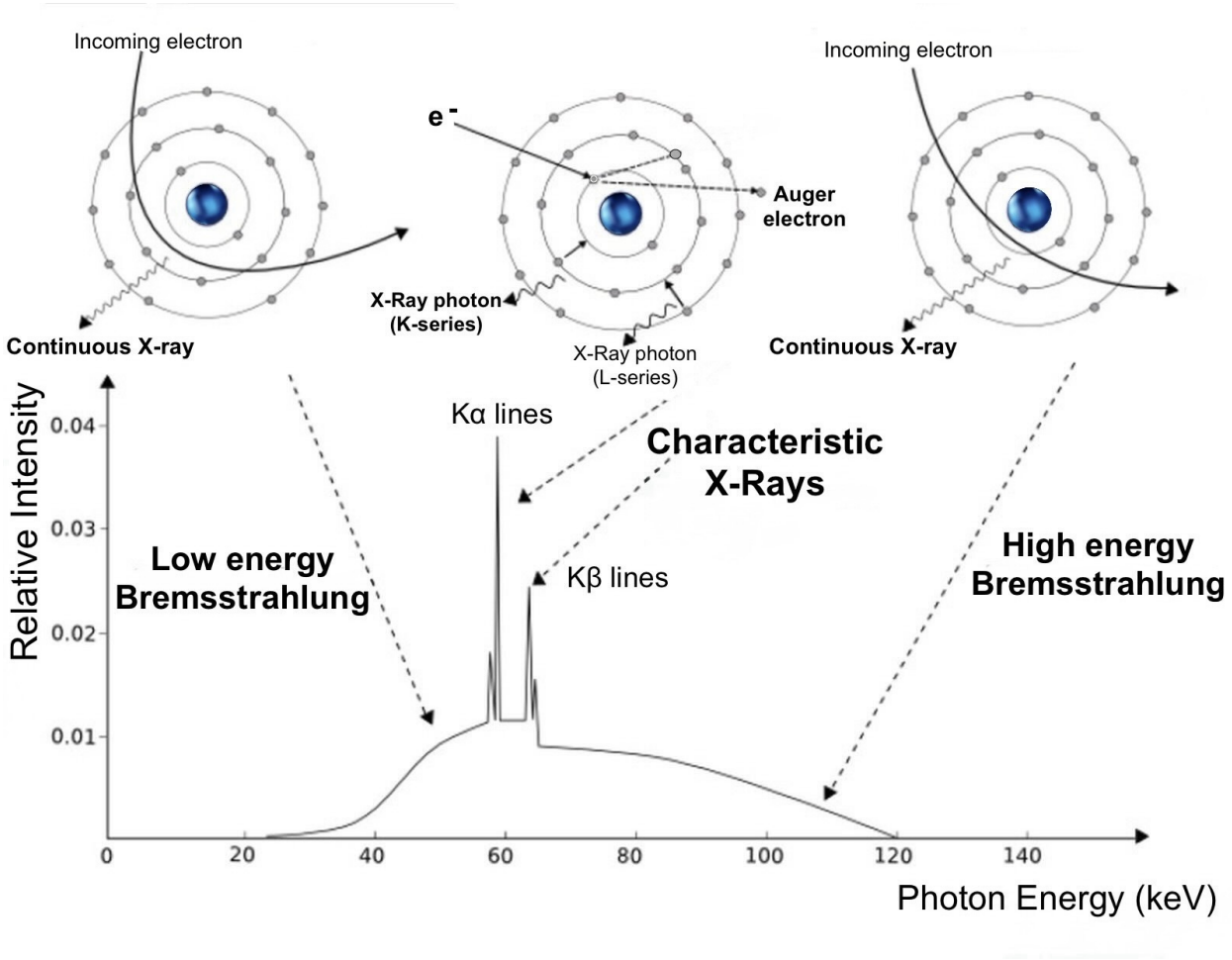

Figure 2.2: Origin of Background and Characteristic X-ray Spectra.

Figure 2.2 visually demonstrates the superposition of the two components. The height and area of the characteristic peaks are used to determine elemental concentrations, while background subtraction is necessary to improve accuracy [23].

2.4 Photon-Matter Interactions

Photons can interact with matter through four main processes, each dependent on the energy of the incident photon and the atomic number (Z) of the medium being traversed, the photoelectric effect, which dominates at low energies and in high atomic number materials; Compton scattering, which prevails at intermediate energies; pair production, which becomes significant at high energies, and Rayleigh scattering, which is negligible compared to the other three processes [24, 25]. Figure 2.3 shows the regions where each interaction dominates, based on the photon energy and the atomic number of the target material.

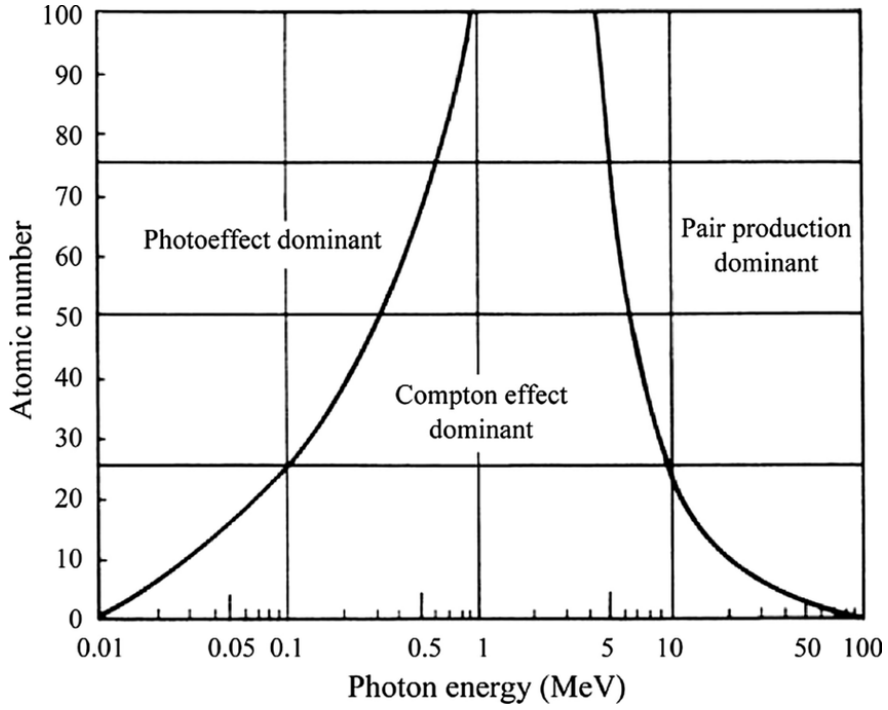

Figure 2.3: Dominant regions of each of the three effects as a function of energy (E) and atomic number (Z).

2.4.1 Photo-Electric Effect

The photoelectric effect shown in 2.1 refers to the interaction in which a gamma photon is absorbed by a bound electron, resulting in the ejection of the electron from its atomic shell. This process predominantly involves the most tightly bound electrons, particularly those in the K-shell, which contribute most significantly to the effect [26].

$$T_{e^-} = E\gamma - E_L \tag{2.4}$$

with:
$E_\gamma = h\nu$ represents the energy of the incident photon
E_L the binding energy of the electron.

2.4.2 Compton Scattering

In Compton scattering, a gamma-ray photon with initial energy $E\gamma$ interacts with a free or loosely bound electron within a material. As a result of this interaction, the photon is deflected at a scattering angle θ emerging with reduced energy $E_{\gamma'}$. The relationship between the energy of the scattered photon $E_{\gamma'}$ and the scattering angle θ is described by

the Compton scattering.

$$E\gamma = T_e + E_{\gamma'} \tag{2.5}$$

$$E_{\gamma'} = E\gamma[1 + \frac{E\gamma}{m_e c^2}(1 - cos\theta)]^{-1} \tag{2.6}$$

where $E_\gamma = h\nu$ represents the energy of the incident photon, $E_{\gamma'}$ the energy of the scattered photon, $m_e c^2$ the rest mass energy of the electron, T_{e^-} the kinetic energy of the compton electron and θ the scattering angle of the photon relative to the incident direction.
During this process, the gamma-ray photon is redirected while losing part of its energy to the electron. When a beam of gamma rays traverses a material, it undergoes successive Compton scattering events, leading to both energy degradation and angular broadening of the beam [26].

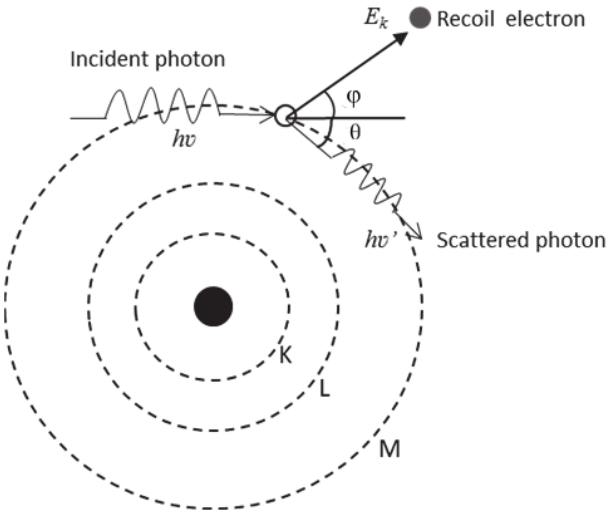

Figure 2.4: Schematic representation of the Compton scattering.

2.4.3 Pair Production

When a gamma-ray photon with energy equal to or greater than 1.02 MeV interacts with an electron, it may undergo pair production. In this process, the photon is annihilated, giving rise to an electron-positron pair. The combined kinetic energies of the positron T_{e^+} and electron T_{e^-}, along with their rest mass energies (equivalent to 1.02 MeV), must be equal to the energy of the incident gamma-ray photon [26].

$$E\gamma = T_{e^-} + T_{e^+} - 2m_e c^2 \tag{2.7}$$

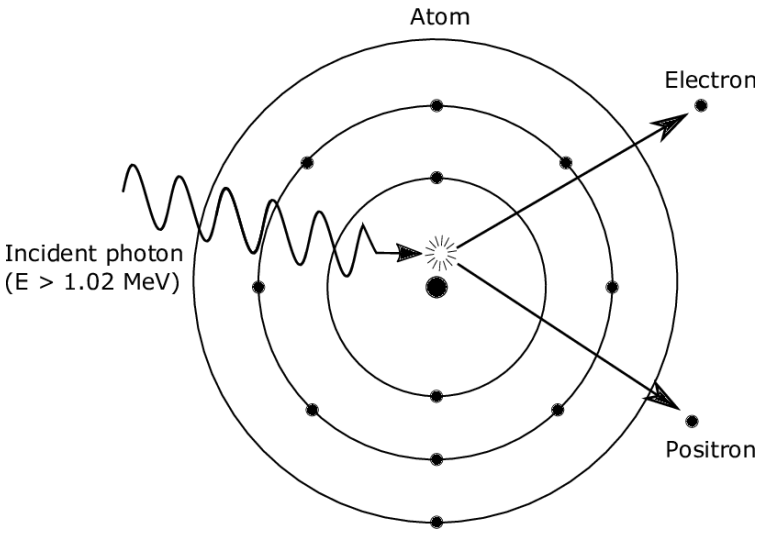

Figure 2.5: Schematic representation of pair production event creating a pair of e^- and e^+.

2.4.4 Rayleigh Scattering

This describes coherent scattering of a photon by the atoms of the material, where there is no energy transfer: the scattered photon retains the same energy as the incident photon but undergoes a change in direction. As a result, photons with shorter wavelengths are scattered more strongly, while photons with longer wavelengths are scattered less [25].

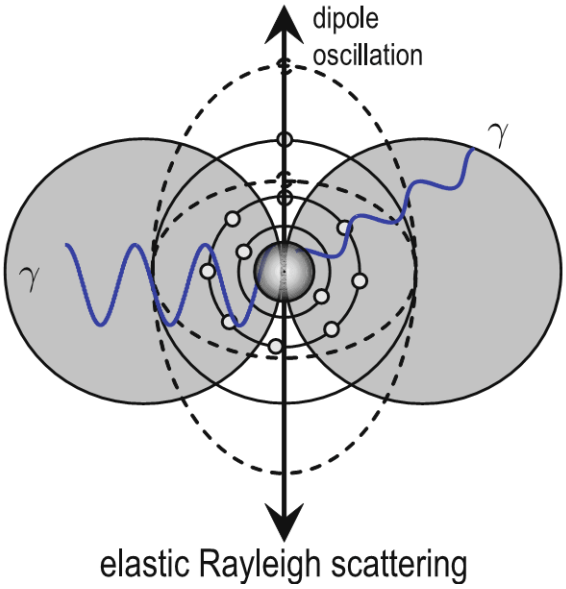

Figure 2.6: Schematic representation of Rayleigh scattering.

2.4.5 Spectrum and Peak Analysis

Gamma ray spectrometry relies on detecting and analyzing the energy of individual gamma photons emitted by radionuclides. Each radionuclide emits gamma rays at specific, discrete energies, which appear as distinct photopeaks in the spectrometer's energy spectrum.

2.4.5.1 Photopeak (Full-Energy Peak)

This is the primary peak formed when a gamma photon deposits all its energy in the detector via the photoelectric effect. Identifying the energy and intensity of a photopeak enables accurate radionuclide identification and quantification.

2.4.5.2 Compton Continuum and Compton Edge

Some gamma photons undergo Compton scattering, depositing part of their energy in the detector before exiting. This results in a broad plateau or "continuum" of counts below the photopeak. The Compton edge marks the maximum energy transferred in a single Compton scatter and is a diagnostic feature of the spectrum.

2.4.5.3 Backscatter Peak

External scatter from surrounding materials like shielding can produce a smaller peak in the lower energy region of the spectrum, known as the backscatter peak typically between 100–250 keV.

2.4.5.4 Annihilation Peak (511 keV)

The 511 keV annihilation peak appears due to pair production, where a high-energy gamma photon (> 1.022 MeV) creates an electron-positron pair. When the positron meets an electron, they annihilate, producing two gamma rays of 511 keV. One of these may be detected, forming the peak.

2.4.5.5 Escape Peaks (Single and Double)

For a high-energy gamma-ray having produced anelectron–positron pair, a full energy peak will be displayed if all the energies of the electron position pairincluding the annihilation photons are dissipated inthe detector material. But one of the annihilation photons or both of them may escape from the detector taking away 0.511 or 1.02 MeV of energy. As aconsequence peaks related to lower energies than the full energy peak will appear in the gamma spectrum a single (or first) escape peak (E_γ–511 keV) and a double (or second) escape peak(E_γ–1022 keV) are displayed in the spectrum [27].

2.4.5.6 Other Peaks

Additional low energy peaks caused by X-rays that are produced by fluorescence interactions with the shielding material of the detector may also appear. Lead X-rays occur in the regions from 74 to 88 keV.

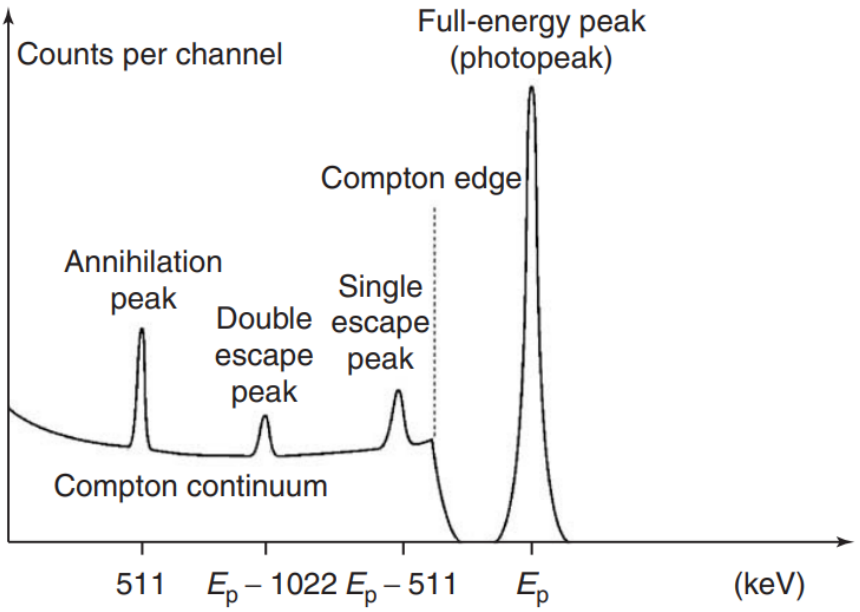

Figure 2.7: Schematic picture of a gamma spectrum.

The spectrum shows the photo-peak (or full-energy peak), corresponding to the energy of the characteristic gamma line of the radionuclide. By Compton scattering electrons with a wide energy distribution are produced (Compton continuum). By pair production and subsequent annihilation of the positron–electron pair apeak of 0.511 MeV (annihilation peak) is produced. If the gamma photons of 0.511 MeV escape from the detector without interaction a single and double escape peak appear in the spectrum (Buchtela, 2005).

2.5 Energy Dispersive X-ray Fluorescence Technique (ED-XRF)

2.5.1 Principle of XRF and EDXRF Operation

X-ray fluorescence (XRF) is a widely employed technique for elemental analysis of solid, powdered, and liquid samples. It is based on the detection of secondary fluorescent X-rays emitted by atoms after excitation by an incident primary X-ray beam. The intensity of these characteristic emissions is proportional to elemental concentration and can be used for both qualitative and quantitative analysis [19]. Modern XRF spectrometers operate in two main configurations:

A. Wavelength Dispersive XRF (WDXRF): This setup uses a diffraction crystal to separate emitted X-rays by wavelength before detection. It provides higher resolution and sensitivity but involves more complex instrumentation and longer measurement times [28].

B. Energy Dispersive XRF (EDXRF): Here, the detector directly measures the energy of incoming X-rays.

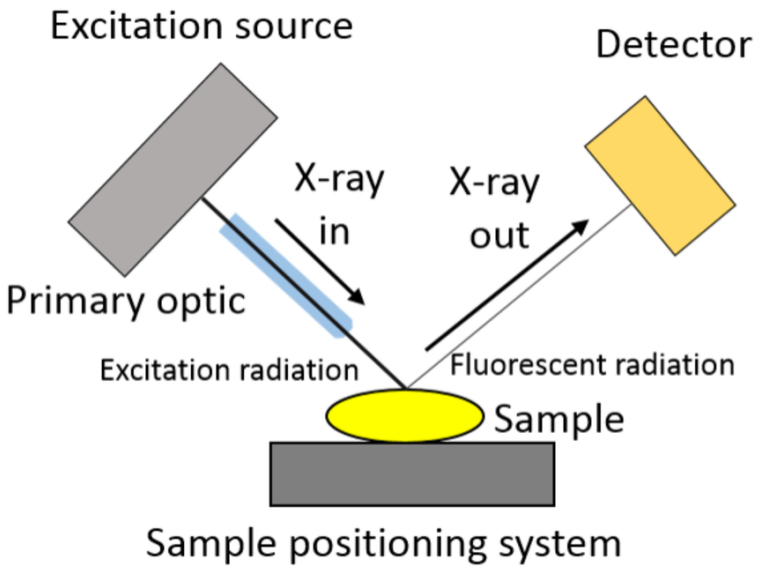

Figure 2.8: Schematic of a general XRF setup. In EDXRF systems, the 'primary optic' may refer to beam-shaping filters or collimators rather than wavelength-selective optics used in WDXRF.

This thesis focuses primarily on the EDXRF technique, which allows for the analysis of a broad range of elements from sodium (Z = 11) to uranium (Z = 92), with detection limits reaching the sub-ppm level and typical uncertainties in the range of 0.2–0.4% in solids. It captures all emitted photon energies simultaneously using a solid-state detector, eliminating the need for wavelength-dispersive components [29].

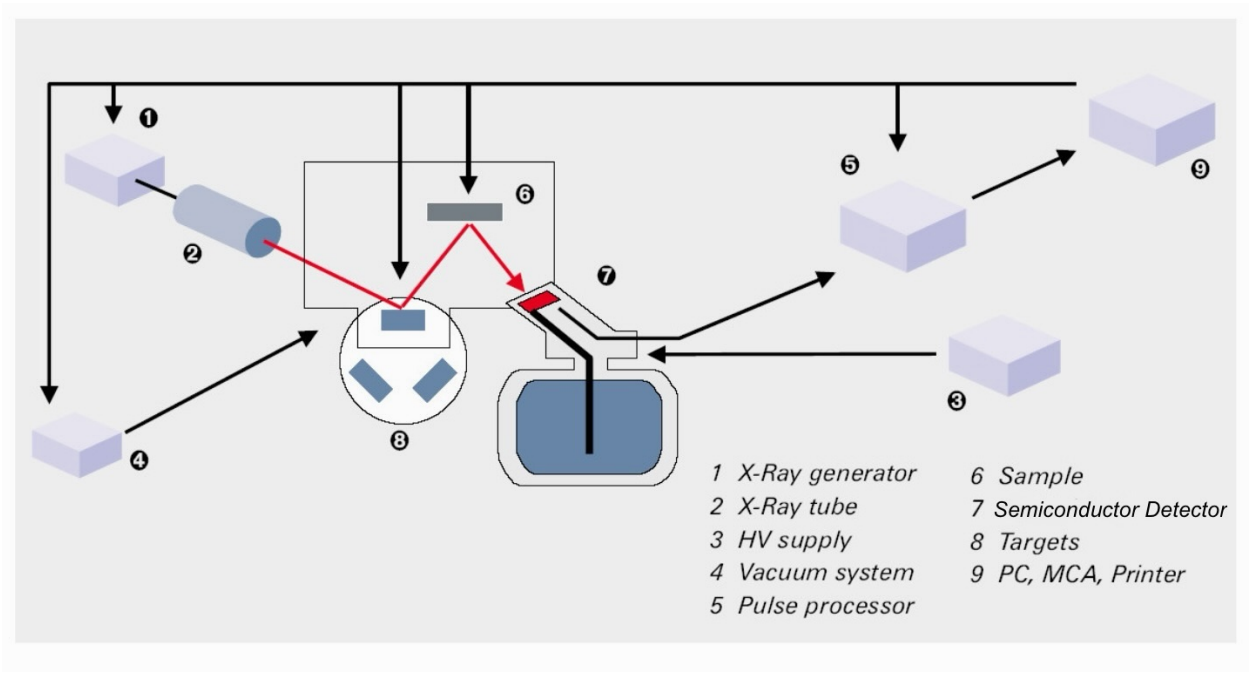

Figure 2.9: General Components of an EDXRF Spectrometry System.

2.5.2 X-ray Tube and Excitation Source

The excitation source in EDXRF is typically an X-ray tube that produces primary radiation by accelerating electrons toward a metal target, usually rhodium or molybdenum. When these high-energy electrons decelerate upon hitting the anode, they emit Bremsstrahlung radiation along with characteristic X-rays of the target material. The energy of the emitted X-rays depends on the accelerating voltage applied to the tube, which is typically adjustable usually 4–50 kV to optimize excitation for different elements.

In direct excitation setups, this beam is aimed at the sample. Alternatively, some systems employ secondary targets or beam filters to tailor the spectral profile for specific analytical needs. Filters are thin materials placed between the X-ray tube and the sample to selectively shape the incident beam [30].

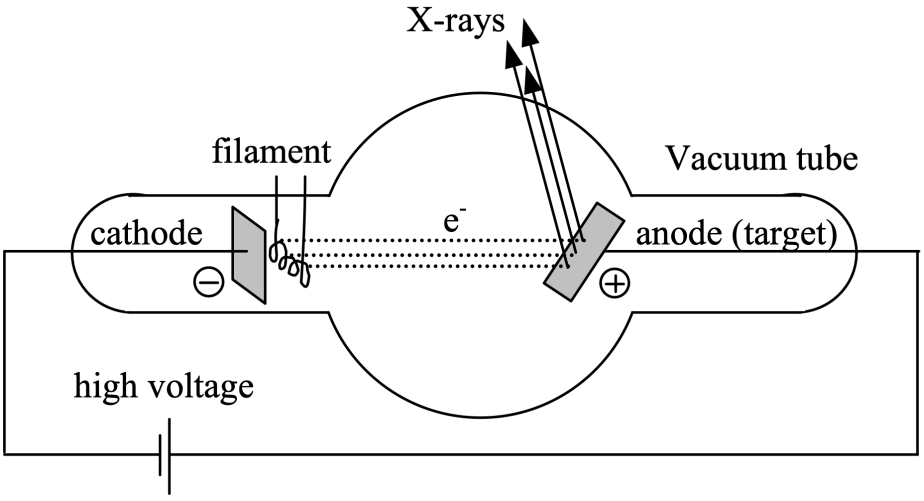

Figure 2.10: X-ray Tube Configuration as the Excitation Source in EDXRF.

2.5.3 Silicon Drift Detectors

Silicon Drift Detector (SDD) are used to measure the energy of characteristic X-rays emitted by the sample after excitation. The SDD is a type of semiconductor detector that employs a series of concentric electrodes to create a radial electric field within a fully depleted high-purity silicon wafer. This field causes the charge cloud produced by an absorbed X-ray photon to drift toward a small central anode. As shown in Figure 2.11.

The small size of the anode results in low capacitance, which allows for fast signal processing with reduced electronic noise. The voltage signal generated at the anode is proportional to the energy of the incident X-ray, enabling elemental identification based on spectral analysis [31].

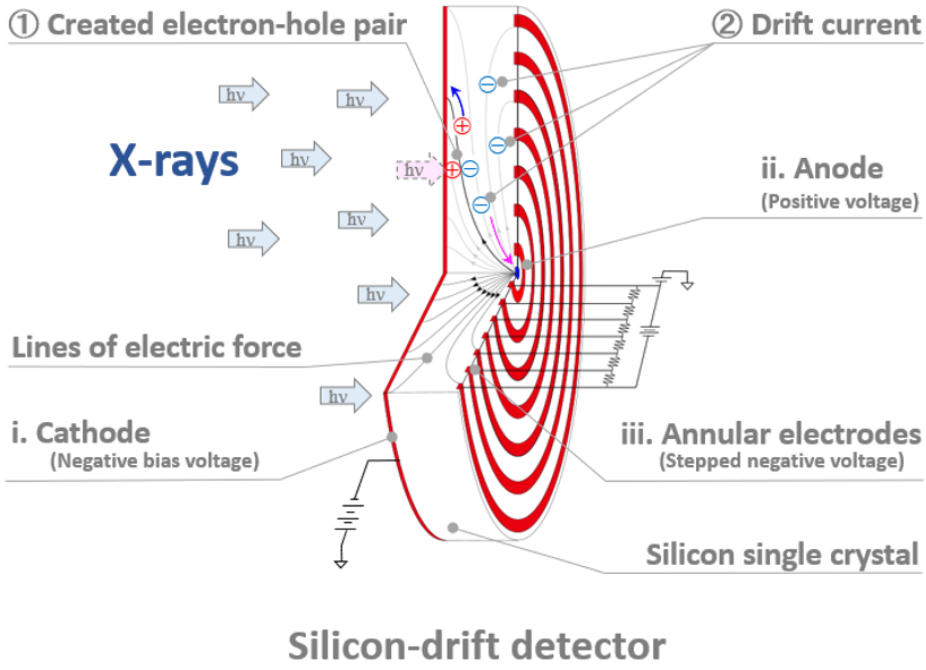

Figure 2.11: Diagram of an SDD, a Common Example of Semiconductor Detectors Used in EDXRF [32].

2.5.4 Calibration and Quantification

In quantitative XRF, the emitted X-ray intensity of a given spectral line is related to elemental concentration through calibration. Depending on the required accuracy and sample characteristics, several calibration strategies are commonly employed [33]:

Fundamental Parameters (FP) Approach

A theoretical model-based calibration that considers X-ray interactions, matrix composition, geometry, and detector efficiency. It enables semi-quantitative or quantitative analysis even without matrix-matched standards. This method was not employed in the current study.

Empirical Calibration

Involves the use of primary standards with known elemental concentrations to establish a direct relationship between intensity and concentration. This approach is typically used to verify instrument performance or calibrate the system before analysis.

Matrix-matched calibration

A more specific form of empirical calibration, where secondary standards are prepared using a blank matrix similar to the sample (e.g., food powder). This allows more accurate quantification by minimizing matrix effects.

In this study, external standard calibration was used, applying the following equation:

$$C_i = C_{st}.\frac{I_{i\,sp}}{I_{i\,st}} \tag{2.8}$$

Where:
C_i: Concentration of element i in the sample
C_{st} : Concentration of the element in the standard
$I_{i\,sp}$: Net intensity (peak area) in the sample
$I_{i\,st}$: Net intensity in the standard

Measurement uncertainties were estimated through propagation of relative errors, following the standard formula:

$$\delta C_i = C_i.\sqrt{(\frac{\delta C_{st}}{C_{st}})^2 + (\frac{\delta I_{sp}}{I_{sp}})^2 + (\frac{\delta I_{st}}{I_{st}})^2} \tag{2.9}$$

Depending on the element and application, results are typically reported in weight percent (wt%) or parts per million (ppm), which is numerically equivalent to the mass to mass ratio mg/kg.

2.5.5 Matrix Effects

The linear relationship between fluorescence intensity and elemental concentration is often affected by matrix effects—interactions among elements within the sample that influence the intensity of the measured signal.

The two primary types are:

A. Absorption Effects

Occur when the fluorescent X-rays emitted by an analyte are partially absorbed by surrounding matrix material, reducing the detectable signal.

B. Enhancement Effects

Happen when characteristic radiation from matrix elements further excites the analyte, increasing its fluorescence yield beyond that caused by the primary source.

Additional challenges include spectral overlaps, surface roughness, and particle size effects, all of which can introduce analytical errors. These are typically addressed through matrix-matched standards, empirical corrections, or computational modeling. Specific methods will be discussed in the next chapter [34].

2.5.6 Application and Advantages

Energy Dispersive X-ray Fluorescence is a versatile technique used in fields such as environmental monitoring, cultural heritage studies, forensic science, and increasingly, food safety assessment. Its strength lies in the ability to analyze samples with minimal preparation while preserving sample integrity [35]. Additionally, EDXRF showed stable performance

even when sample mass varied slightly, which is important when analyzing powdered food pellets, where achieving perfect homogeneity can be challenging. The short acquisition time enabled high-throughput screening, making the technique suitable for routine laboratory monitoring [36].

2.5.7 Detection Limits

The detection limits in EDXRF typically range from 1 to 100 ppm, depending on the element, matrix composition, and instrumental configuration. It is estimated by:

$$LD = 3c \times \frac{\sqrt{B}}{N} \tag{2.10}$$

Where:
C: Concentration
B: Background count
N: Net peak intensity

Sensitivity for lighter elements (Z < 11) remains limited due to low X-ray yields and strong attenuation in air or detector windows [37].

In this study, several strategies were employed to enhance detection sensitivity and minimize background interference. Beam filtration was applied to improve the signal-to-noise ratio by selectively reducing the Bremsstrahlung component of the X-ray spectrum. Additionally, acquisition parameters were optimized to ensure sufficient statistical confidence, particularly for trace elements with low-intensity peaks. These refinements allowed detection limits to approach regulatory thresholds established by bodies such as the Codex Alimentarius and the World Health Organization, thereby supporting reliable identification of heavy metal contaminants in food samples. Specific implementation details are presented in the following chapter.

2.5.8 Health Risk Assessment Factors

A. The Estimated Intake :

The Estimated Daily Intake (EDI) refers to the amount of a toxic metal that an individual is expected to consume on a daily basis through food. Similarly, the Estimated Weekly Intake (EWI) calculates this exposure on a weekly scale, providing a broader view of cumulative intake. These estimates are then compared to reference values such as the Provisional Tolerable Weekly Intake (PTWI), which represents the maximum amount of a toxic metal that can be ingested weekly over a lifetime without posing a significant health risk, as established by international health authorities. The Estimated Daily Intake (EDI) is calculated using the following formula:

$$EDI = \frac{C \times IR}{BW} \tag{2.11}$$

Where:
C: Concentration of the metal in the sample (mg/kg)
IR: Daily ingestion rate of the food (kg/day)
BW: Body weight (kg) of the consumer

B. The Hazard Index and Hazard Quotient :

The Hazard Quotient (HQ) and Hazard Index (HI) are key indicators for evaluating non-carcinogenic health risks from dietary exposure to heavy metals. HI reflects the combined effect of multiple toxic elements, with values $\leq$1 indicating low risk, while values >1 suggest potential health concerns that may require further investigation or intervention.

The Hazard Index (HI) is defined as the sum of individual Hazard Quotients (HQi) for each metal:

$$HI = \sum_i HQ_i = \sum_i \left(\frac{EDI}{RfD_i} \right) \tag{2.12}$$

Where:

HQ i is the Hazard Quotient for metal i
EDI i is the Estimated Daily Intake of metal i (mg/kg body weight/day)
RfD i is the Reference Dose of metal i (mg/kg body weight/day)

C. Metal Pollution & Contamination Indices :

The Metal Pollution Index (MPI) provides an overall indication of heavy metal contamination in a food or environmental sample. It is calculated as the geometric mean of the concentrations of multiple metals:

$$MPI = (C_1 \times C_2 \times \cdots \times C_n)^{\frac{1}{n}} \tag{2.13}$$

Where C1, C2 ..., Cn are the concentrations (mg/kg) of the n different metals in the sample. Typically, higher MPI values reflect greater overall contamination. Although no strict thresholds exist, MPI values approaching or exceeding 1 may suggest potential health concerns.

The Contamination Factor (CF) assesses the contamination level of each individual metal by comparing its concentration in the sample to a reference or background value:

$$CF_i = \frac{C_i}{C_{\text{ref}}} \tag{2.14}$$

Where Cref is the reference concentration (mg/kg) of metal i, typically obtained from regulatory sources such as the Codex Alimentarius. A CF value below 1 indicates low contamination, while a value greater than 6 indicates very high contamination.

Based on CF values, the Pollution Load Index (PLI) is then computed as the geometric mean of all CFs to give an integrated measure of metal pollution. A PLI value of 1 indicates baseline contamination (i.e., no pollution), <1 suggests minimal pollution, and >1 reflects progressive contamination.

2.6 Gamma Spectrometry Technique

Gamma spectrometry being a rapid and efficient method, is held as the optimal non- destructive technique for the radioactivity's (gamma-emitting radionuclides within a sample) identification and quantification. Photons emitted by the source interact with the detection crystal, depositing either all or part of their energy. Over a defined measurement period, these interactions allow the construction of a spectrum that displays the number of detected photons as a function of their energy. By analyzing the resulting signals which correspond to the various photon-detector interactions (photoelectric effect, Compton scattering, and pair production) it becomes possible to determine the specific radioelements present in the sample and to assess their activity levels [24, 38].

2.6.1 Detection Chain

Gamma spectrometry aims to qualitatively identify radionuclides and quantitatively measure the activity of gamma radiation spontaneously emitted by a sample. In this method, photons interacting with the detector are sorted based on their energy. The performance of the measurement system depends on the configuration and settings of each stage. Therefore, it is essential to understand the operation and limitations of each component in order to tailor the system to specific needs.

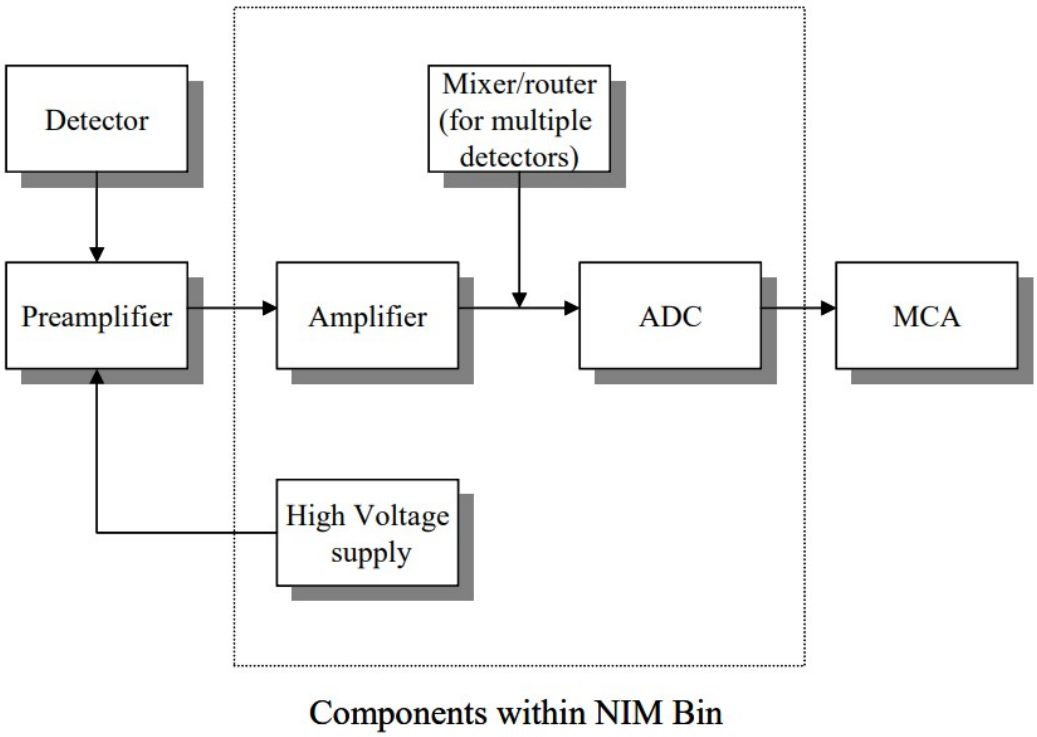

Figure 2.12: Electronic components for a gamma spectrometric system. [39]

2.6.1.1 Detector

The primary element of the gamma spectroscopy system is the detector. The detection material engages with the gamma rays, thereby transferring their energy. This energy is either transferred to positrons during annihilation or to electrons. When these generated particles lose energy within the detector, ionized atoms and ion pairs are formed. The signal from the detector relies on these secondary entities. High purity is essential. The material most widely used for gamma-ray spectrometry systems is germanium.

A. Scintillation detector :

Scintillation is the production of small flashes of light, where crystals, such as sodium iodide (NaI), convert the ionization and excitation produced by radiation into a light pulse or scintillation. The amount of light that is produced is proportional to the energy deposited by the radiation particle/photon. The weak scintillation is transformed into an electrical pulse using a photomultiplier tube (PMT), which amplifies the signal while preserving the energy proportionality. Consequently, the amplitude of the output pulse provides a quantitative measure of the energy of the incident radiation [40].

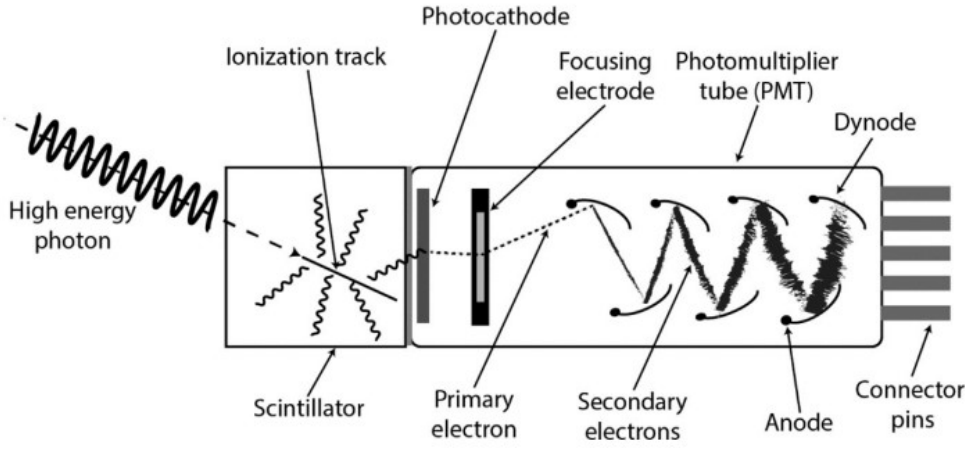

Figure 2.13: Basic components and operating principle of a scintillator detector [41].

B. Semiconductor detector :

Semiconductors do not normally conduct electricity because their crystals do not contain enough free-charged particles to carry the current, but do become conducting when the atoms in the crystal become ionized. The operational mechanism of semiconductor-based radiation detectors is fundamentally governed by the electronic band structure of the crystalline material. In certain semiconductor compounds, notably germanium with a band gap of 0.66 eV at room temperature. It also has a P-I-N diode structure where reverse bias creates a charge-depleted intrinsic (I) region. Incident ionizing radiation can deposit sufficient energy in this depletion zone generate electron-hole pairs that are separated by the applied electric field and collected at their respective electrodes. The resulting charge, proportional to the photon energy, is converted to a voltage pulse via a charge-sensitive preamplifier. Since the depletion depth is inversely proportional to net electrical impurity concentration, and counting efficiency is also dependent on the purity of the material, large volumes of very pure material are needed to ensure high counting efficiency for high-energy photons.
The energy required to produce an electron-hole pair is characteristic of the detector material, with germanium's relatively narrow band gap making it particularly sensitive to radiation detection. The resulting charge carriers can be collected under an applied electric field, producing a measurable signal proportional to the deposited radiation energy.
Both the electron and the hole can migrate through the semiconductor crystal in response to an electric field and can produce an electrical signal that indicates the passage of radiation. Modern semiconductor technology enables the production of ultra-high-purity germanium crystals, forming intrinsic germanium (HPGe) detectors. While these detectors can be stored at room temperature without bias voltage, they require cryogenic cooling to liquid nitrogen temperatures during operation. The detector crystal is enclosed in a Dewar vacuum housing and connected by a copper rod (cold finger) to a reservoir of liquid nitrogen [40, 42].

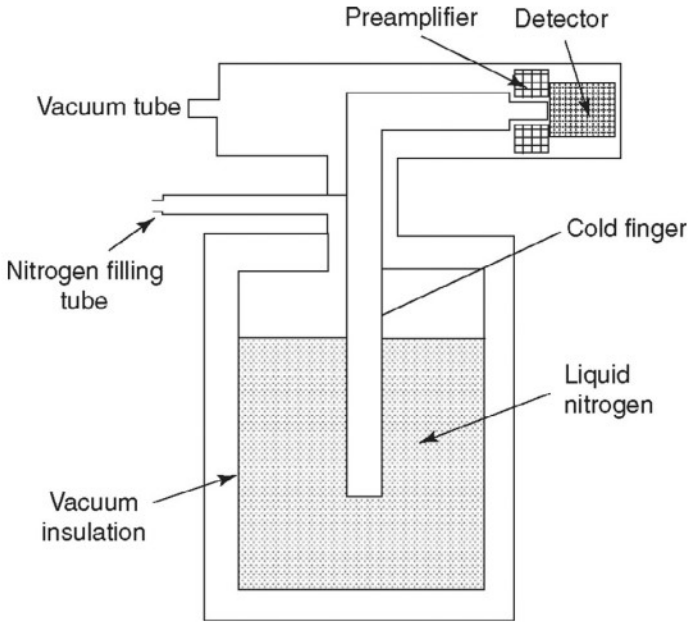

Figure 2.14: Basic components and operating principle of a scintillator detector [40].

2.6.1.2 Preamplifier

A charge-sensitive preamplifier (often FET-based and cryogenically cooled) is used to convert ionization charges into step pulses proportional to gamma energy [40].

2.6.1.3 Amplifier

A shaping amplifier then optimizes these pulses by amplifying, filtering, and reducing noise for improved resolution at typical environmental count rates (< 100 cps) [40].

2.6.1.4 HV Supply

A stable high-voltage bias ($\pm$1–5 kV) ensures efficient charge collection [40].

2.6.1.5 ADC

The analog-digital converter (ADC), is used to convert analog signals into digital signals. This conversion allows the next stage of the system to process data in digital rather than analog form so it digitizes pulses [24].

– **NIM-bin** Components (amplifier, HV supply, ADC) are typically housed in modular NIM-bin racks, ensuring compatibility across manufacturers.

2.6.1.6 MCA

The Multichannel Analyzer (MCA) sorts electrical pulses according to their amplitude. It uses internal memory to store these signals in channels that correspond to specific voltage intervals and subsequently transfers the data to a connected computer. The resulting output is presented as a spectrum, commonly referred to as "pulse height differential spectra."It enables qualitative and quantitative analysis of these spectra via data acquisition software [24].

2.6.2 Main Characteristics of a Detector

2.6.2.1 Detector Efficiency

In general, the sensitivity of an HPGe system is directly related to the detector's efficiency. Detector efficiency refers to the proportion of gamma rays that produce measurable pulses essentially, the fraction of photons emitted by the source or sample (A) that result in a detectable event within the detector (N). This ratio defines the detector's efficiency ϵ [43].

$$N = \epsilon.A \tag{2.15}$$

A. Absolute Efficiency :

It depends on the detection geometry and the probability of photon interaction within the detector. In this context, two types of efficiency are defined: full-energy peak efficiency (FEPE) and total absolute efficiency [24].

– **Full-energy peak efficiency (FEPE) :** It is defined as the percentage of photons detected at a given energy (originating from the photoelectric interaction) relative to the total number of photons emitted by the source. It is expressed as follows:

$$\epsilon_{FEPE} = \frac{N_{PE}}{A.I.\Delta t} \tag{2.16}$$

Where A is the activity of the source, I is the emission intensity of the energy line E, and Δt is the acquisition time.

– **Total absolute efficiency :** The ratio between the total number of photons detected and the total number of photons emitted by the source. It is expressed as follows:

$$\epsilon_{abs} = \frac{N_{ray}\, detected}{N_{ray}\, emitted\, by\, the\, source} \tag{2.17}$$

B.Intrinsic Efficiency :

The ratio of the number of pulses produced by the detector to the number of gamma rays striking the detector. It depends on the type of radiation, its energy, and the material that makes up the detector [43, 24].

$$\epsilon_{in} = \frac{N_{ray}\, detected}{N_{ray}\, received\, by\, the\, detector} \tag{2.18}$$

Both types of efficiency, absolute and intrinsic, are related by this following relation:

$$\epsilon_{abs} = \frac{\Omega}{4\pi}.\epsilon_{in} \tag{2.19}$$

Where $\frac{\Omega}{4\pi}$ The geometric efficiency corresponds to the ratio between the number of photons that reach the detector and the number of photons emitted by the source, with Ω representing the solid angle between the source and the detector, as described in the following Figure 2.15:

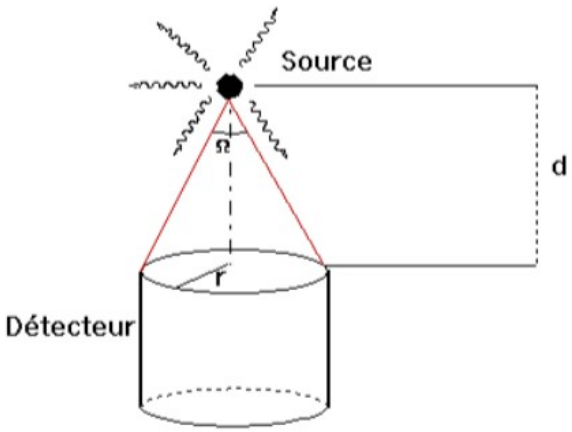

Figure 2.15: Descriptive diagram of the solid angle of a point source. [24]

2.6.2.2 Detector Resolution

Energy resolution is a measure of the width (full width at half maximum, FWHM) of a single energy peak at a specific energy. It reflects a detector's ability to distinguish between two closely spaced gamma peaks in the spectrum. This width can be expressed either in absolute keV (as with Germanium Detectors) or as a percentage of the energy at that point (as with Sodium Iodide Detectors). In practice, the full-energy absorption peaks appear as Gaussian curves, with the FWHM varying with energy (Figure 2.16). The broadening of the peak is primarily caused by fluctuations in the number of charge carriers created, the non-uniformity of charge collection, and noise from the electronic components (electronic chain noise) [43, 24]. The energy resolution of a detector is typically approximated by the following relation:

$$R = \frac{FWHM}{E_0} \tag{2.20}$$

In the case of a peak with an ideally Gaussian distribution, the full width at half maximum (FWHM) is related to the standard deviation σ(E) of the distribution:

$$FWHM = 2.35\,\sigma_E \tag{2.21}$$

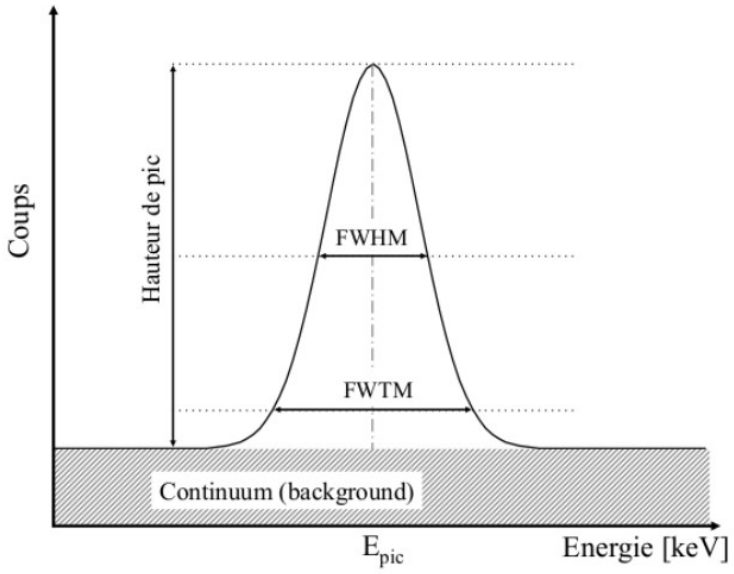

Figure 2.16: Definition of the resolution for a perfectly Gaussian peak.

2.6.2.3 Dead Time

During the time interval in which the acquisition system processes the signal generated by a photon's interaction with the detector, the system becomes insensitive to any other incoming photons. Any event occurring during this period is considered lost or ignored, as the input is electronically blocked.
Thus, dead time represents the minimum time required to separate two events or interactions so that they can be processed as distinct pulses. The count loss due to dead time increases with the activity of the source, since a higher activity raises the likelihood that two photons will interact with the detector within a time shorter than the dead time.
The spectrum acquisition software estimates this dead time based on two parameters: real time and live time. These correspond respectively to the total duration during which measurements were taken, and the actual time the detector was active and able to record events. The dead time (in %) is then defined as the ratio :

$$dead\,time\,(\%) = \frac{real\,time - live\,time}{real\,time} \times 100 \tag{2.22}$$

2.6.3 Radioactivity

2.6.3.1 Definition

Some unstable nuclides can spontaneously transform over time. They present an excess of protons, neutrons, or both, leading them to transform into other atomic nuclei with the emission of particles, sometimes followed by characteristic electromagnetic radiation. The resulting nucleus may itself be radioactive and undergo further transformations, or it may be stable [44].

2.6.3.2 Types of Decay

Radioactive decay is the process by which a radionuclide transitions from an unstable state to a stable one, releasing energy in the form of radiation such as alpha, beta, or gamma rays [45]. The main decay modes of a radionuclide are the emission of α or β particles, often accompanied by γ radiation. Other possible decay processes include electron capture, spontaneous fission, and the emission of a proton (following a decay or electron capture) or a neutron (following a β^- decay) [46], as shown in table 2.1 :

Type of decay	Equation
α decay	${}^{A}_{Z}X \xrightarrow{\alpha} {}^{A-4}_{Z-2}Y + {}^{4}_{2}He$
β^+ decay	${}^{A}_{Z}X \xrightarrow{\beta^+} {}_{Z-1}{}^{A}Y + e^+ + \nu$
β^- decay	${}^{A}_{Z}X \xrightarrow{\beta^-} {}_{Z+1}{}^{A}Y + e^- + \nu^-$
Electron capture	${}^{A}_{Z}X + e^- \longrightarrow {}_{Z-1}{}^{A}Y + \nu$
γ decay	${}^{A}_{Z}X^* \longrightarrow {}^{A}_{Z}X + \gamma$

Table 2.1: Decay types

2.6.3.3 Origins of Radioactivity

A. Natural radioactivity : Natural radioactivity originates from cosmic rays and the radioisotopes found in the Earth's crust. In the first case, it results from the de-excitation of unstable nuclei formed by the bombardment of energetic cosmic ray particles, primarily of galactic origin and, to a lesser extent, of solar origin. In the second case, it involves the de-excitation of primordial radionuclides. Natural radioactivity is present in rocks, soil, water, and even in our building materials [47, 48].

B. Artificial radioactivity : Artificial radioactivity is produced by converting stable nuclei into unstable ones, which then emit energetic particles (such as electrons or α particles) or radiation (such as photons) after a certain period. This transformation is typically achieved by bombarding target nuclei with projectile particles, most commonly protons, neutrons, or helium or deuterium nuclei [49].

2.6.3.4 Radioactive Decay Chains

A radioactive decay chain is defined as the successive disintegration of a radionuclide through the natural emission of particles primarily alpha and beta, until a stable state is reached. The process is considered a decay chain when the daughter nucleus is also radioactive. Each step in the chain is characterized by its own decay constant, which is related to the half-life of the radioactive element [50]. This sequence of decays is typically represented by a series of equations of the form:

$$\mathrm{X}_1{}^* \xrightarrow{1} \mathrm{X}_2{}^* \xrightarrow{2} \mathrm{X}_3{}^* \xrightarrow{3} \ldots \xrightarrow{n-1} \mathrm{X}_n$$

where λ_i denotes the decay probability (or decay constant) of the nucleus X_i. This constant defines the rate at which each radionuclide transforms. The collection of radioisotopes involved in such a decay chain is referred to as a radioactive family or decay series [45].
The nuclei that undergo successive natural decays are grouped into three series, which are considered among the heaviest chemical elements in the periodic table.

A. The $^{238}_{92}U$ series : Uranium is the heaviest naturally occurring chemical element found on Earth in trace amounts. Due to its large and unstable nucleus, it can spontaneously transform into a more stable state, emitting ionizing radiation (α, β, *gamma*, and X-rays) in the process. In addition to its common decay modes, uranium-238 can also undergo spontaneous fission a very rare and weak nuclear process in which the nucleus splits into two lighter fragments, releasing neutrons and energy without being triggered by an external particle [46]. Uranium has fourteen known radioactive isotopes, ranging from ^{226}U to ^{240}U. However, only those with sufficiently long half-lives have persisted on Earth to the present day. These include ^{238}U, ^{235}U and ^{234}U [51], whose radioactive half-lives and current relative abundances are shown in Table 2.2 :

Table 2.2: Periods (years) and relative abundances of the main isotopes of uranium

Isotopes	Radioactive half-life (years)	Current relative abundance on Earth (in % of natural U)
^{234}U	2.46×10^5	0.0055
^{235}U	7.04×10^8	0.7200
^{238}U	4.46×10^9	99.2745

The starting element, or parent element, is uranium with an atomic mass of 238. It decays very slowly, eventually transforming into stable lead through a process that involves 14 successive decays, emitting 8 α particles and 6 β^- particles.

Radon ^{222}Rn is the sixth descendant in the radioactive decay chain of uranium-238. It originates from the decay of radium ^{226}Ra and itself decays into polonium ^{218}Po in a matter of days, emitting an alpha particle during the process [52].

B. The $^{235}_{92}U$ series : Also called the Actinium series, it originates from $^{235}_{92}U$, which has a half-life of 7.1×10^8 years and represents 0.72% of natural uranium. The final stable product of this decay chain is the lead isotope $^{207}_{82}Pb$ [52].

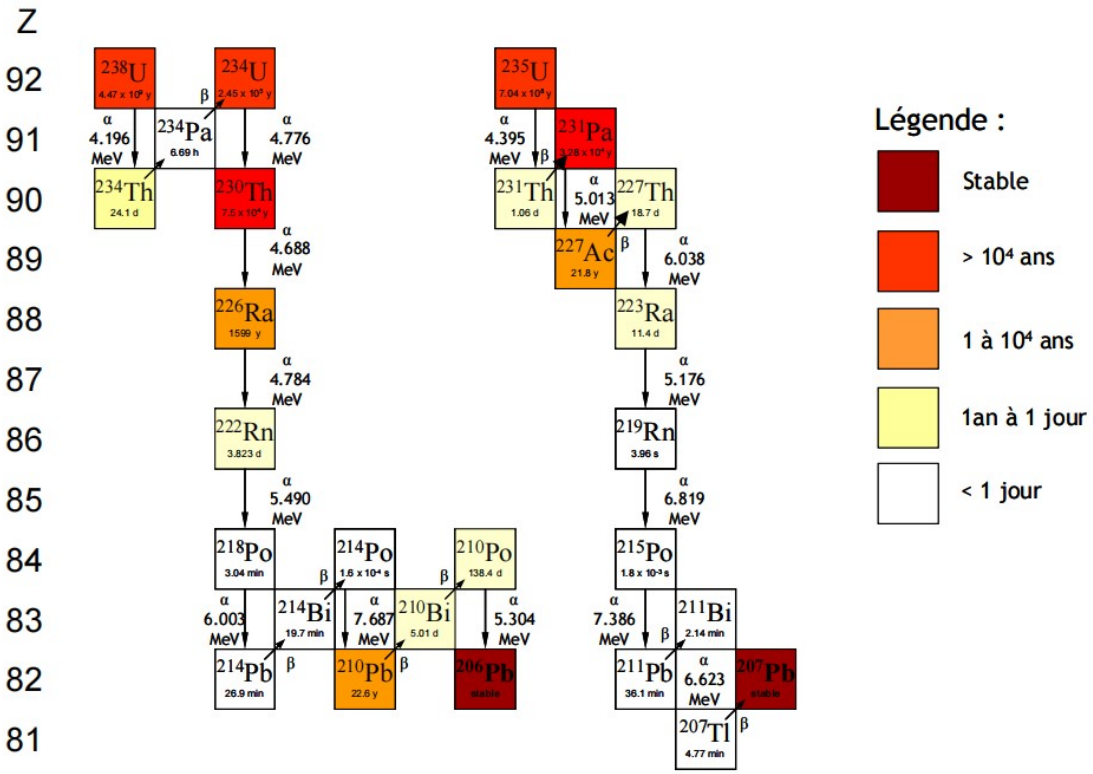

Figure 2.17: Decay chains of the two main isotopes of uranium. The color code uses light colors to represent short half-lives and dark colors to represent long half-lives [51].

C. The $^{232}_{90}Th$ series: The first element in this series is $^{232}_{90}Th$, with a half-life of 1.405×10^9 years, and the final element is lead $^{206}_{82}Pb$. $^{232}_{90}Th$ accounts for all naturally occurring thorium. During the decay of the various nuclei in this chain, 6 alpha particles and 4 beta particles are emitted. All descendants of $^{232}_{90}Th$, like the parent nucleus, have mass numbers that are multiples of 4 [53].

D. The ^{40}K series : Natural potassium is composed of three isotopes, $^{40}_{19}K$ being the least stable. It decays over a long period via two distinct pathways, resulting in the formation of two daughter products: calcium $^{40}_{20}Ca$ and argon $^{40}_{18}Ar$.

2.6.3.5 Secular Equilibrium

Secular equilibrium is achieved when the half-life of the parent nucleus is much longer than that of its daughter nuclei, this is typically the case in decay chains involving radionuclides with very long half-lives. In such cases, λ_1 (the decay constant of the parent) is much smaller

than λ_2 (the decay constant of the daughter). Under these conditions, Equation (2.23) simplifies to:

$$A_2 = A_1(1 - e^{-\lambda_2 t}) \tag{2.23}$$

After a certain amount of time, λ_2 increases, and the exponential term in Equation (2.23) becomes negligible. At this point, a secular equilibrium is reached, in which the activities of the parent and daughter become equal and constant over time:

$$A_1 = A_2 \tag{2.24}$$

2.6.3.6 Law of Radioactive Emission

A. Radioactive Decay Constant : Each radioactive substance, consisting of a population of identical atoms, has a certain probability of decaying per unit time. The number of atoms that decay during a time interval dt is given by the following expression :

$$dN(t) = -\lambda N(t)dt \tag{2.25}$$

where N(t) is the number of atoms present at time t, and λ is the decay constant, a characteristic value for each radionuclide. This constant represents the probability that a nucleus will decay per unit time.

The number of radioactive nuclei in a sample decreases exponentially over time, leading to the following solution:

$$N(t) = N_0 e^{-\lambda t} \tag{2.26}$$

where N_0 is the number of atoms present in the sample at the initial time (t=0) [55].

B. Radioactive Half-Life : The radioactive half-life $T_{\frac{1}{2}}$ of a radionuclide is the time required for half of the initially present radioactive atoms to decay. Using equation (2.26), the number of atoms remaining after one half-life is:

$$N(T_{\frac{1}{2}}) = N_0 e^{\lambda T_{\frac{1}{2}}} = \frac{N_0}{2} \tag{2.27}$$

hence :

$$T_{\frac{1}{2}} = \frac{ln2}{\lambda} \tag{2.28}$$

The time needed for the quantity to reduce from N_0 to $\frac{N_0}{2}$ is the same from $\frac{N_0}{2}$ to $\frac{N_0}{4}$ and so on, therefor. The number of atoms remaining after n half-lives is given by:

$$N(nT_{\frac{1}{2}}) = \frac{N_0}{2^n} \tag{2.29}$$

C. Activity : The activity A is defined as the average number of decays per second :

$$\frac{dN}{dt} = -\lambda N \tag{2.30}$$

From the equation (2.26) the time evolution of the activity is :

$$A(t) = \lambda N(t) = \lambda N_0 e^{-\lambda t} = A_0 e^{-\lambda t} \tag{2.31}$$

The unit of activity is the Becquerel (Bq), which corresponds to one disintegration per second. Another common unit is the Curie (Ci), defined as the activity of 1 gram of radium: $1Ci = 3.7 \times 10^{10} Bq$.

D. Mass-Activity Relationship : The activity per unit mass of a radionuclide is known as its specific activity A_s. It represents the activity A associated with a mass m of N atoms [44]:

$$m = \frac{M}{\lambda N_A} A \tag{2.32}$$

With Avogadro's number $N_A = 6.023 \times 10^{23}$.

2.6.4 Radiological Hazard Assessment :

A. Annual Committed Effective Dose :

The annual committed effective dose (AED) (Sv/yr) was calculated using the activity concentration of all radionuclides detected and analyzed in the samples as followed [56]:

$$AED = \sum e(g)_j \times A_J \times U_j \tag{2.33}$$

where $e(g)_j$ is the effective dose conversion factor for ingestion of nuclide j (Sv/Bq) (ICRP PUB 72)[57], A_j is the activity concentration of nuclide j (Bq/kg) and U_j is the consumption rate of food (kg/yr). According to the International Commission on Radiological Protection (ICRP), the recommended dose limit for the public from all artificial and natural sources, excluding medical and occupational exposure, is **1 mSv/year**. This threshold serves as a reference for evaluating the radiological safety of dietary intake.

B. Internal Hazard Index (Hin):

The internal exposure to radon and its short-lived daughters (H_{in}) was quantified using the activity concentration of ^{40}K, ^{238}U, and ^{232}Th using the following equation(2.34) [26]:

$$H_{in} = \frac{C_U}{185} + \frac{C_{Th}}{259} + \frac{C_K}{4810} \tag{2.34}$$

Where C_U, C_{Th} and C_K are the activity concentrations of ^{238}U, ^{232}Th and ^{40}K in $Bq.kg^{-1}$. According to the United States Environmental Protection Agency (USEPA),[58], the internal hazard index should be <1 Bq/kg to ensure the material or food item does not pose significant internal exposure risks to human health.

C. Excess Lifetime Cancer Risk (ELCR) :

Excess Lifetime Cancer Risk (ELCR) follows the linear no-threshold model recommended by the International Commission on Radiological Protection (ICRP) [59, 60], which assumes that even the smallest dose has some risk. A fatal cancer risk factor (RF) of 0.05 Sv^{-1} is used reported by International Atomic Energy Agency (IAEA), indicating a 5% increased cancer risk per sievert received throughout his entire life [ICRP Pub 103]. The AED (Sv/yr) in food is estimated to determine the cancer risk of an adult using equation(2.35) [59, 61]:

$$(ELCR) = AED \times LE \times RF \tag{2.35}$$

where AED is the annual committed effective dose (Sv/year), LE is the life expectancy (assumed to be 76 years in Algeria) by (WHO), and RF is the risk factor. According to the United States Environmental Protection Agency (USEPA), the acceptable ELCR range for radiation exposure from environmental sources is typically between 10^{-6} and 10^{-4} [58]. Values above this range may indicate a potential radiological health concern, depending on exposure duration and population vulnerability.

Chapter 3

Material and Methods

3.1 Introduction

This chapter presents the materials and analytical methods used to evaluate contamination in food samples sourced from the Algerian market. It begins with the description and selection criteria of the seven commercial and non-commercial food samples analyzed in this study. The chapter then details the sample preparation procedures adapted for EDXRF and gamma spectrometry, along with the operating conditions, calibration steps, and data processing techniques applied to ensure accurate and reliable results.

3.2 Description and Selection of Food Samples

A total of seven food product samples were selected for analysis to assess their elemental composition. These included:

3.2.1 Commercial Food Samples

The selected commercial samples, all sourced from the Algerian market (Algiers), include widely consumed products such as green tea and bread [62], as well as powdered items like baby formula and broth cubes. The latter were selected for their homogeneous form, which facilitates easier sample preparation. This selection balances dietary relevance with practical considerations for analysis. The following table presents their brand name, few relevant ingredients which were obtained directly from the product packaging, and potential contaminants.

Table 3.1: Commercial Food Samples and Potential Contaminants.

Sample	Brand Name	Ingredients	Possible Contaminants
Baby Formula	Célia - Confort Digestif 1	Skimmed milk, vegetable fats, maltodextrin, vitamins, 12 minerals, additives	Heavy metals: Fe, Zn, Cu contaminants in additives and packaging migration. NORMs: ^{238}U, ^{226}Ra, ^{210}Pb, ^{210}Po, ^{40}K via added minerals and dairy feed.
Broth Cube	Jumbo - bouillon de poulet	Salt, MSG, flavor enhancers, palm fat, spices, preservatives, coloring	Pb, Cd: from salt/spices, artificial additives (E621, E635), processing residues. NORMs via natural salts and dehydrated vegetables.
Bread	Rayane - Pain de Mie Complet	Wheat flour, sugar, salt, yeast, dough improver, preservative	Al from baking, heavy metals in flour. NORMs via wheat and salt content.
Green Tea	E'raki - Thé vert de chine	Natural green tea	Pb, As, Cd common in tea leaves from soil uptake. NORMs via soil uptake as well.

3.2.2 Non-commercial Samples

These include field-harvested samples such as dates a widely consumed and exported Algerian food and wheat, one of the most consumed products in Algeria [62]. Fish feed was also analysed to assess potential contamination in aquaculture-based seafood. The following table presents a summary of each sample's description, origin, and possible contaminants based on their source and composition.

Table 3.2: Non-Commercial Food Samples and Potential Contaminants.

Sample	Description	Origin	Possible Contaminants
Dates	High in sugars, potassium; contains Mg, Ca, Zn, Fe, Cu, Mn, Se [63].	Tolga, Biskra.	Pb, Cd from soil and irrigation water. NORMs: ^{238}U, ^{226}Ra, ^{210}Pb, ^{210}Po, ^{40}K via root uptake from soil and water.
Fish Feed	Nutrient-rich shrimp and floating feed (macro/micro minerals).	Algerian Market.	Hg, Pb, Zn from marine ingredients and additives. NORMs via mineral supplements and fishmeal.
Wheat	Whole grain, rich in carbs, proteins, minerals like Fe, Zn, Mg [63].	Setif.	Cd, As, Zn from phosphate fertilizers and soil. NORMs via soil, fertilizers, and irrigation water.

3.3 Sample Preparation

Due to the organic and often heterogeneous nature of food samples, careful sample preparation is essential to ensure homogeneity and reliable results.

3.3.1 Drying

Moisture was first removed to avoid x-ray scattering, matrix absorption, and inconsistent elemental detection. All samples were dried in a controlled oven at 60 °C for 24 to 48 hours, or until a constant weight was achieved. The low drying temperature was selected to avoid decomposition of organic material and prevent elemental loss, especially of volatile or light elements.

3.3.2 Grinding and Homogenization

Dried samples were ground into fine powder. A non-contaminating mill (Teflon or agate) was used to eliminate the risk of metal contamination from stainless steel or iron-based grinders. Further manual grinding was performed to ensure uniformity and homogeneity across the sample batch.

Figure 3.1: The preparation process for Dates and Wheat samples.

3.4 ED-XRF Analysis

3.4.1 Sampling

EDXRF is highly surface-sensitive and affected by matrix effects such as moisture, particle size, and surface flatness. From each ground and homogenized sample 2 grams with a particle size between $125\mu m$ and $250\mu m$ were weighed and placed into individual EDXRF sample cups which were approximately 31 mm in diameter and 17 mm in height, double open-ended, covered with a thin Mylar film featuring a pin-hole for pressure equalization, and sealed with plastic wrap to prevent contamination.

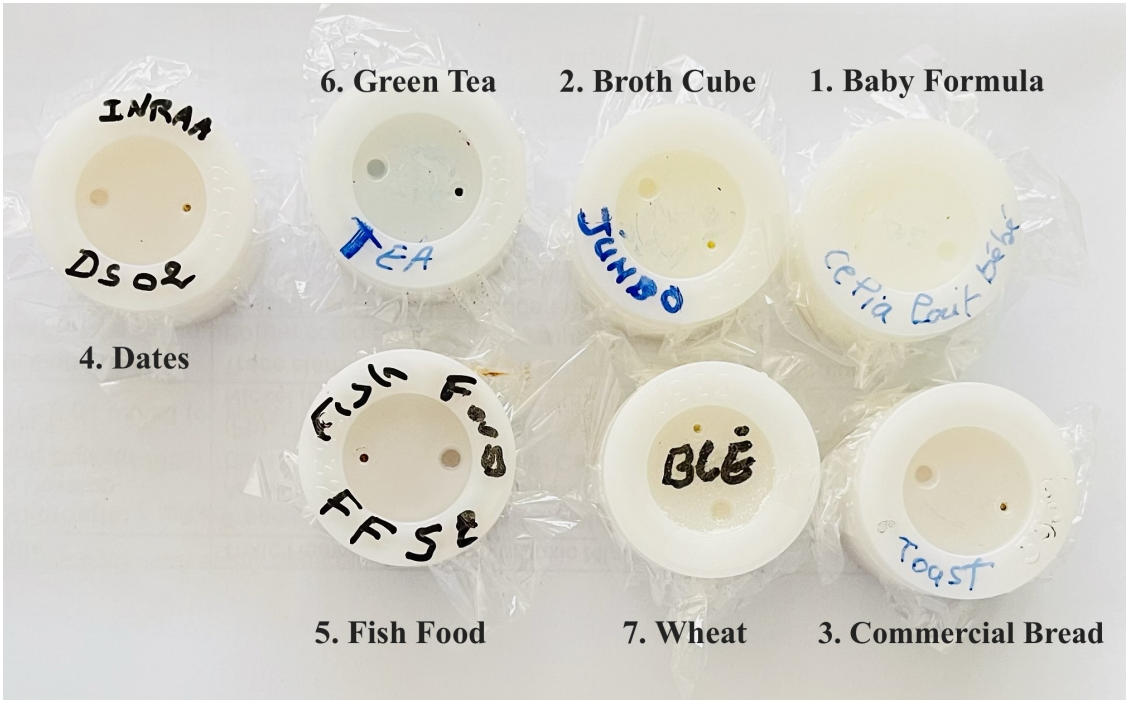

Figure 3.2: Prepared EDXRF Sample Cups for Analysis

3.4.2 Measurement and Operating Conditions

The elemental analysis of toxic heavy metals in food samples was performed using the Thermo Scientific ARL QUANT'X Energy Dispersive X-ray Fluorescence Spectrometer, a system well suited for multi-elemental screening in complex organic matrices. The instrument is equipped with a rhodium (Rh) anode X-ray tube and a 0.05 mm beryllium window, delivering up to 50 W of excitation power, which allows effective stimulation of both light and heavy elements. Detection is carried out by a Silicon Drift Detector with a 30 mm^2 active area, offering the energy resolution and sensitivity necessary to resolve closely spaced peaks. The system also features an automated 10-position sample changer, which ensures consistent, reproducible analysis and increases throughput when handling multiple food samples. These specifications make the ARL QUANT'X particularly suitable for trace-level detection of heavy metals in heterogeneous food matrices [64].

Each sample was analyzed using multiple excitation conditions, combining different filters and voltages tailored to detect low, medium, and high atomic number elements (see Table 3.3). Parameters such as current, atmosphere, and expected element groups are also listed to illustrate the analytical setup. These conditions were applied sequentially, resulting in a total measurement time of approximately 1–2 minutes per sample.

Table 3.3: Excitation Conditions for EDXRF Analysis.

Condition	Used filter	Voltage (kV)	Auto current	Atmos-phere	Count rate	Elements
High Zb	Cu Thick	50	1.00	Air	Medium	Cd, Ba.
Low Za	No filter	4	2.00	Air	Medium	Mg, Al, Si, P, S.
Mid Za	Pd Thin	16	2.00	Air	Medium	Ti, V, Cr, Mn, Fe, Ni, La, Nd, Ce, Ba.
Mid Zc	Pd Thick	30	1.66	Air	Medium	Ni, Cu, Zn, As, Rb, Sr, Y, Zr, Pb, Th, Ga, Br, Mo, Nb.
Low Zb	C Thick	8	2.00	Air	Medium	K, Ca, Sc.

Figure 3.3: EDXRF Experimental Set Up.

3.4.3 Data Processing and Quantitative Analysis

Energy Calibration

Before measurements, the energy scale of the EDXRF system was calibrated using a copper (Cu) standard. This step establishes the relationship between channel number and photon energy, ensuring accurate identification of spectral peaks.

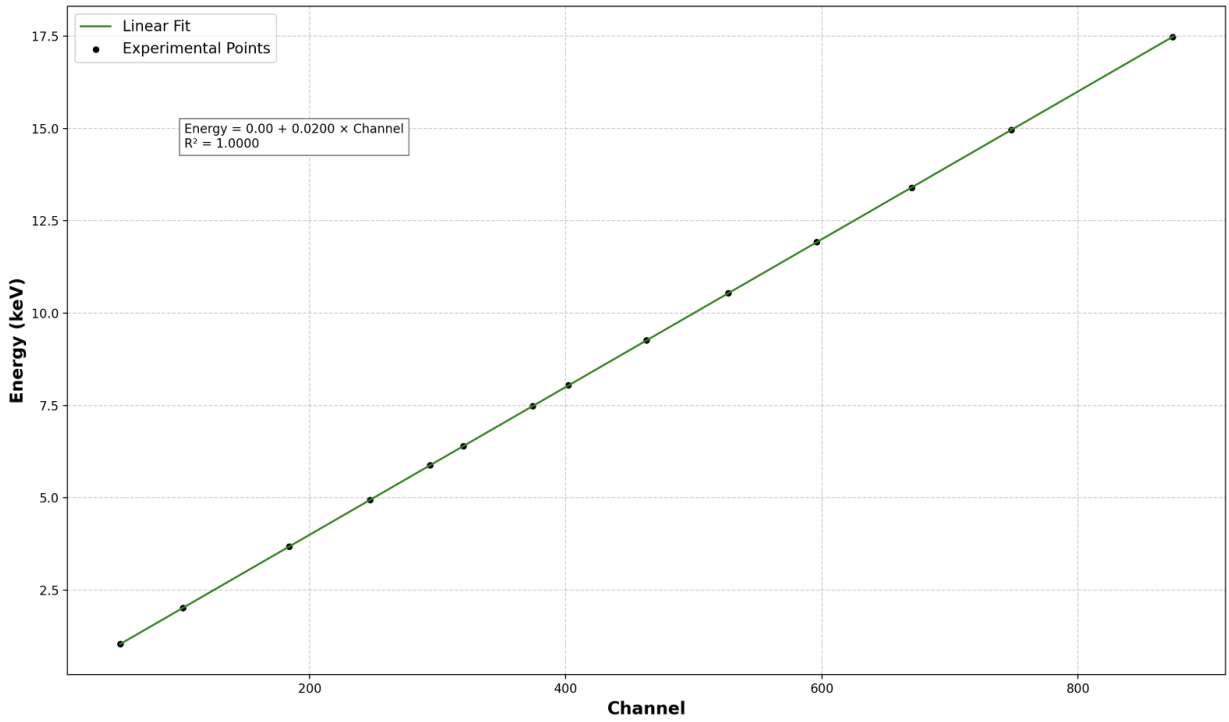

Figure 3.4: The Energy Calibration Curve for ED-XRF

Standard-Based Calibration

Certified Reference Materials (CRMs) were used to calibrate the system for plant- and soil-based food matrices. These standards contain known concentrations of elements, allowing reliable quantification of the elements present in the samples.

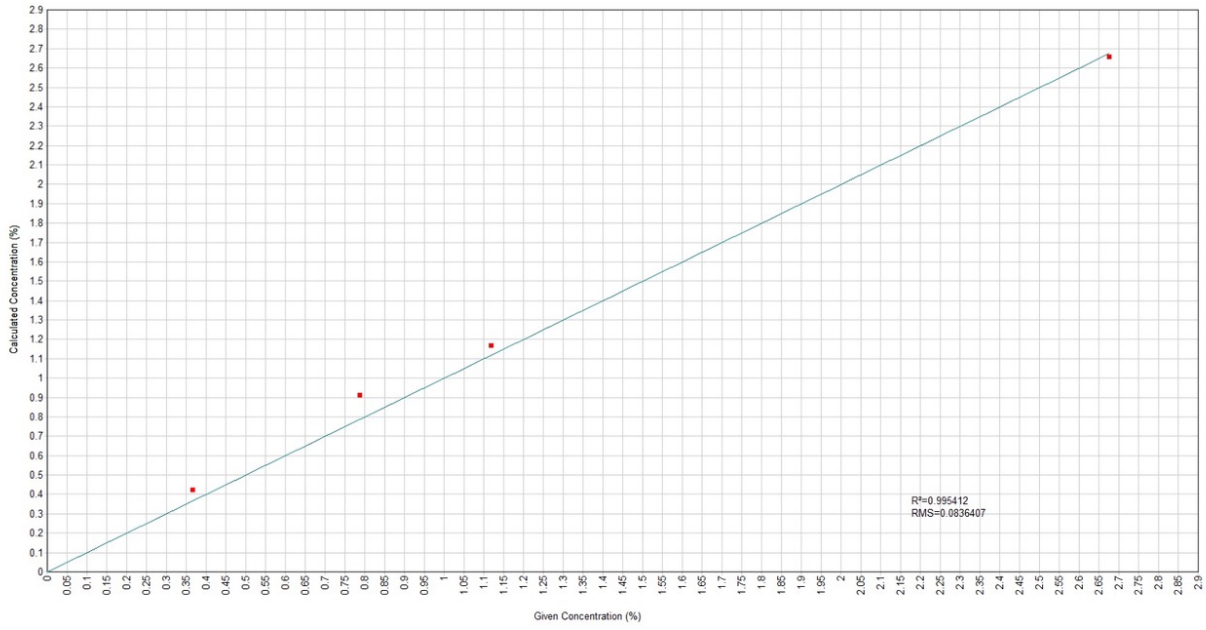

Figure 3.5: Calibration Curve for Potassium (K) Using Certified Reference Materials

Spectrum Analysis

The spectra obtained from the EDXRF measurements were processed using two main software tools:

A. Axil : performs peak fitting and deconvolution using iterative least-squares methods to accurately determine the intensities of overlapping spectral lines. This is particularly important in this study, where several toxic heavy metals such as As, Cd, and Pb produce closely spaced peaks e.g. As Kα (10.543 keV) vs Pb Lα (10.551 keV) [65].

B. WinTrace : processes net peak areas obtained via AXIL, applies calibration curves based on CRMs, and corrects for matrix effects using empirical models to account for inter-element absorption and enhancement. This procedure follows the quantitative approach outlined in Equation 2.8 from Chapter Two, converting spectral data into accurate concentration values [64].

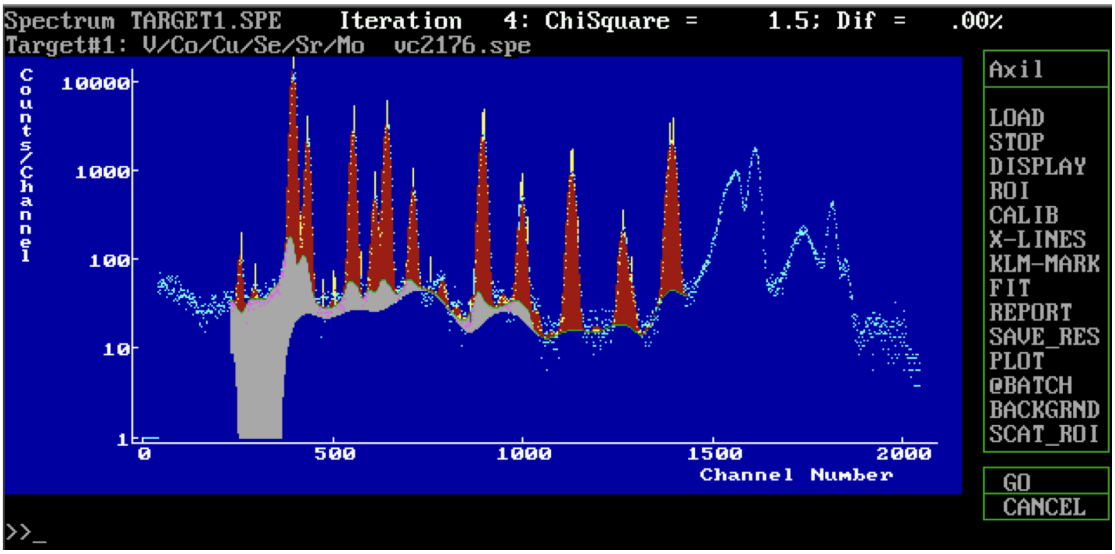

Figure 3.6: Example of spectrum deconvolution using AXIL software.

3.4.4 EDXRF Results

Table 3.4 presents the concentrations of the elements detected by Energy Dispersive X-Ray Fluorescence across the seven analyzed food samples. All values are expressed in parts per million (ppm). Values < LOD are below the detection limit.

Table 3.4: Metal Concentrations Across the Seven Food Samples

Element	Baby Formula	Bread	Broth Cubes	Dates	Fish Feed	Green Tea	Wheat
Al	277	410	218	174.86	288	23	251
As	< LOD	0.033	0.033	< LOD	0.364	0.038	< LOD
Ba	< LOD	154	< LOD	< LOD	< LOD	< LOD	< LOD
Ca	6473.2	1750	1230	804	16621	5797.5	981
Cd	0.029	0.093	< LOD	0.024	0.034	< LOD	0.032
Cl	3465	9767	28200	2400	2672	872.4	980.7
Co	0.069	0.019	0.031	0.15	0.39	0.160	0.049
Cr	0.32	0.7	< LOD	11.8	8.3	1.153	13.6
Cu	5.48	2.12	1.21	4.39	6.44	12.00	8.23
Fe	89.44	17.7	7.20	122.75	751.3	179.4	160.31
Hg	0.021	0.062	0.029	0.117	0.160	0.042	0.016
K	6505.4	2900	1124	11217	5316.6	16482	4508.8
Mg	2700	560	800	400	3100	550	1600
Mn	1.07	8.67	2.08	5.76	20.44	808.84	29.31
Mo	< LOD	0.212	< LOD	0.45	< LOD	< LOD	< LOD
Na	5049.44	185	12.11	30.72	46.44	< LOD	108.202
Ni	0.56	0.47	0.308	1.02	1.70	2.81	0.99
P	2163.4	101.5	820	224.8	5869	1427.5	1835.9
Pb	< LOD	0.22	< LOD	0.40	3.986	0.48	0.39
Rb	2.45	2.67	1.20	5.79	4.28	68.05	3.74
S	2433.2	2309.2	1700	1200	4189.2	2600	1500
Sb	0.480	< LOD	0.443	< LOD	0.35	0.134	< LOD
Se	0.030	< LOD	0.032	0.123	0.51	0.041	< LOD
Sc	< LOD	0.008	< LOD	< LOD	< LOD	< LOD	0.0125
Sr	1.84	2.19	5.41	3.04	75.44	34.24	4.39
V	0.23	< LOD	0.215	0.34	0.58	0.13	0.26
Zn	68.11	14.01	4.28	7.13	61.91	28.58	41.27

3.5 Gamma Spectrometry Analysis

Gamma spectrometry is used to identify and quantify radioactive elements within a food matrix. The measurement of radioactivity is performed either by analyzing directly the specific radionuclides or indirectly through their decay products, such as ^{226}Ra and ^{232}Th are assessed by detecting their respective decay products : lead-214 and bismuth-214 for radium-226, and actinium-228 and lead-212 for thorium-232.

3.5.1 Sampling

Unlike EDXRF, gamma spectrometry requires larger sample quantities with identical volumes for accurate comparison. Each food sample was ground, homogenized, and sieved to achieve a particle size of less than $250\mu m$. From these, between 70 and 110 grams of the powdered sample were weighed to ensure that all samples occupied the same volume in the counting containers. In contrast to EDXRF, where samples can be analyzed directly, gamma spectrometry requires the establishment of secular equilibrium between the parent radionuclides and their decay products. Therefore, all seven samples were sealed and placed in containers to allow secular equilibrium to be established between radon-222 and radium-226, as this equilibrium is practically reached after approximately seven half-lives of radon ($T_{1/2}$ of Rn = 3.8 days). This was done prior to measurement using the HPGe (High-Purity Germanium) detector system.

Figure 3.7: Prepared Samples for gamma spectrometry Analysis.

3.5.2 Characteristics of the Gamma Spectrometry Chain

The gamma spectrometry detector employed in our study is a high-purity p-type coaxial germanium detector (HPGe), model GX-3519. To minimize background interference, the detector is enclosed in a shielding chamber consisting of a 114 mm thick lead layer and a 1.5 mm copper lining. This setup offers a relative efficiency of 35% at an energy of 1.33 MeV when compared to a standard NaI(Tl) detector and provides an energy resolution of 1.85

keV (FWHM) at 1332.5 keV.
Data acquisition and system control are managed using Genie 2000 software by Canberra Industries. This software facilitates spectrum acquisition and storage, isotope identification, and calibration of both energy and efficiency parameters for the detection system.

Before any measurements are conducted, the spectrometric system must be carefully calibrated for both energy and efficiency to ensure accurate and reliable results, which will guarantee that the recorded data accurately represent the characteristics of the analyzed samples.

Figure 3.8: Gamma spectrometry Experimental Set up.

3.5.3 Energy Calibration

Energy calibration involves establishing a relationship between the channel number and the energy deposited in the crystal. It is essential to conduct a qualitative analysis to identify the radioelements present in the samples. It requires the experimental determination of a function, typically a first-degree polynomial, that describes the energy dependence of the channel count in the spectrum, with the following equation:

$$E = aC + b \tag{3.1}$$

With E energy corresponding to channel (keV), a coefficient to be determined and C channel number.

An europium ^{152}Eu source was employed to carry out the calibration. The obtained results are summarized in (Table 3.5), which served as the basis for plotting the calibration curve (Figure 3.9) and deriving the corresponding equation. The curves and equations were generated using Origin software, which allows for precise curve fitting and optimization.

Table 3.5: Energy calibration of the gamma spectrometry chain.

Radioelement	Energy (keV)	Channel
	121.4	331
	243.9	659
	344.7	931
	409.9	1107
^{152}Eu	442.5	1195
	777.4	2099
	964.1	2603
	1085.6	2931
	1112.3	3003
	1408.6	3803

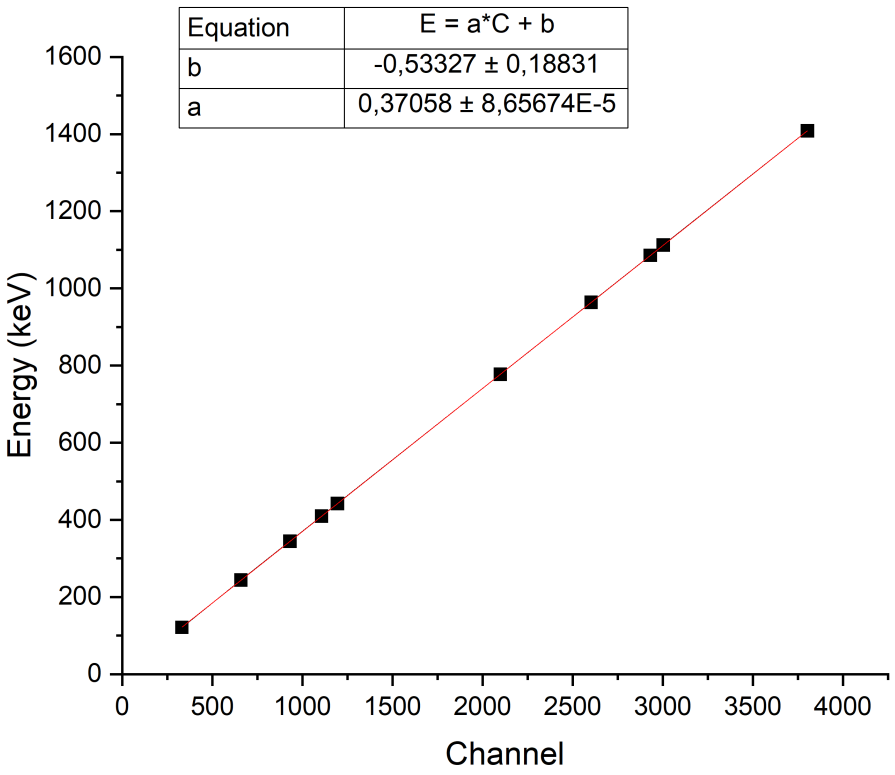

Figure 3.9: Energy calibration curve using a point source of ^{152}Eu.

As illustrated in Figure 3.9, the linear energy calibration equation obtained for the detector is:

$$E = 0,37058 \times C - 0,53327 \tag{3.2}$$

3.5.4 Efficiency Calibration

A careful efficiency calibration of the detector is a must to ensure precise and accurate measurements with minimal activity errors. It establishes a relationship between the counting rate and the actual activity of the source. Efficiency calibration necessitates the use of standard radioactive sources, unlike energy calibration, the reference source used in this case must closely match the nature and shape (sharing the same volume and density) of the sample being analyzed. The absolute efficiency of the Ge (HP) detector is influenced by its relative efficiency, which depends on the geometry and materials of the matrix. The absolute efficiency of the detector is given by :

$$\epsilon = \frac{N_x}{A.m.\gamma.t_m} \tag{3.3}$$

Where :

ϵ :Absolute efficiency.

N_x :Intensity or area of the photoelectric peak.

A: Activity of the source at the time of measurement (Bq).

m: Mass of the sample in kilograms.

γ : ranching ratio.

t_m :Measurement time (seconds).

The efficiency calculation for unknown elements in plant samples is carried out using the calibration curve that relates gamma energy ($E\gamma$) to efficiency $\epsilon(E\gamma)$:

$$\epsilon = A_1 \times exp(\frac{-E}{t_1}) + A_2 \times exp(\frac{-E}{t_2}) + y_0 \tag{3.4}$$

Where y_0, t_1, and t_2 are constants to be determined.

The error on the efficiency is given by the relation:

$$\delta\epsilon = \epsilon\sqrt{(\frac{\delta A}{A})^2 + (\frac{\delta N_x}{N_x})^2 + (\frac{\delta t_m}{t_m})^2 + (\frac{\delta\gamma}{\gamma})^2 + (\frac{\delta m}{m})^2} \tag{3.5}$$

3.5.4.1 Preparation of the Mixed Source

Experimental approach utilizes standardized sources (calibration sources or Mixed source) with composition, density, and geometry that are as close as possible to the measured samples. The direct measurement of different calibration sources containing γ-ray emitters within the energy range of interest, and their subsequent fitting to a parametric function, yields the best results [66].

Experimental efficiency was determined using a standard gamma mixed solution type ERX certified by Czech Metrology Institute. The mixed solution is made of ^{241}Am, ^{109}Cd, ^{139}Ce, ^{57}Co, ^{60}Co, ^{137}Cs, ^{51}Cr, ^{113}Sn, ^{85}Sr and ^{88}Y , covering the energy range of 59.54–1836.12 keV. About 21 ml of the standard solution distributed in three layers equally were injected directly in a spiral shape into a soil matrix with a density of 1.15 $g.cm^{-3}$ and then put into the sample container [38].

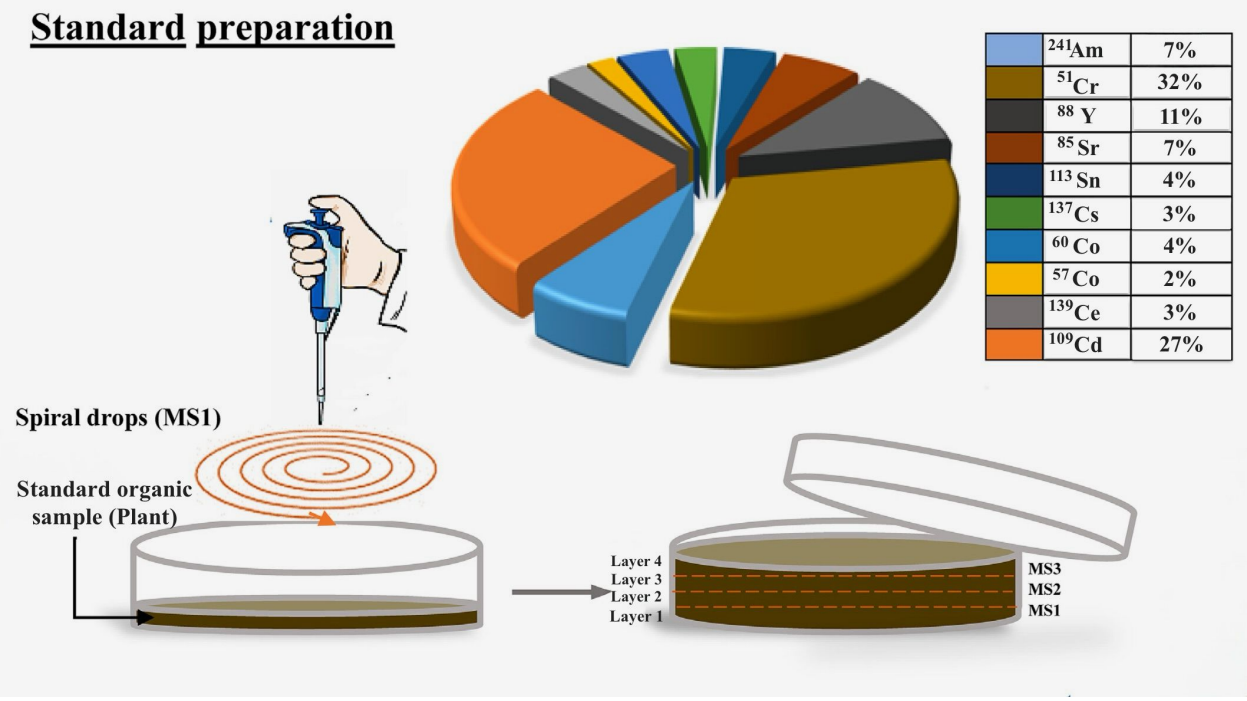

Figure 3.10: Diagram illustrating the preparation of the mixed source.

3.5.4.2 Mixed Source in a Plant Matrix

Measurements conducted using the prepared mixed source with gamma spectrometry are summarized in Table 3.6. From these data, a calibration curve is plotted (Figure 3.11), and the associated calibration equation is derived.

Table 3.6: Energy calibration of the gamma spectrometry chain.

Radioelement	**Energy (keV)**	$I\gamma(\%)$	ϵ	$\delta\epsilon$
Am-241	59.54	35.9	0,07596	0,00402
Cd-109	88.03	3.644	0,07899	0,00418
Co-57	122,06	85.6	0,07191	0,00381
Co-57	136,47	10.68	0,07003	0,00374
Ce-139	165,85	79.9	0,05627	0,00298
Cr-51	320,08	9.191	0,03751	0,00206
Sn-113	391,69	64.97	0,03091	0,00164
Sr-85	514	96	0,02448	0,0013
Cs-137	661,65	85.1	0,01993	0,00106
Y-88	898,04	93.7	0,01443	7,64286E-4
Co-60	1173,23	99.85	0,01186	6,28257E-4
Co-60	1332,49	99.983	0,01062	5,62399E-4
Y-88	1836,06	99.2	0,00802	4,24812E-4

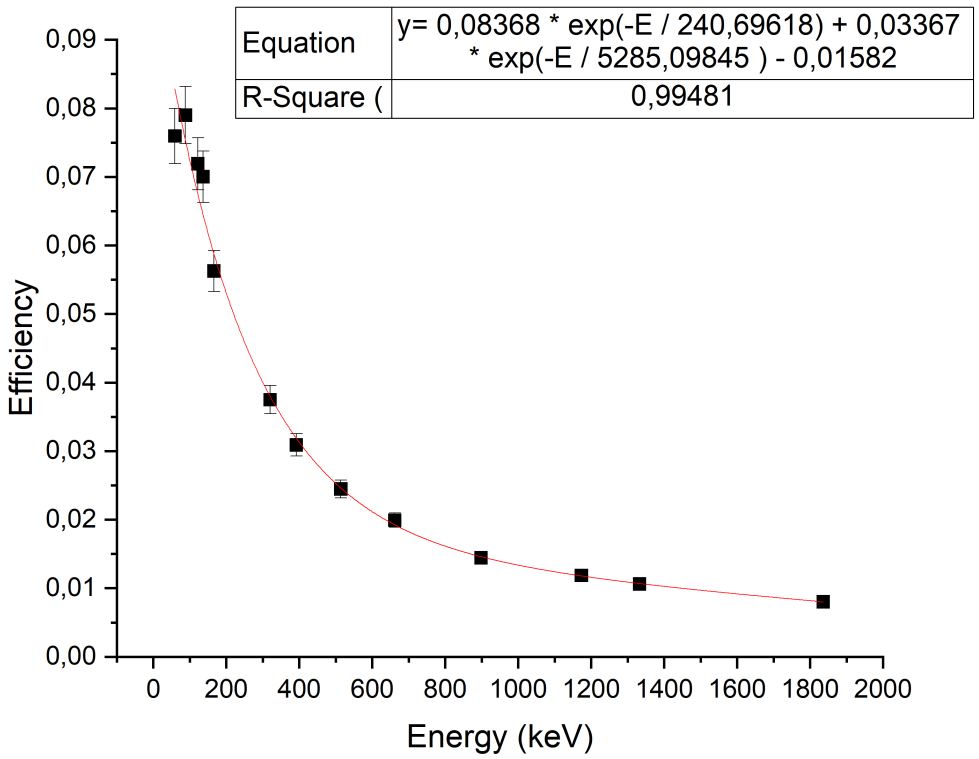

Figure 3.11: Efficiency calibration curve of the detector using a mixed plant-based source.

As illustrated in Figure 3.11, the characteristic equation describing the fitted relationship between efficiency and energy for a plant-based sample is:

$$\epsilon = 0,08368 \times exp(\frac{-E}{240,69618}) + 0,03367 \times exp(\frac{-E}{5285,09845}) - 0,01582 \tag{3.6}$$

3.5.5 Analysis of Food Samples

Qualitative Analysis :

Food samples analyzed typically contain various radioelements. Based on the recorded data from the multi-gamma spectrum it is possible to identify different radioelements according to their characteristic energies (qualitative analysis) and subsequently determine their activity levels (quantitative analysis).

Quantitative Analysis :

Specific activity is defined as the activity per unit mass of the sample and can be measured using the following relation:

$$A_s = \frac{N_x}{\epsilon.m.\gamma.t_m} \tag{3.7}$$

Where :

A_s :Specific activity of the radioelement (Bq).
N_x :Intensity or area of the photoelectric peak.
ϵ:Detector efficiency for a cylindrical geometry.
m: Mass of the sample in kilograms.
γ : Banching ratio.
t_m :Measurement time (seconds).

3.5.6 Gamma Spectrometry Results

Table 3.7 presents the concentrations of the elements detected by Gamma spectrometry across the seven analyzed food samples. All values are expressed by ($Bq.kg^{-1}$), accompanied by the corresponding standard deviations.

Table 3.7: Gamma spectrometry results

Product Category	**Food**	**Activity** ($Bq.kg^{-1}$)				
		^{235}U	^{232}Th	^{226}Ra	^{137}Cs	^{40}K
Fruit	**Dates**	<LOD	<LOD	<LOD	<LOD	297.88 ± 14.894
Cereal Grain	**Wheat**	1.4±0.05	<LOD	0.29 ± 0.014	<LOD	116.37 ± 5.818
	Bread	<LOD	1.21 ± 0.06	<LOD	<LOD	69.2 ± 3.46
Beverages	**Green tea**	<LOD	4.11 ± 0.2	1.915 ± 0.095	<LOD	508.15 ± 25.407
Flavour Enhancers	**Broth cubes**	1.04 ± 0.052	1.15 ± 0.057	0.61 ± 0.03	<LOD	60.69 ± 3.034
Milk	**Baby formula**	<LOD	0.47 ± 0.023	0.41 ± 0.02	<LOD	161.88 ± 8.091
Fish	**Fish feed**	<LOD	<LOD	0.04 ± 0.002	<LOD	181.52 ± 9.076

<LOD : Below Limit of Detection

Chapter 4

Results and Discussion

4.1 Interpretation of EDXRF Results

This section presents the interpretation of toxic metal concentrations detected in food samples using the EDXRF technique. While the analysis provides valuable insight into specific food items, it does not represent a full Total Diet Study (TDS), nor does it estimate total dietary exposure. Allocation or location factors, which account for how much a food contributes to overall intake were not applied.

Ingestion rates (IR, kg/day) used in exposure calculations were taken from literature and reflect commondietary patterns in Algeria. An average body weight of 70.2 kg was used for adults [67] and 6.7 kg for infants under six months [68].

For fish feed, which is not directly consumed by humans, metal concentrations were approximated to those found in fish. However, this does not fully account for bioaccumulation, which remains an important consideration for future evaluations.

4.1.1 Toxic Heavy Metals

4.1.1.1 Measured Concentrations and Regulatory Comparison

The concentrations of As, Cd, Hg, and Pb were compared to two reference sets: (1) Codex standards (JECFA via WHO/FAO) and (2) includes regulatory limits and health-based guidelines published by the European Union (EU), the European Food Safety Authority (EFSA), as well as the Chinese National Food Safety Standard (GB 2762-2022). Tables 4.2 and 4.3 show measured values, reference limits, and compliance status. Exceedances are expressed as multipliers (e.g., $\times$ 17 Codex).

Table 4.1: Regulatory Comparison for Commercial Food Samples

Toxic Heavy Metals Concentrations (mg/kg)						
Commercial Samples		Measured	Reference 1	Reference 2	Compliance Status	Exceedance Ratio
Baby Formula	As	< LOD	ALARA	0.02 [90]	Within limits	-
	Cd	0.029	ALARA	0.01 [90]	**Exceeded**	**×2.9 EU**
	Hg	0.021	0.004 [10](1)	-	Within limits(1)	-
	Pb	< LOD	0.01 [10]	0.02 [90]	Within limits	-
Broth Cubes	As	0.033	-	0.1 [91]	Within limits	-
	Cd	< LOD	-	0.1 [91]	Within limits	-
	Hg	0.029	0.004 [10](1)	-	Within limits(1)	-
	Pb	< LOD	GMP	1.5 [91]	Within limits	-
Bread	As	0.033	-	0.5 [91]	Within limits	-
	Cd	0.093	0.2 [10]	0.15 [90]	Within limits	-
	Hg	0.062	-	0.02 [91]	**Exceeded**	**×3.1 GB**
	Pb	0.222	0.20 [10]	0.20 [90]	**Exceeds limits**	**×1.1 Both limits**
Green Tea	As	0.038	-	2.0 [92]	Within limits	–
	Cd	< LOD	-	1.00 [92]	Within limits	–
	Hg	0.042	-	0.3 [92]	Within limits	–
	Pb	0.481	GMP	5.0 [91]	Within limits	–

Table 4.2: Regulatory Comparison for Non-Commercial Food Samples

Toxic Heavy Metals Concentrations (mg/kg)						
Non-Commercial Samples		Measured	Reference 1	Reference 2	Compliance Status	Exceedance Ratio
Dates	As	< LOD	0.015 [10][(1)(2)]	-	Within limits[(1)]	-
	Cd	0.024	-	0.05 [90]	Within limits	-
	Hg	0.117	0.004 [10][(1)]	-	Within limits[(1)]	–
	Pb	0.393	0.10 [10]	0.10 [90]	**Exceeds both limits**	**×3.9 Both limits**
Fish Feed	As	0.364	-	10 [93]	Within limits	-
	Cd	0.034	-	0.5 [93]	Within limits	-
	Hg	0.160	-	0.2 [93]	Within limits	-
	Pb	3.986	-	5 [93]	Within limits	-
Wheat	As	< LOD	-	0.02 [91]	Within limits	-
	Cd	0.032	0.20 [10]	0.15 [90]	Within limits	-
	Hg	0.016	-	0.02 [91]	Within limits	-
	Pb	0.393	0.20 [10]	0.20 [90]	**Exceeds both limits**	**×1.9 Both limits**

Notes: [(1)]In the absence of established regulatory maximum levels, exposure was assessed by comparing the EWI to the PTWI.

[(2)]This PTWI has been withdrawn and is no longer in effect due to updated risk assessments

ALARA, As Low As Reasonably Achievable. This principle applies particularly to infant foods, where manufacturers are expected to minimize contaminant levels as much as possible due to the heightened vulnerability of the target population [111].

GMP, Good Manufacturing Practice. Indicates that no numerical maximum limit is currently defined; in many cases, previously established limits were withdrawn [112].

4.1.1.2 Estimated Weekly Intake and Compliance

IR values were used in formula 2.11 to calculate EDI and EWI. Tables 4.3 and 4.4 present these estimates alongside PTWI for compliance assessment. EWI reflects intake from the analyzed samples only, while PTWI covers total weekly exposure.

Table 4.3: Estimated Weekly Intake of Toxic Heavy Metals (Commercial)

		IR (kg/day)	EWI (mg/kg/week)	PTWI (mg/kg/week)	Compliance Status
Commercial Samples					
Baby Formula	As	0.117 [97]	0.000	0.0004 [96](1)	Within the limit
	Cd		0.004	0.006 [10]	Within the limit
	Hg		0.003	0.004 [10]	Within the limit
	Pb		0.000	0.025 [10](2)	Within the limit
Broth Cubes	As	0.0024 [98]	0.000	0.0004 [96](1)	Within the limit
	Cd		0.000	0.006 [10]	Within the limit
	Hg		0.000007	0.004 [10]	Within the limit
	Pb		0.000	0.025 [10](2)	Within the limit
Bread	**As**	0.3013 [99]	0.001	0.0004 [96](1)	**Exceeds the limit by 2.5**
	Cd		0.003	0.006 [10]	Within the limit
	Hg		0.002	0.004 [10]	Within the limit
	Pb		0.007	0.025 [10](2)	Within the limit
Green Tea	As	0.0008 [100]	0.000003	0.0004 [96](1)	Within the limit
	Cd		0.000	0.006 [10]	Within the limit
	Hg		0.000003	0.004 [10]	Within the limit
	Pb		0.00004	0.025 [10](2)	Within the limit

Table 4.4: Estimated Weekly Intake of Toxic Heavy Metals (Agricultural)

		IR (kg/day)	EWI (mg/kg/week)	PTWI (mg/kg/week)	Compliance Status
Commercial Samples					
Dates	As	0.063 [101]	0.000	0.0004 [96](1)	Within the limit
	Cd		0.0001	0.006 [10]	Within the limit
	Hg		0.001	0.004 [10]	Within the limit
	Pb		0.002	0.025 [10](2)	Within the limit
Fish	As	0.011 [102]	0.0004	0.0004 [96](1)	Within the limit
	Cd		0.00004	0.006 [10]	Within the limit
	Hg		0.0002	0.004 [10]	Within the limit
	Pb		0.004	0.025 [10](2)	Within the limit
Wheat	As	0.6 [103]	0.000	0.0004 [96](1)	Within the limit
	Cd		0.002	0.006 [10]	Within the limit
	Hg		0.001	0.004 [10]	Within the limit
	Pb		0.024	0.025 [10](2)	Within the limit

Notes: (1)This value was estimated based on the reference dose (mg/kg/day) provided in a recent EPA study (January 2025), as the PTWI previously established by WHO was withdrawn following new epidemiological evidence (JECFA, 2010).

(2)This PTWI value has been withdrawn due to updated toxicological assessments and emerging scientific evidence. Currently, no official PTWI has been established (EFSA, 2010; WHO, 2011).

4.1.1.3 Risk Indices: Hazard and Pollution Metrics

Table 4.5 summarizes the calculated hazard quotient (HQ), hazard index (HI), contamination factor (CF), metal pollution index (MPI), and pollution load index (PLI), based on the formulas and reference values detailed in Chapter 2. EDI and RfD are included for HQ and HI calculations. These metrics offer complementary perspectives: HQ and HI assess potential health risks, while CF, MPI, and PLI characterize the level and extent of environmental contamination across samples.

Table 4.5: HQ and HI Values Based on EDI and RfD

		EDI (mg/kg/day)	RfD (mg/kg/day)	HQ	HI
Food Samples					
Baby Formula	As	0.000	0.00006 [96]	0.000	**1.149**
	Cd	0.0005	0.001 [106]	0.506	
	Hg	0.0003	0.00057 [10]	0.643	
	Pb	0.000	0.0036[(1)]	0.000	
Broth Cubes	As	0.000001	0.00006 [96]	0.017	0.019
	Cd	0.000	0.001 [106]	0.000	
	Hg	0.000001	0.00057 [10]	0.002	
	Pb	0.000	0.0036[(1)]	0.000	
Bread	As	0.0001	0.00006 [96]	1.600	**3.732**
	Cd	0.0004	0.001 [106]	0.400	
	Hg	0.0002	0.00057 [10]	0.467	
	Pb	0.0009	0.0036[(1)]	0.265	
Green Tea	As	0.000	0.00006 [96]	0.000	0.001
	Cd	0.000	0.001 [106]	0.000	
	Hg	0.000	0.00057 [10]	0.000	
	Pb	0.000005	0.0036[(1)]	0.001	
Dates	As	0.000	0.00006 [96]	0.000	0.304
	Cd	0.00002	0.001 [106]	0.022	
	Hg	0.0001	0.00057 [10]	0.184	
	Pb	0.0004	0.0036[(1)]	0.098	
Fish	As	0.00006	0.00006 [96]	0.950	**1.172**
	Cd	0.000005	0.001 [106]	0.005	
	Hg	0.00003	0.00057 [10]	0.0438	
	Pb	0.0006	0.0036[(1)]	0.173	
Wheat	As	0.000	0.00006 [96]	0.000	**1.447**
	Cd	0.0003	0.001 [106]	0.274	
	Hg	0.0001	0.00057 [10]	0.240	
	Pb	0.003	0.0036[(1)]	0.933	

Notes: [(1)]There is no currently established RfD for lead, as both the US EPA and JECFA have withdrawn previous values due to new toxicological evidence. However, a daily intake threshold of 0.0036 mg/kg bw/day is sometimes used in dietary risk assessments based on the former JECFA Provisional Tolerable Weekly Intake (PTWI) of 25 μg/kg bw, which has since been withdrawn (EFSA, 2010; WHO, 2011) [105].

Table 4.6: Contamination Metrics: CF, MPI, and PLI for Toxic Metals

		CF	MPI	PLI
Food Samples				
Baby Formula	As	0.000	0.024	**1.475**
	Cd	2.900		
	Hg	0.750		
	Pb	0.000		
Broth Cubes	As	0.330	0.030	0.024
	Cd	0.000		
	Hg	0.0017		
	Pb	0.000		
Bread	As	0.066	0.080	0.570
	Cd	0.465		
	Hg	3.100		
	Pb	1.110		
Green Tea	As	0.019	0.091	0.063
	Cd	0.000		
	Hg	0.140		
	Pb	0.096		
Dates	As	0.000	0.103	0.778
	Cd	0.480		
	Hg	0.250		
	Pb	3.930		
Fish Feed	As	0.036	0.298	0.199
	Cd	0.068		
	Hg	0.800		
	Pb	0.797		
Wheat	As	0.000	0.058	0.695
	Cd	0.213		
	Hg	0.800		
	Pb	1.965		

4.1.2 Other Elements

4.1.2.1 Guideline Values

Regulatory threshold values for mineral and trace elements have been established by three major bodies: the U.S. Environmental Protection Agency (EPA), the JECFA, and European agencies (EFSA/SCF). These thresholds include the Reference Dose (RfD), Adequate Intake (AI), Provisional Tolerable Weekly Intake (PTWI), Tolerable Daily Intake (TDI), and Upper Intake Level (UL) or Recommended Daily Intake (RDI). Values expressed per body weight are given in mg/kg /day or mg/kg/week; absolute intake limits are in mg/day. Where applicable, adult and infant (0–6 months old or other age ranges) values are specified separately. Inequality symbols (e.g., < or =) indicate whether the value represents an upper limit or a recommended intake.

Table 4.7: Regulatory Threshold for Essential and Non-essential Minerals

	U.S. Environmental Protection Agency (EPA)	FAO/WHO		European Agencies (EFSA, SCF)
	RfD/AI (mg/kg/day)	PTWI (mg/kg/week)	TDI (mg/kg/day)	UL/RDI/AI (mg/day)
Trace elements				
Al		2 [46]	1.0 [104]	
Cr			0.3 [73]	
Cu	< 0.04 [108]			< 5 for adults, < 1 for infants (0–6 m) [70]
Fe			0.8 [71]	= 6 for infants (0.5–1 y) [74]
K			3510 [75]	= 650 for infants (4–12 m) [77]
Mg				= 350 for adults, = 60 for infants (0–6 m) [72]
Na			2000 [75]	= 110 for infants (0–6 m) [76]
Ni	< 0.02 [107]		0.011 [69]	
P				= 550 for adults, = 400 for infants (0–12 m) [78]
Sb			0.006 [79]	
Se	< 0.005 [107]			< 0.3 for adults, < 0.06 for infants (0–6 m) [70]
Zn	< 0.3 [107]			< 25 for adults, < 7 for infants (0–6 m) [70]

4.1.2.2 Non-Essential and Potentially Toxic Elements

Table 4.8: Exposure and Risk Indices for Non-Essential Elements (Al, Cr, Ni, Sb)

		EDI (mg/kg/day)	MPI (mg/kg)	HQ	Compliance Status	HI
Food Samples						
Baby Formula	**Al**	4.837	2.209	4.837	**Exceeds limits**	**6.641**
	Cr	0.005		0.016	Within limits	
	Ni	0.009		0.488	Within limits	
	Sb	0.008		1.3	**Exceeds limits**	
Broth Cubes	Al	0.007	3.098	0.007	Within limits	0.008
	Cr	0.000		0.000	Within limits	
	Ni	1.0e-5		0.0005	Within limits	
	Sb	1.0e-5		0.001	Within limits	
Bread	**Al**	1.759	5.128	1.759	**Exceeds limits**	**1.869**
	Cr	0.003		0.01	Within limits	
	Ni	0.002		0.100	Within limits	
	Sb	0.000		0.000	Within limits	
Green Tea	Al	0.0002	1.778	0.0002	Within limits	0.001
	Cr	1.313e-05		4.3e-05	Within limits	
	Ni	3.202e-05		0.001	Within limits	
	Sb	1.527e-06		0.0002	Within limits	
Dates	Al	0.156	12.815	0.156	Within limits	0.231
	Cr	0.010		0.030	Within limits	
	Ni	0.0009		0.045	Within limits	
	Sb	0.000		0.000	Within limits	
Fish	Al	0.045	6.141	0.045	Within limits	0.070
	Cr	0.0013		0.004	Within limits	
	Ni	0.0002		0.013	Within limits	
	Sb	5.0e-5		0.008	Within limits	
Wheat	**Al**	2.145	15.006	2.145	**Exceeds limits**	**2.954**
	Cr	0.116		0.386	Within limits	
	Ni	0.0084		0.423	Within limits	
	Sb	0.000		0.000	Within limits	

4.1.2.3 Essential Trace Elements

For essential trace elements, a Nutritional Exposure Index (NEI) was estimated by dividing the EDI by the corresponding reference intake values listed in Table 4.7 This provides a simplified measure of dietary adequacy relative to recommended intake levels. Compliance status indicates whether the mineral content is due to enhanced content (such as added nutrients in baby formula) or is simply above baseline levels. The geometric means of concentrations and NEI values are also shown to provide an average estimate across the samples.

Table 4.9: Estimated Daily Intake and Nutrition Exposure from Essential Minerals

		EDI (mg/kg/day)	NEI	Compliance Status	Geometric Mean	
					Concatenation (mg/kg)	NEI
Food Samples						
Baby Formula	Cu	0.095	2.392	Enhanced content	81.37	0.308
	Fe	1.561	1.952	Enhanced content		
	K	113.601	0.032	Within limit		
	Mg	47.149	5.265	Enhanced content		
	Na	0.881	0.0004	Within limit		
	P	37.778	0.632	Within limit		
	Se	0.0005	0.104	Within limit		
	Zn	1.189	3.964	Enhanced content		
Broth Cubes	Cu	4.0e-5	0.001	Within limit	17.92	0.0001
	Fe	0.0002	0.0003	Within limit		
	K	0.038	1.0e-5	Within limit		
	Mg	0.027	0.0054	Within limit		
	Na	0.0004	2.0e-7	Within limit		
	P	0.028	0.003	Within limit		
	Se	1.0e-6	0.0002	Within limit		
	Zn	0.0001	0.0004	Within limit		
Bread	Cu	0.009	0.227	Within limit	76.99	0.037
	Fe	0.075	0.094	Within limit		
	K	12.446	0.003	Within limit		
	Mg	2.403	0.482	Within limit		
	Na	0.794	0.0003	Within limit		
	P	0.435	0.055	Within limit		
	Se	0.000	0.000	Within limit		
	Zn	0.060	0.200	Within limit		
Green Tea	Cu	0.0001	0.003	Within limit	85.22	0.0009
	Fe	0.002	0.002	Within limit		
	K	0.187	5.0e-5	Within limit		
	Mg	0.006	0.001	Within limit		
	Na	0.000	0.000	Within limit		
	P	0.016	0.002	Within limit		

	Se	4.672e-07	0.000	Within limit		
	Zn	0.0003	0.001	Within limit		
Dates	Cu	0.003	0.098	Within limit	44.23	0.011
	Fe	0.110	0.137	Within limit		
	K	10.066	0.002	Within limit		
	Mg	0.358	0.072	Within limit		
	Na	0.027	1.0e-5	Within limit		
	P	0.201	0.025	Within limit		
	Se	0.0001	0.022	Within limit		
	Zn	0.0063	0.021	Within limit		
Fish	Cu	0.0010	0.025	Within limit	169.65	0.008
	Fe	0.117	0.147	Within limit		
	K	0.833	0.0002	Within limit		
	Mg	0.485	0.097	Within limit		
	Na	0.007	4.0e-6	Within limit		
	P	0.919	0.117	Within limit		
	Se	8.0e-5	0.016	Within limit		
	Zn	0.009	0.032	Within limit		
Wheat	Cu	0.070	1.758	Above baseline	258.93	0.258
	Fe	1.370	1.712	Above baseline		
	K	38.536	0.010	Within limit		
	Mg	13.675	2.742	Above baseline		
	Na	0.924	0.0004	Within limit		
	P	15.691	2.002	Above baseline		
	Se	0.000	0.000	Within limit		
	Zn	0.352	1.175	Above baseline		

4.1.3 Element-Specific Discussion

Aluminum (Al)

Aluminum was found at 277-410 pm in baby formula and bread, ∼250-290 ppm in fish feed and wheat, and lower in other foods. These values are extremely high by dietary standards, WHO 's tolerable weekly intake for Al is 2 mg/kg body-weight/day [110]. For example, a 0-6-month Algerian infant (∼6.7 kg) drinking ∼0.12 kg formula/day at 277 mg/kg would intake ∼30 mg/kg/week > 15x the WHO's PTWI. A typical Algerian adult consuming 300g of bread would get ∼10 mg/kg-week above the PTWI, repeated high intake from multiple sources (bread, vegetables, canned goods) could accumulate. In infants, however, formula is the critical source, high Al in formula is a known issue [80] sources include additives, packaging, or soil contamination of ingredients. Chronic aluminum exposure in infants is linked to cognitive delays, motor impairment, and increased risk of neurodevelopmental disorders [81]. Al levels in the baby formula sample far exceed any safe guideline, indicating a clear exposure risk to infants.

Arsenic (As)

Inorganic arsenic was low or undetected in most samples: 0 in baby formula, dates and wheat; trace in broth cubes (0.033 mg/kg) and green tea (0.038 mg/kg); but high in fish feed (0.364 mg/kg). The latter is not directly eaten by people but could bioaccumulate in farmed fish however that exposure was not directly assessed here. Dietary arsenic is a serious carcinogen, with no safe threshold. The old WHO PTWI (15 μg/kg-week) has been withdrawn as inadequate [10]. For Bread, a weekly intake of 1 μg/kg was estimated which can cause a concern especially when paired with other potentially contaminated food items. For perspective, a cup of brewed tea (2g leaves) and one broth cube (80 g) gives 66 and 304 nanograms of As, respectively. Thus, dietary As from broth cubes or tea is negligible. In summary, aside from indirect fish concerns and bread consumption in the Algerian population, arsenic in the tested foods is low and not near any intake guideline, but any further exposure (e.g. from rice or water) adds to cumulative risk [96].

Cadmium (Cd)

Cadmium appeared at 0.029 mg/kg in infant formula, 0.093 mg/kg in bread, and ∼0.02–0.03 mg/kg in wheat, fish feed, and dates, with zero detected in tea and broth cubes. The Codex PTWI for Cd is 6 μg/kg bw [10]. The EWI for infants aged 0–6 months was 4 μg/kg bw, which is concerning, especially since WHO emphasizes applying the ALARA principle for infants [111]. The observed increase in cadmium levels from raw wheat to commercial bread (by a factor of 0.3) underscores the contribution of industrial processing to contamination. With an EWI of 3 μg/kg bw, regular high intake of bread could approach or exceed the Cd PTWI in adults, especially when combined with other sources. A typical serving of dates of 40 grams (2 to 4 dates) is only ∼0.8 μg making it negligible. In sum, baby formula and cereal staples could potentially be harmful. Infants fed this formula would exceed the EU regulatory limit by 190%, posing a possible kidney toxicity risk [90]. While moderate consumption of bread and wheat may not exceed tolerable limits in adults, high consumers, particularly in populations reliant on these staples, face increased risk of chronic cadmium accumulation, which can cause kidney and bone toxicity [109].

Mercury (Hg)

Total Hg concentrations ranged from approximately 0.117–0.160 mg/kg in dates and fish feed, 0.042–0.062 mg/kg in green tea and bread, and were lower in broth cubes, baby formula, and wheat. The Chinese National Safety Standards set a regulatory threshold of 0.02 mg/kg for cereal products, which was exceeded by the bread sample [91]. JECFA's PTWI for inorganic Hg is 4 μg/kg bw/week [10]; none of the estimated weekly intakes based on the Algerian diet exceeded this limit. Fish feed showed an EWI of 0.2 μg/kg bw/week, which remains well below the PTWI. Methylmercury, primarily derived from fish, is more toxic [109]; once more, no speciation or bioavailability corrections were applied in this assessment. Infant formula stands out: while its Hg level remains within safety margins, exposure should be carefully monitored due to infant's heightened sensitivity during early development. We conclude that mercury content in formula and any similar infant foods is a potential concern. Adult dietary exposure to Hg from these sources is generally low, except in the specific toast bread sample analyzed. Cumulative exposure (fish, etc.) should still be minimized.

Lead (Pb)

Estimated weekly intake values for Pb ranged from zero to 0.024 mg/kg bw/week across the seven sampled food items. The highest Pb concentration was observed in Fish Feed (3.986

mg/kg), contributing to a weekly intake estimate of 0.004 mg/kg bw/week. Wheat and Dates both presented Pb concentrations of around 0.4 mg/kg, resulting in respective EWI values of 0.024 and 0.002 mg/kg bw/week. Bread, with a Pb level of 0.222 mg/kg, yielded an estimated intake of 0.007 mg/kg bw/week. In contrast, Baby Formula and Broth Cubes showed undetectable levels of Pb and correspondingly no estimated intake, while Green Tea, despite a moderate Pb content (0.481 mg/kg), contributed minimally to weekly exposure (0.00004 mg/kg/week) due to lower consumption rates. Overall, the estimated weekly intakes did not exceed the provisional tolerable weekly intake (PTWI) for Pb [105]. The highest observed EWI (0.024 mg/kg bw/week), linked to Wheat consumption, approached the PTWI threshold, suggesting potential concern under high-consumption scenarios or cumulative exposure from multiple sources.

Chromium (Cr)

Total Cr ranged from ∼0.3-0.7 mg/kg in formula and bread up to 13.6 mg/kg in wheat and 11.8 mg/kg in dates. This mostly reflects trivalent Cr (CrIII), an essential nutrient, rather than toxic hexavalent Cr(VI). EFSA has set a Tolerable Daily Intake (TDI) for Cr of 0.3 mg/kg bwt/day [73]. For a 70 kg adult this is ∼21 mg/day. Even with 13.6 mg/kg in wheat, eating 200g wheat provides ∼2.7 mg Cr which is well under 21 mg. Thus, even the highest observed Cr levels are far below risk thresholds. In infants, a similar margin applies. We therefore conclude that chromium poses no immediate dietary risk in these samples. Except if environmental C(VI) contamination existed, additional risk would apply, but total Cr by XRF does not specify valence.

Nickel (Ni) and Antimony (Sb)

Nickel (Ni) and Antimony (Sb) concentrations varied across food samples. The most notable concern was observed in infant formula, where the EDI for Ni reached 0.009 mg/kg bw/day—approaching the U.S. EPA's tolerable daily intake of 0.02 mg/kg bw/day—and for Sb, it exceeded the WHO/FAO TDI of 0.006 mg/kg bw/day, reaching 0.008 mg/kg bw/day. Other food items either showed negligible levels or concentrations below the detection limit. These findings are particularly relevant for infants, who are more vulnerable to the toxic effects of heavy metals due to their developing organs and lower body weight, and because infant formula often constitutes their sole source of nutrition, making even low concentrations relatively more significant in terms of exposure. Nickel can enter infant formula through contaminated raw materials or processing equipment, often due to industrial emissions or wastewater. Antimony typically originates from mining, smelting, or leaching from Sb-containing packaging. Chronic exposure, particularly in infants, may lead to allergic reactions and kidney toxicity (Ni), or liver and gastrointestinal effects (Sb). To minimize such risks, adherence to Good Manufacturing Practices (GMP), as recommended by the WHO [83], is essential throughout food production and packaging processes.

Manganese (Mn)

Manganese levels varied greatly: modest in formula (1.07 mg/kg) and bread (8.67 mg/kg), but extremely high in green tea (808.8 mg/kg) and elevated in wheat (29.3 mg/kg) and fish feed (20.4 mg/ kg). Tea plants concentrate Mn from soil - as documented [88], foods usually <5 mg/kg but tea leaves can be >>10 mg/kg. A brewed cup of tea (2 g leaves) can contain ∼0.4-1.3 mg Mn. Typical adult intakes are ∼1-9 mg/day; EFSA/SC suggest an adequate intake of a few mg (no formal UL was set, but some guidance points to ∼2-8 mg/day as safe for adults [70]). In our samples, 1-2 cups of tea would supply ∼1-2.5 mg Mn, about half or less of the adult adequacy range. Elderly, smokers or those with

impaired excretion (liver disease) can accumulate Mn. For infants, absorption of Mn is higher; formula and cereals also contribute small amounts (1.07 mg/kg in formula means ∼0.85 mg in 0.8 kg, or -0.11 mg/kg-bw/day for a 7.5 kg baby, ∼0.8 mg/kg-week, well above the adequate intake). Regular consumption of Mn-rich tea along with bread and formula could cumulatively reach the upper safe range, especially in children. While Mn is essential, excessive intake (particularly inhalation in industry) causes neurotoxicity; dietary risk is low but not zero. In summary, high Mn in tea is a known trend, so recommendations may advise limiting tea for infants/children to avoid cumulative Mn load.

4.1.4 Statistical and Visual Interpretation

4.1.4.1 Multivariate Classification Analysis

To assess cumulative toxicological risk, a Partial Least Squares Discriminant Analysis (PLS-DA) was performed using normalized exceedance scores for eight toxic metals Al, As, Cd, Cr, Hg, Ni, Sb, Pb across seven food samples. The resulting biplot (Figure 4.1) depicts the separation of samples based on their relative exceedance percentages compared to individual guideline values.

Baby formula with a 100 % exceedance score projects at the extreme positive end of PLS1, underscoring its status as the highest-risk item. Bread, Dates, and Wheat occupy central positions with 48.4 %, 47.8 %, and 34.4 % exceedance, respectively; reflecting moderate but distinct patterns of metal contributions. In contrast, Broth Cubes, Green Tea, and Fish Feed all 0 % exceedance cluster at the negative extreme of PLS1, indicating full compliance with regulatory limits. PLS2, which is orthogonal to PLS1, is mainly driven by arsenic (As: 0.454) and mercury (Hg: 0.515). Their influence is due to extremely low guideline limits responding to their high toxicological effects, which make even small differences in concentration stand out across samples.

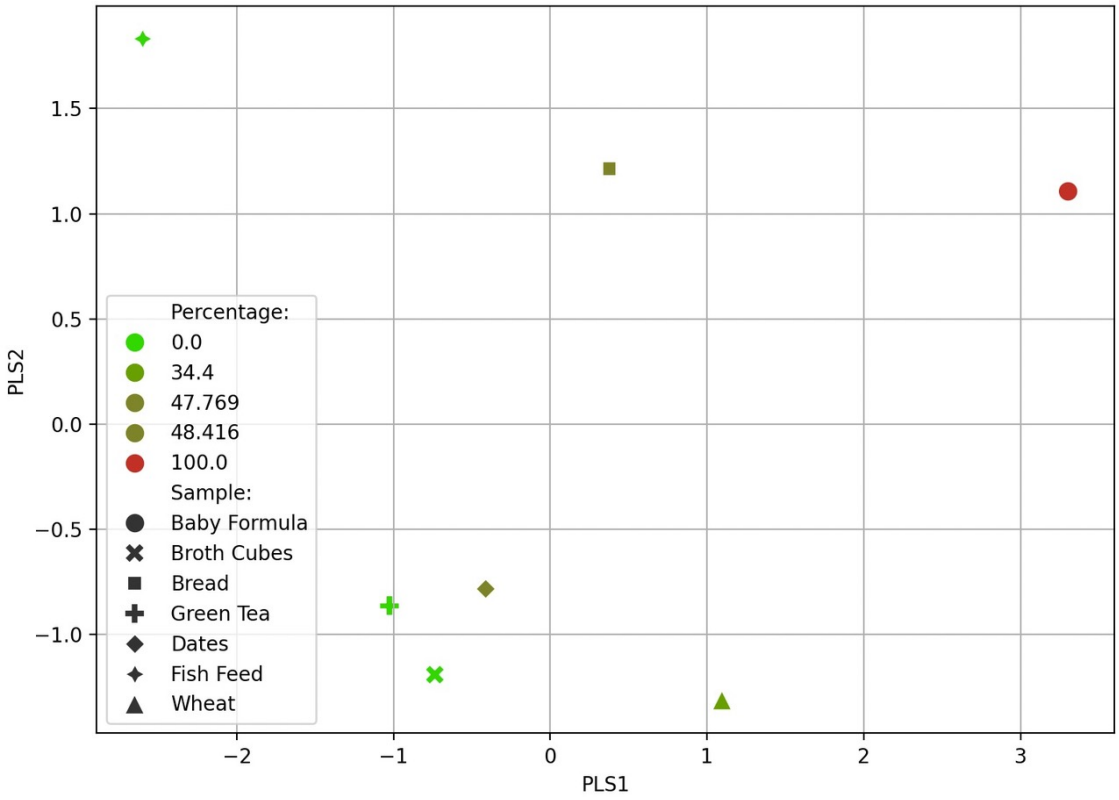

Figure 4.1: PLS-DA Biplot Based on Normalized Toxic Metal Exceedance Scores

4.1.4.2 Histogram Representation of Elemental Groups

To visualize the elemental composition of the analyzed food samples, three histograms were generated based on EDXRF results. Figure 4.2 illustrate the concentration levels of essential minerals, nonessential trace elements, and toxic heavy metals across seven different commercial and non-commercial food items. Among the toxicants, lead (Pb) exhibited the highest concentrations, particularly in wheat and fish feed samples, where levels markedly exceeded those observed in other samples. In contrast, cadmium (Cd) and mercury (Hg) were detected in comparatively lower amounts across all food types. Aluminum (Al) and potassium (K) exhibited the highest concentrations among non-essential and essential minerals, respectively. Most other elements were either present at zero, or below the instrument's limit of detection.

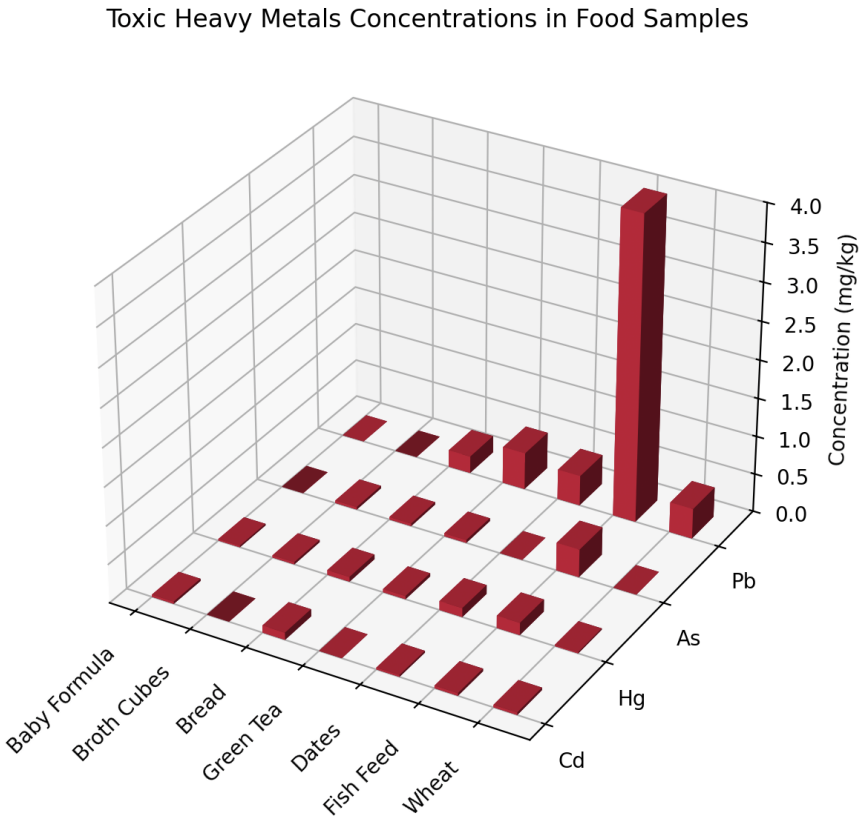

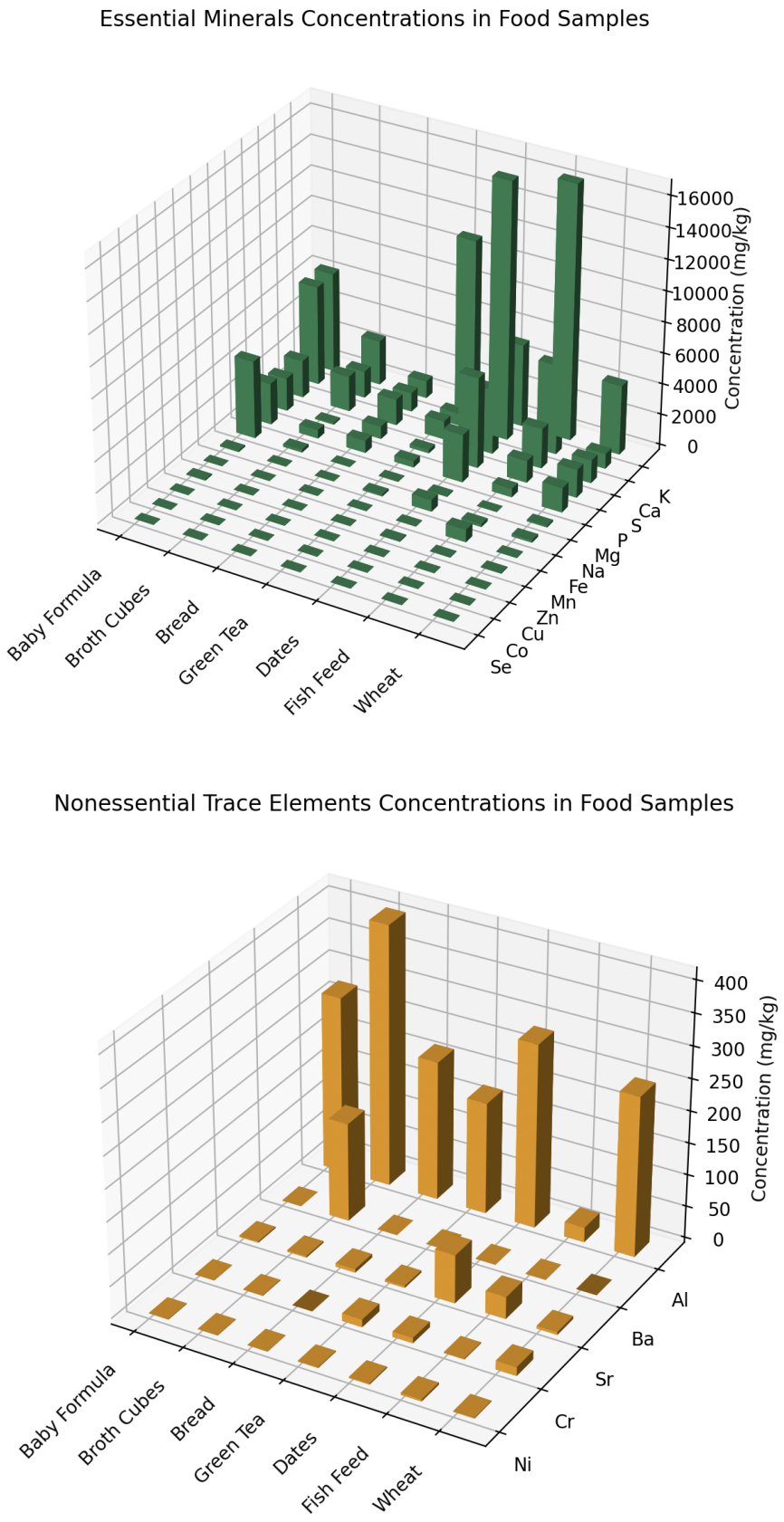

Figure 4.2: Histograms of Elemental Concentrations (Essential, Non-Essential, and Toxic Metals)

4.1.5 International Comparison of Exposure Levels

While this is not a Total Diet Study (TDS), the estimated daily intakes (EDI) offer a comparative snapshot of dietary exposure relevant to the Algerian population. To provide context, selected values are compared with recent findings from other countries (e.g., France, Cameroon) and regional studies. Table 4.10 presents these comparisons as part of a broader analysis aimed at situating Algerian exposure levels within an international framework.

Table 4.10: Comparative Analysis of EDXRF Results

		Measured EDI (µg/kg/day)	Reference EDI (µg/kg/day)	Country	Sources
Food Categories					
Baby Formula	As	0.0	1.03	Turkey	Tugba Dumir et al. [87]
	Cd	0.5	0.019	Turkey	Tugba Dumir et al. [87]
	Hg	0.3	0.026	Turkey	Tugba Dumir et al. [87]
	Pb	0.0	0.15	Turkey	Tugba Dumir et al. [87]
	Al	4837	2.56	Turkey	Tugba Dumir et al. [87]
	Cu	95	4.38	Turkey	Tugba Dumir et al. [87]
	Zn	1186	56.20	Turkey	Tugba Dumir et al. [87]
Broth Cubes (Flavourings)	As	0.001	0.006(1)	France	ANSES (N. Arnich et al.) [84]
	Cd	0.0	0.001(1)	France	ANSES (N. Arnich et al.) [84]
	Pb	0.0	0.002(1)	France	ANSES (N. Arnich et al.)[84]
	Al	7.0	4.25(1)	Cameroon	M.-M. Gimou et al. [82]
	Cu	0.04	0.6(1)	Cameroon	M.-M. Gimou et al. [82]
	Ni	0.01	0.03(1)	France	ANSES (N. Arnich et al.) [84]
	Sb	0.01	0.001 (P95) (1)	Cameroon	M.-M. Gimou et al. [82]
Green Tea (Beverages)	As	0.0	0.013(1)	France	ANSES (N. Arnich et al.) [84]
	Cd	0.0	0.001(1)	France	ANSES (N. Arnich et al.)[84]
	Pb	0.005	0.006(1)	France	ANSES (N. Arnich et al.) [84]
	Al	0.2	5.10(1)	France	ANSES (N. Arnich et al.) [84]
	Cu	0.1	2.25(1)	Cameroon	M.-M. Gimou et al. [82]
	Ni	0.03	0.09(1)	France	ANSES (N. Arnich et al.) [84]
	Sb	0.001	0.003(1)	France	ANSES (N. Arnich et al.) [84]
Dates	As	0.0	0.04 - 0.30	Saudi Arabia	Khaled F Salama et al. [86]
	Cd	0.02	0.005 - 0.28	Saudi Arabia	Khaled F Salama et al. [86]
	Pb	0.4	0.67 - 70.82	Saudi Arabia	Khaled F Salama et al. [86]
	Al	156.0	1.29 - 21.41	Saudi Arabia	Khaled F Salama et al. [86]
	Sb	0.0	1.03 - 2.32	Saudi Arabia	Khaled F Salama et al. [86]

	Cr	10	0.02 - 0.10	Saudi Arabia	Khaled F Salama et al. [86]
Fish	As	0.06	0.009 (P95) [1]	France	ANSES (N. Arnich et al.) [84]
	Cd	0.005	0.007 (P95) [1]	France	ANSES (N. Arnich et al.) [84]
	Pb	0.6	0.2 (P95) [1]	Cameroon	M.-M. Gimou et al. [82]
	Al	45.0	35.3 (P95) [1]	Cameroon	M.-M. Gimou et al. [82]
	Cu	1.0	1.150[1]	Cameroon	M.-M. Gimou et al. [82]
	Ni	0.2	0.277[1]	Cameroon	M.-M. Gimou et al. [82]
	Sb	0.05	0.002 (P95) [1]	France	ANSES (N. Arnich et al.) [84]
Cereals [2]	As	0.1	0.008[1]	France	ANSES (N. Arnich et al.) [84]
(Wheat, Toast)	Cd	0.3	0.18 (P95) [1]	Cameroon	M.-M. Gimou et al. [82]
		Only wheat 0.3	3.47 e-06	Morocco	O.Hammani et al. [85]
	Hg	0.15	1.13[1]	France	ANSES (N. Arnich et al.) [84]
	Pb	1.95	0.12 (P95) [1]	Cameroon	M.-M. Gimou et al. [82]
		Only wheat 3.0	2.28 e-06	Morocco	O.Hammani et al. [85]
	Al	1952	27.8 (P95) [1]	Cameroon	M.-M. Gimou et al. [82]
	Cr	59.5	1.99 (P95) [1]	France	ANSES (N. Arnich et al.) [84]
	Cu	39.5	5.87[1]	Cameroon	M.-M. Gimou et al. [82]
	Ni	5.2	0.22 (P95)	France	ANSES (N. Arnich et al.) [84]
	Sb	0.0	0.001[1]	France	ANSES (N. Arnich et al.) [84]

Notes: [1] Value represents an Estimated Dietary Exposure not an Estimated Daily Intake. [2]The mean value of the EDI was taken.

4.2 Interpretation of Gamma Spectrometry Results

This section presents the results of natural and artificial radionuclide activity concentrations detected in specific Algerian food samples using gamma spectrometry.

While international agencies such as the IAEA, WHO, and Codex Alimentarius have established guideline or maximum permissible levels for artificial radionuclides like ^{137}Cs and ^{90}Sr particularly in the context of nuclear accidents, there are currently no universally accepted, legally binding limits for naturally occurring radionuclides , such as ^{238}U, ^{235}U, ^{232}Th, ^{226}Ra and ^{40}K, across specific food categories. This regulatory gap is largely due to the variability of natural background radiation, which depends on local geology and environmental factors. As a result, most international bodies recommend evaluating based on committed effective dose assessments rather than fixed concentration thresholds.

Ingestion intake of natural radionuclides depends on the consumption rates of food, although it does not represent a complete Algerian diet, ingestion rates (IR, kg/year) given in Table 4.11 used in exposure calculations were derived from the literature and reflect common dietary patterns in Algeria. The Algerian life expectancy, 76 years, was taken from the World Health Organization data base (WHO)[113].

For fish feed, which is not directly consumed by humans, radionuclide concentrations were compared to those found in fish. For baby formula, it is considered as the full diet of an infant. The ingestion dose coefficients shown in Table 4.12 used to calculate the annual committed effective dose were taken from ICRP Publication 72 [57], and the coefficients for radionuclides in baby formula corresponds to a 1-year-old infant.

Table 4.11: Ingestion Rate of Food in Algeria

Food	Ingestion Rate (kg/year)
Dates	22.995
Wheat	219
Bread Toast	109.974
Green Tea	0.292
Broth Cubes	0.876
Baby Formula	42.705

Table 4.12: Ingestion Dose Coefficients for Each Radionucleid

e(g) (Sv/Bq)		
Radioncleid	**Adult**	**1yr Baby**
^{238}U	4.50E-008	1.20E-007
^{235}U	4.70E-08	1.30E-07
^{232}Th	2.30E-07	4.50E-007
^{226}Ra	2.80E-07	9.60E-007
^{40}K	6.20E-009	4.20E-008
^{137}Cs	1.30E+008	1.20E-008

4.2.1 Mesured Radionuclide Activity Concentrations and Regulatory Comparison

In the absence of explicit limits, scientific references such as the UNSCEAR 2000 Report (Annex B)[114] provide representative intake values and typical activity concentrations for food categories including meat, milk, cereals, vegetables/fruits, and fish, and CODEX [115] for infant and adult food. In this study, measured activity concentrations of ^{235}U, ^{232}Th, ^{226}Ra, ^{137}Cs, ^{40}K, and ^{137}Cs in Algerian food samples were compared against these reference values.

These are guidance values, not enforceable limits, and will be interpreted in the context of risk based metrics such as the annual committed effective dose, internal hazard index, and cancer risk assessment to determine potential health impacts.

Table 4.13: Comparison of Measured Activity Concentrations with International Reference Guideline Levels

Product Category	**Food**	**Radionuclide**	**Activity** ($mBq.kg^{-1}$)			
			Measured	**[UNSCEAR]**	**[CODEX][115]**	**GL(1)**
Fruit	**Dates**	^{235}U	<LOD	0.1	10^5	-
		^{232}Th	<LOD	0.5	-	-
		^{226}Ra	<LOD	30	-	-
		^{137}Cs	<LOD	-	10^6	-
		^{40}K	297×10^3	-	-	-

Product Category	Food	Radionuclide	Activity ($mBq.kg^{-1}$)			
			Measured	[UNSCEAR]	[CODEX][115]	GL(1)
Cereal Grain	Wheat	^{235}U	1.4×10^3	1	10^5	Within
		^{232}Th	<LOD	3	-	-
		^{226}Ra	290	80	-	Exceeds
		^{137}Cs	<LOD	-	10^6	-
		^{40}K	116×10^3	-	-	-
	Bread Toast	^{235}U	<LOD	1	10^5	-
		^{232}Th	1.21×10^3	3	-	Exceeds
		^{226}Ra	<LOD	80	-	-
		^{137}Cs	<LOD	-	10^6	-
		^{40}K	69.2×10^3	-	-	-
Beverages	Green Tea	^{235}U	<LOD	-	10^5	-
		^{232}Th	4.11×10^3	-	-	-
		^{226}Ra	1.9×10^3	-	-	-
		^{137}Cs	<LOD	-	10^6	-
		^{40}K	508×10^3	-	-	-
Flavour Enhancers	Broth Cubes	^{235}U	1.04×10^3	-	10^5	Within
		^{232}Th	1.15×10^3	-	-	-
		^{226}Ra	610	-	-	-
		^{137}Cs	<LOD	-	10^6	-
		^{40}K	60.69×10^3	-	-	-
Milk	Baby Formula	^{235}U	<LOD	0.05	10^5	-
		^{232}Th	470	0.3	-	Exceeds
		^{226}Ra	410	5	-	Exceeds
		^{137}Cs	<LOD	-	10^6	-
		^{40}K	161×10^3	-	-	-

Product Category	Food	Radionuclide	Activity (mBq.kg^{-1})			
			Measured	[UNSCEAR]	[CODEX][115]	GL(1)
Fish	Fish Feed	^{235}U	<LOD	-	10^5	-
		^{232}Th	<LOD	10	-	-
		^{226}Ra	40	100	-	Within
		^{137}Cs	<LOD	-	10^6	-
		^{40}K	181×10^3	-	-	-

Notes: (1)Guideline Level

4.2.2 Radionuclids Discussion

The comparison values used for naturally occurring radionuclides in this study are reference guideline levels provided by sources such as the UNSCEAR 2000 Report (Annex B) [114]. These are not regulatory limits, but rather typical concentration ranges compiled from global dietary intake studies. They are intended to provide a baseline for contextual evaluation and should not be interpreted as strict thresholds for safety or compliance.

Uranium (^{235}U)

Uranium-235 (^{235}U) was below detection limits in dates, green tea, toast bread, fish feed and baby formula, but detected in wheat ($1.40 \pm 0.05 Bq.kg^{-1}$) and broth cubes (1.04 ± 0.052 $Bq.kg^{-1}$). In wheat, the level exceeded UNSCEAR's reference value yet remained within Codex Alimentarius guidance levels, while for both cubes, the value was within both reference ranges. The presence of ^{235}U in broth cubes despite being a processed product, could be attributed to their complex composition, which includes ingredients like vegetables, herbs, spices, cereals, and hydrolyzed proteins [116], potentially introducing trace uranium through multiple natural sources. In contrast, the absence of detectable ^{235}U in other foods may result from low environmental uranium uptake by source plant or animals, geochemical differences in cultivation areas, differences in soil origin and agricultural inputs or processing dilution that reduce residual uranium content.

Thorium (^{232}Th)

Thorium-232 (^{232}Th) was below detection limits in dates, wheat, and fish feed, while detectable levels were observed in green tea (4.11 ± 0.20 $Bq.kg^{-1}$), toast bread (1.21 ± 0.06 $Bq.kg^{-1}$) which exceeded the UNSCEAR 2000 reference guideline value of 03 $mBq.kg^{-1}$, broth cubes (1.15 ± 0.057 $Bq.kg^{-1}$), and baby formula (0.47 ± 0.023 $Bq.kg^{-1}$) exceeding the reference guideline value of 0.3 $mBq.kg^{-1}$ which is not a strict safety thresholds. The highest concentration in green tea is consistent with its direct uptake of minerals from soil, as tea plants tend to accumulate trace elements including thorium. The presence of ^{232}Th in processed foods such as toast bread, broth cubes, and baby formula may result from ingredient diversity and the use of additives. Bread includes yeast, salt, and fortifying agents, and broth cubes contain spices, vegetables, and hydrolyzed proteins, all of which can contribute small thorium amounts depending on their origin. Although fish feed often includes fish meal and processing byproducts, the absence of detectable thorium may be attributed to limited

uptake in marine environments or to purification and dilution during formulation. These observations suggest that food processing can either introduce, retain trace radionuclides or reduce them depending on the raw materials and the nature of the manufacturing methods.

Radium (^{226}Ra)

Radium-226 (^{226}Ra) showed the highest concentration in green tea ($1.195 \pm 0.095\ Bq.kg^{-1}$), followed by baby formula ($0.41 \pm 0.02\ Bq.kg^{-1}$) and wheat ($0.29 \pm 0.014\ Bq.kg^{-1}$), which exceeded the UNSCEAR 2000 reference guideline value of 0.05 $mBq.kg^{-1}$ and 80 $mBq.kg^{-1}$ respectively for baby formula and wheat. Fish feed exhibited the lowest detectable level ($0.04 \pm 0.002\ Bq.kg^{-1}$), well within the guideline level of 100 $mBq.kg^{-1}$. In contrast, ^{226}Ra was below detection limits in dates and toast bread. The elevated level in green tea is likely due to the plant's efficiency in uptaking radium directly from mineral rich soils. For baby formula and wheat, the presence of ^{226}Ra could stem from calcium rich ingredients or fertilizers, as radium chemically mimics calcium. The absence of detectable levels in dates and toast bread may result from limited soil to fruit translocation and processing steps that remove or dilute radium during preparation or cooking.

Radionuclide levels in dates were mostly below detection due to limited transfer through the plant. Since fruits like dates are at the end of the nutrient transport chain, most radionuclides accumulate in roots, stems, or leaves, leading to minimal presence in the edible part.

Potassium (^{40}K)

The highest activity concentrations observed in Table 4.13 correspond to the naturally occurring radionuclide potassium-40 (^{40}K) present in all samples. The maximum concentration was recorded in the Green Tea sample, measured at 508.15 ± 25.41 Bq.kg^{-1}, while broth Cubes sample at 60.69 ± 3.03 Bq/kg and Bread Toast ($69.2 \pm 3.46 Bq.kg^{-1}$) recorded the lowest values. This elevated ^{40}K level in green tea is consistent with its botanical origin and natural potassium content, as tea plant's natural tendency to absorb potassium directly from the soil. Since tea leaves are typically harvested and consumed in dried form with minimal processing, the naturally accumulated potassium ^{40}K remains concentrated in the final product. In contrast, broth cubes and toast are more processed food products, likely prepared with lower potassium ingredients and subjected to dilution during manufacturing. This indicates a wide variability in ^{40}K levels across different food types. Although ^{40}Kconsistently contributed the highest activity in all food samples. However, it is important to note that potassium-40 is a naturally essential element involved in biological functions, and its concentration in human tissues is tightly regulated through metabolic processes. As a result, no specific guideline levels for ^{40}K in food have been established by international agencies, and its presence is generally considered a baseline component of natural radioactivity in the human diet.

Cesium (^{237}Cs)

Cesium-137 ^{137}Cs was below the detection limit in all analyzed samples, indicating the absence of significant artificial radionuclide contamination. This aligns with expectations for food products not affected by recent nuclear incidents, and suggests no residual fallout influence in the sampled regions.

It is important to emphasize that for naturally occurring radionuclides (NORMs) such as ^{238}U, ^{235}U, ^{232}Th, ^{226}Ra, and ^{40}K, there are no internationally binding limits set by the ICRP, UNSCEAR, or WHO. Instead, most available figures are reference guideline levels,

intended to serve as rough benchmarks rather than strict regulatory thresholds. These values, often derived from limited datasets or average global intake estimates, can vary widely from one publication or region to another. Consequently, the differences between the measured activity concentrations in Algerian food samples and these reference values may appear significant. However, such discrepancies are expected and can be attributed to local geological, environmental, agricultural, and dietary factors, which strongly influence the uptake and accumulation of natural radionuclides in food. Therefore, instead of relying solely on comparison to these generic guideline levels, dose-based assessments such as the Annual Committed Effective Dose (AED) and risk indices like Hazard Index (Hin) and Excess Lifetime Cancer Risk (ELCR) offer a more meaningful approach to evaluating the potential health impact of these naturally present radionuclides.

4.2.3 Radiological Hazard Assessment

To better understand the potential health implications of the measured activity concentrations, radiological risk indicators were calculated, including the Annual Committed Effective Dose (AED), Internal Hazard Index (Hin), and excess lifetime cancer risk (ELCR). These indicators allow for a more meaningful assessment of ingestion-related radiation exposure, especially in the absence of fixed activity concentration limits for naturally occurring radionuclides in food. The following values in Table 4.14 were derived based on standard ingestion dose coefficients (Table 4.12) and food consumption (Table rates 4.11) relevant to the local population.

In the following radiological hazard assessments (AED, Hin, and ELCR), only food samples relevant to human dietary intake were considered. Fish feed was excluded, as it is not consumed directly by humans and therefore not representative of ingestion exposure. Baby formula was also treated separately, since it is specifically consumed by infants for a limited period (typically within the first year of life) and does not reflect long-term dietary patterns in the general population.

Table 4.14: Radiological Hazard Assessment

Food	AED(mSv/yr)	Hin(Bq/kg)	ELCR
Dates	4.25E-05	0.0619	1.61E-04
Wheat	1.90E-04	0.0242	7.23E-04
Bread Toast	7.78E-05	0.0191	2.96E-04
Green Tea	1.35E-06	0.122	5.14E-06
Broth Cubes	7.54E-07	0.0171	2.86E-06
Baby Formula	3.16E-04	0.0355	0.0012
Fish Feed	-	-	-
Cumulative Exposure	3.13E-04	0.244	1.19E-03
Threshold Compliance	< 1	< 1	$> 1 \times 10^{-4}$

Annual Committed Effective Dose (AED)

The calculated AED values for all food samples remain well below the internationally recommended public exposure limit of 1 mSv/year (ICRP 60 [117], UNSCEAR 2000). The highest AED was observed in wheat at 1.90×10^{-4} mSv/year, followed by baby formula 3.16×10^{-4} this value is safe in context, as it reflects a one-year dietary exposure typical for infants, rather than a full lifetime intake., while the lowest dose was recorded in broth cubes at 7.54×10^{-7} mSv/year. These findings indicate that, when consumed individually, none of the analyzed food items pose a significant radiological health risk. Even when considering cumulative exposure from multiple food items, the total estimated AED 3.13×10^{-4} remains safely under the 1 mSv/year threshold, suggesting that the dietary intake of naturally occurring radionuclides from these foods is not a concern under current consumption patterns.

Internal Hazard Index (Hin)

The Internal Hazard Index (Hin) values calculated for all food samples were found to be well below the safety threshold of 1 Bq/kg, indicating negligible radiological risk from internal exposure. The highest HiN was recorded in green tea at 0.122 Bq/kg, while the lowest was observed in bread toast at 0.0191 Bq/kg. Even when considering the combined intake of all food in a regular diet, the cumulative Hin remains safely below at 0.244 Bq/kg the critical limit. These results confirm that, based on current activity concentrations and standard ingestion rates, the selected food products do not pose internal radiological hazards to consumers.

Excess Lifetime Cancer Risk (ELCR)

The Excess Lifetime Cancer Risk (ELCR) values show noticeable variation among the analyzed food samples. The highest individual ELCR was observed in baby formula at 1.2×10^{-6}, followed by wheat (7.23×10^{-6}) both exceeding the internationally recommended upper limit of 1×10^{-4} for the public (ICRP 60, USEPA). Similarly, dates and toast bread also presented ELCR values exceeding this threshold. In contrast, green tea and broth cubes showed much lower ELCRs, on the order of 10^{-6}, well within the acceptable range. When considering the cumulative dietary ELCR from all analyzed food samples, the total value reaches approximately 1.19×10^{-3}, which also exceeds the recommended limit. These findings highlight the potential cumulative radiological risk if such food items form a regular part of the diet, and reinforce the importance of ongoing monitoring, especially for foods consumed frequently or by vulnerable groups.

4.2.4 Visual Interpretation of Gamma Spectrometry Results

4.2.4.1 Radioactivity Distribution

To illustrate the distribution of natural and industrial radionuclides in the analyzed food samples, a three-dimensional histogram was generated based on the gamma spectrometry measurements (Figure 4.3). The activity concentrations are presented in Bq/kg. The artificial radionuclide Cs-137 was below the detection limit in all samples. The highest activity was recorded for the naturally occurring K-40, with green tea showing the highest concentration. In contrast, Ra-226 exhibited the lowest activity levels, with fish feed presenting the lowest concentration among the samples.

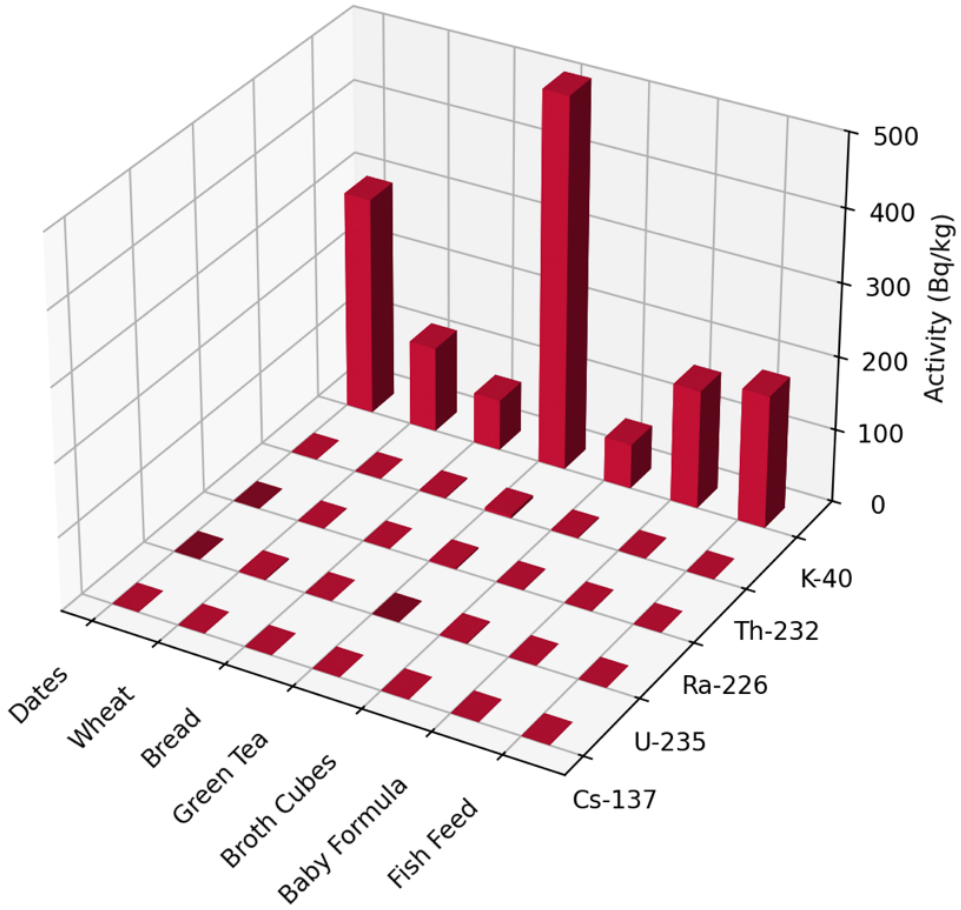

Figure 4.3: Measured Radioactivity Levels in Food Samples

4.2.4.2 Radiological Hazards

To assess potential radiological risks, the hazard indices were visualized in a grouped bar chart (Figure 4.4). The Hazard Index (Hin) remained below the recommended safety limit of 1 Bq/kg for all samples, indicating no significant radiological risk. Green tea exhibited the highest Hin and annual effective dose (AED) among the samples, although the AED values for all samples were well below the 1 mSv/year benchmark. Regarding the Excess Lifetime Cancer Risk (ELCR), all samples except broth cubes and green tea exceeded the conservative threshold limit of 1×10^{-4}, suggesting a potential lifetime carcinogenic risk associated primarily with these two samples.

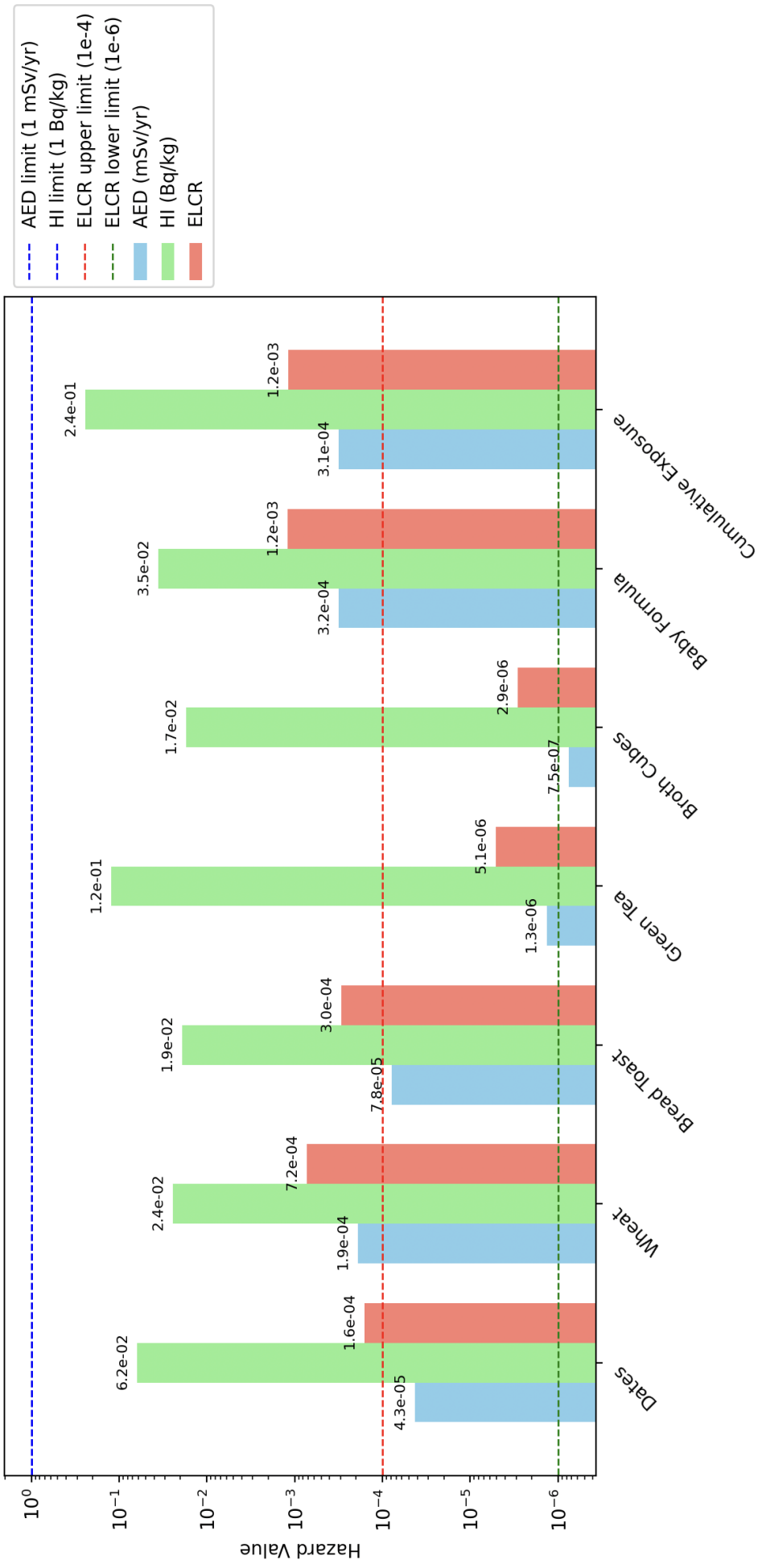

Figure 4.4: Radiological Hazard Assessment in Food Samples

4.2.5 Comparison with Other Counties

To provide context for the measured activity concentrations in Algerian food samples, the following Table 4.15 presents a comparison with values reported in other countries. These reference values are drawn from reports, including UNSCEAR 2000 and relevant regional studies. While not regulatory limits, they serve as useful benchmarks for evaluating the relative presence of naturally occurring radionuclides in various food categories.

Table 4.15: Comparison of Measured Activity Concentrations with Those Reported in Other Countries

Product Category	**Food**	**Radionuclide**	**Activity** (Bq.kg^{-1})			
			Measured	**UK**	**Germany**	**China**
Cereal Grain	**Wheat**	^{235}U	1.4	-	-	0.5×10^{-3}[114]
		^{232}Th	<LOD	0.012[114]	-	0.013[114]
		^{226}Ra	0.29	0.7×10^{-3}-5.2[114]	0.134[119]	0.62[118]
		^{137}Cs	<LOD	-	-	0.22[118]
		^{40}K	116	-	-	105[118]
	Bread Toast	^{235}U	<LOD	-	-	0.5×10^{-3}[114]
		^{232}Th	1.21	0.012[114]	-	0.013[114]
		^{226}Ra	<LOD	0.7×10^{-3}-5.2[114]	0.134[119]	0.62[118]
		^{137}Cs	<LOD	-	-	0.22[118]
		^{40}K	69.2	-	-	105[118]
Beverages	**Green Tea**	^{235}U	<LOD	-	-	-
		^{232}Th	4.11	-	-	-
		^{226}Ra	1.9	-	-	1.09[118]
		^{137}Cs	<LOD	-	-	0.33[118]
		^{40}K	508	-	-	305[118]

Product Category	Food	Radionuclide	Activity (Bq.kg^{-1})			
			Measured	UK	Germany	China
Flavour Enhancers	Broth Cubes	^{235}U	1.04	-	-	-
		^{232}Th	1.15	-	-	-
		^{226}Ra	0.610	-	-	-
		^{137}Cs	<LOD	-	-	-
		^{40}K	60.69	-	-	-
Milk	Baby Formula	^{235}U	<LOD	-	-	0.6×10^{-3}[114]
		^{232}Th	0.47	-	-	1.2×10^{-3}[114]
		^{226}Ra	0.41	0.4×10^{-3}-0.2[114]	0.0615[119]	1.13[118]
		^{137}Cs	<LOD	-	-	0.79[118]
		^{40}K	161	-	-	228[118]
Fish	Fish Feed	^{235}U	<LOD	-	-	0.5×10^{-3}[114]
		^{232}Th	<LOD	-	-	1.3×10^{-3}[114]
		^{226}Ra	0.04	8.5×10^{-3}-2.1	0.0196[119]	0.55[118]
		^{137}Cs	<LOD	-	-	0.04[118]
		^{40}K	181	-	-	67.5[118]

Wheat

^{235}U measured at 1.4 Bq/kg, significantly higher than China's reported 0.5×10^{-3} Bq/kg, indicating possible localized enrichment or soil composition differences. ^{232}Th is below detection limits, while other countries reported low levels (0.012–0.01 Bq/kg). ^{226}Ra measured at 0.29 Bq/kg, higher than Germany (0.134 Bq/kg) but lower than China (0.62 Bq/kg), within global variation. ^{137}Cs not detected, aligning with the UK's and Germany's non-reports and below China's 0.22 Bq/kg. ^{40}K at 116 Bq/kg, slightly above China's 105 Bq/kg, but within expected natural variation.

Bread Toast

^{235}U is not detected, similar to other countries' lack of data or trace levels.^{232}Th at 1.21 Bq/kg exceeds the reference values (UK and China 0.012–0.013 Bq/kg), likely due to additives or enriched ingredients. ^{226}Ra is below detection limit, while other countries report measurable levels, possibly due to differences in flour source or baking salt. ^{137}Cs is not detected, contrasting with China's 0.22 Bq/kg. ^{40}K at 69.2 Bq/kg, lower than China's 105 Bq/kg.

Green Tea

^{235}U is not detected, no data for comparison. ^{232}Th 4.11 Bq/kg no direct comparison, but is at a high value. ^{226}Ra 1.9 Bq/kg, slightly higher than China's 1.09 Bq/kg. ^{137}Cs not detected, whereas China reports 0.33 Bq/kg may reflect differences in contamination sources or tea origin. ^{40}K: 508 Bq/kg, considerably higher than China's 305 Bq/kg, consistent with natural potassium accumulation in tea leaves.

Broth Cubes

No international data for comparison for all radionuclides.

Baby Formula

^{235}U is not detected consistent with China's very low 0.6×10^{-3} Bq/kg. ^{232}Th at 0.47 Bq/kg slightly higher than China's 1.2×10^{-3} Bq/kg. ^{226}Ra at 0.41 Bq/kg within the wide UK range (0.4×10^{-3}–0.2), higher than Germany, but below China (1.13 Bq/kg). ^{137}Cs Not detected, lower than China (0.79 Bq/kg). ^{40}K at 161 Bq/kg slightly lower than China (228 Bq/kg).

Fish Feed

^{235}U and ^{232}Th both not detected matches low values reported in China ($0,5 \times 10^{-3} Bq/kg$ and 1.3×10^{-3} Bq/kg respectively). ^{226}Ra at 0.04 Bq/kg lower than china (0.55 Bq/kg). ^{137}Cs: Not detected consistent with China's 0.04 Bq/kg. ^{40}K 181 Bq/kg higher than China (67.5 Bq/kg).

As shown in Table 4.15 the comparison shows significant variation in natural radionuclide levels across foods and regions, influenced by geology, environment, farming, diet, and processing. Variability in sampling and measurement methods also affects reported values. Since there are no universal limits for natural radionuclides in food, reference levels help provide context. These findings emphasize the importance of region specific data and dose-based risk assessments over fixed concentration thresholds in evaluating food safety.

4.2.5.1 Dates Comparison

To better understand the significance of the measured activity concentrations, results for dates were compared with those reported in other countries where dates are a common dietary component, as shown in Table 4.16.

Table 4.16: Comparison of Activity Concentrations in Dates with Those Reported in Other Countries

Food	Radionuclide	Activity ($Bq.kg^{-1}$)					
		Measured	**UAE[120]**	**Iran[122]**	**Tunisia[122]**	**SA 1$^{(1)}$[122]**	**SA 2$^{(2)}$[121]**
Dates	^{235}U	<LOD	-	-	-	-	-
	^{232}Th	<LOD	<LOD-1.79	-	-	-	2.8 ± 0.4
	^{226}Ra	<LOD	<LOD-1.47	1.6 ± 0.3	1.3 ± 0.3	1.3 ± 0.3	5.6 ± 1.2
	^{137}Cs	<LOD	-	-	-	-	-
	^{40}K	297	277-370	214 ± 10	180 ± 9	163 ± 8	181 ± 17

Notes: $^{(1)}$Saudi Arabia reference 1. $^{(2)}$Saudi Arabia reference 2.

For ^{40}K, the measured value in this study was within the same range reported in studies from the United Arab Emirates, and slightly exceeded those reported in other countries such as Saudi Arabia, Iran, and Tunisia. However, the differences were not significant, and all values remained within the expected natural variability for potassium in dates, likely reflecting regional soil composition and environmental conditions. Thorium-232 was also below detection limits, consistent with values reported in the UAE (range: <LOD–1.79 Bq/kg). However, a higher concentration was noted in Saudi Arabia (2.8 Bq/kg, Ref 2), indicating potential regional variations in soil-to-fruit transfer, though overall accumulation of thorium in date fruits appears to be minimal. Radium-226 was below detection limits in the present study. This is comparable to the range reported in the UAE (<LOD–1.47 Bq/kg), while higher concentrations were observed in Saudi Arabia (up to 5.6 ± 1.2 Bq/kg, Ref 1) and Tunisia (2.3 Bq/kg). These differences may reflect variations in local soil composition and environmental conditions influencing radium uptake.

Conclusion

This study aimed to assess the contamination levels of both natural radionuclides and toxic heavy metals in food products commonly consumed in Algeria, using two advanced nuclear analytical techniques: High-Purity Germanium (HPGe) gamma-ray spectrometry and Energy Dispersive X-ray Fluorescence (EDXRF). The integration of these two complementary techniques provided a robust and multifaceted approach to evaluating radiological and toxicological risks in the selected food samples.

EDXRF analysis revealed varying levels of toxic heavy metal concentrations, particularly of aluminum (Al), lead (Pb), cadmium (Cd), mercury (Hg), and arsenic (As). While most samples complied with Codex Alimentarius and EU standards, significant exceedances were observed especially in infant formula (for Al and Cd) and bread (for Hg and Pb). The risk assessment using Hazard Quotients (HQ), Hazard Index (HI), and pollution metrics such as Contamination Factor (CF), Metal Pollution Index (MPI), and Pollution Load Index (PLI) indicated elevated toxicological risk in specific samples. Notably, baby formula exhibited 100% exceedance across toxic metal guidelines, reinforcing the need for stricter regulatory control and routine monitoring, particularly for vulnerable populations.

Gamma spectrometry analysis complemented these findings by detecting naturally occurring radionuclides such as Potassium-40 (^{40}K), Uranium-235 (^{235}U), Thorium-232 (^{232}Th), and Radium-226 (^{226}Ra). Cesium-137 (^{137}Cs), an artificial radionuclide, was not detected in any sample, indicating no recent artificial contamination. Activity concentrations varied significantly among the food items, with ^{40}K being the most abundant radionuclide, particularly in green tea and wheat. Comparative analysis with international data indicated general conformity, though certain food types showed elevated levels. These deviations highlight the importance of contextualizing results within local geological, agricultural, and dietary frameworks.

Radiological hazard indices including the Annual Committed Effective Dose (AED), Internal Hazard Index (Hin), and Excess Lifetime Cancer Risk (ELCR) were calculated to evaluate potential health risks. All food items, individually and in aggregate, remained below the international limit of 1 mSv/year for AED. The Hin values were all under the safety threshold of 1, suggesting no significant internal hazard. However, ELCR values for some items (notably bread toast and wheat) exceeded the reference risk level of 1×10^{-4}, raising concerns for long-term exposure under high-consumption scenarios. Conversely, infant targeted products like baby formula, when evaluated under realistic short-term consumption assumptions, showed the highest ELCR value.

Together, these findings underscore the value of nuclear techniques in food safety surveillance. Gamma spectrometry offers sensitive detection of low-level radionuclides, while EDXRF enables rapid screening of elemental contaminants. The dual approach allows for a comprehensive risk profile of food products, addressing both radioactive and chemical hazards. Although the majority of analyzed foods remain within international safety margins, certain exceedances particularly in infant and staple foods warrant further investigation and may

inform future policy revisions on food quality standards in Algeria.

In conclusion, this thesis highlights the utility of combining gamma spectrometry and EDXRF for national food safety assessment. It advocates for continued investment in analytical infrastructure and routine surveillance programs to protect public health, especially among high risk groups such as infants and high consumption adults. Particular attention should be given to evaluating complete dietary exposure, as individual food items may appear safe in isolation but contribute to cumulative risks when consumed regularly as part of a full diet. Future work should expand the sample size and diversity, include speciation analysis for metals like arsenic and chromium, and evaluate bioavailability to better quantify exposure and health effects. The integration of such comprehensive methods into national food control systems will be crucial for enhancing Algeria's food safety framework and ensuring long-term consumer protection.

References

[1] Henson, S., & Caswell, J. A. (1999). Food safety regulation: Contemporary issues. Agricultural Economics, 18(2), 117-125.

[2] Turkish Journal of Agriculture - Food Science and Technology. (2022). 10(8), 1342-1351.

[3] World Health Organization (WHO). (2024). Newsroom: Food Safety, 4 October.

[4] United Nations Scientific Committee on the Effects of Atomic Radiation (UNSCEAR). (1988). Sources, Effects, and Risks of Ionizing Radiation. United Nations, New York.

[5] International Atomic Energy Agency (IAEA). (1980). Elemental Analysis of Biological Materials. Vienna.

[6] International Atomic Energy Agency (IAEA). (1982). Generic Models and Parameters for Assessing the Environmental Transfer of Radionuclides from Routine Releases, Exposure of Critical Groups. Safety Series, No. 57.

[7] Naturally Occurring Radioactive Material (NORM V). (2008). Thorium and Uranium Bioaccumulation in Wheat and Rye Plants. August 15.

[8] Handbook of Mineral Elements in Food. (2015). The Toxic Element. Málaga, Spain.

[9] Handbook of Mineral Elements in Food. (2015). Dietary Intake of Minerals. Chatham, UK.

[10] Food and Agriculture Organization (FAO) / World Health Organization (WHO). (1995). General Standard for Contaminants and Toxins in Food and Feed. Codex Alimentarius Commission.

[11] An Overview of Algerian Food Quality Legislation, Regulation, and Control Authorities. (2023). The 4th International Electronic Conference on Foods, 15–30 October.

[12] International Atomic Energy Agency (IAEA). (2011). Radiation Protection and Safety of Radiation Sources: International Basic Safety Standards. GSR Part 3.

[13] Handbook of Mineral Elements in Food. (2015). Human Risk Assessment and Regulatory Framework for Minerals in Food. Valencia, Spain.

[14] Global NEST Journal. (2024). Assessment of Heavy Metals Accumulation in Food Crops Irrigated with Wastewater in Boumerzoug Sub-Basin, Algeria.

[15] Analytical Methods. (2020). Mass Spectrometry Approaches to Ensure Food Safety. Issue 9.

[16] International Atomic Energy Agency (IAEA). (2001). Advanced Separation Techniques in Radiochemical Analysis of Environmental Samples. Slovakia.

[17] Knoll, G. F. (2015). Measurement and Detection of Radiation. 4th Edition, Chapter 7, p. 236.

[18] Clapera, R. S. (2006). Energy Dispersive X-ray Fluorescence: Measuring Elements in Solid and Liquid Matrices.

[19] Salamó Clapera, R. Energy Dispersive X-ray Fluorescence: Measuring Elements in Solid and Liquid Matrices.

[20] Tsoulfanidis, N., & Landsberger, S. (2015). Measurement and Detection of Radiation (4th ed.). CRC Press.

[21] Knoll, G. F. (2010). Radiation Detection and Measurement (4th ed.). John Wiley & Sons.

[22] Yao, M., Wang, D., & Zhao, M. (2015). Element analysis based on energy-dispersive X-ray fluorescence. Advances in Materials Science and Engineering, 2015.

[23] Sokoltsova, T. (2021). Development of a Standardless Miniature XRF Setup for the Analysis of Actinides: Coupling MC Methods with Fundamental Parameters (Doctoral dissertation, Université Paris-Saclay).

[24] Arectout, A. (2023, July). Étude et optimisation des caractéristiques des détecteurs dédiés à la spectrométrie gamma moyennant la méthode des plans d'expériences (Doctoral thesis, Abdelmalek Essaâdi University). ResearchGate.

[25] Courtine, F. (2007, March). Étalonnage d'un spectromètre gamma en vue de la mesure de la radioactivité naturelle : Mesures expérimentales et modélisation par techniques de Monte-Carlo (Doctoral dissertation, Université Blaise Pascal – Clermont-Ferrand II). INIS IAEA Database.

[26] Bigelow, R. A. (n.d.). Radiation interactions in matter [PDF]. University of Hawai'i Physics Department. Retrieved June 14, 2025

[27] Buchtela, K. (2005). Radiochemical methods: Gamma-ray spectrometry [Technical report]. Atominstitut der Österreichischen Universitäten. Elsevier.

[28] Oliveira, M. F., et al. (2018). Direct determination of Ca, K, Mg, Na, P, S, Fe and Zn in bivalve mollusks by wavelength dispersive X-ray fluorescence (WDXRF) and laser-induced breakdown spectroscopy (LIBS). Food Chemistry, 273, 620 627.

[29] Bengroun, M. (2023). Study of Radioelements and Heavy Metal Transfer from Soil to Plants: Nuclear Techniques Optimization by Monte Carlo Simulation for Quantitative Analysis (PhD thesis, Université de Béjaïa).

[30] Jaklevic, J. M., & Giauque, R. D. (1993). Energy-dispersive X-ray fluorescence analysis using X-ray tube excitation. In R. Van Grieken & A. Markowicz (Eds.), Handbook of X-ray Spectrometry: Methods and Techniques (pp. 151–180). Marcel Dekker.

[31] Van Grieken, R., & Markowicz, A. A. (Eds.). (2002). Handbook of X-ray Spectrometry: Methods and Techniques (2nd ed.). Marcel Dekker.

[32] JEOL Ltd. (2012, October 24). Scanning electron microscopy terms. JEOL.

[33] Marguí, E., Queralt, I., & Hidalgo, M. (2009). Application of X-ray fluorescence spectrometry to determination and quantitation of metals in vegetal material. TrAC Trends in Analytical Chemistry, 28(3), 362–372.

[34] Huang, H., et al. (2023). Improving the accuracy of EDXRF results in gold alloy analysis by matrix effect correction. Spectrochimica Acta Part B: Atomic Spectroscopy, 201, 106629.

[35] Li, F., Meng, L., Ding, W., et al. (2022). Review of energy-dispersive X-ray fluorescence on food elements detection. X-Ray Spectrometry, 51(1), 3–13.

[36] Perring, L., & Andrey, D. (2016). Development and validation of an ED-XRF method for the fast quantification of mineral elements in dry pet food samples. Food Analytical Methods, 9(9), 2598–2606.

[37] IXRF Systems. (n.d.). Ultralight Elemental Analysis by EDXRF. Retrieved April 17, 2025.

[38] Jouini, D., Azbouche, A., ElMahroug, Y., Benarous, S., Tellili, B., Souga, C., & Labidi, S. (2023). HPGe efficiency calibration using GEANT4-GAMOS code for study environmental materials: Radioactivity transfer study nearby the phosphate area in southern Tunisia. International Journal of Environmental Analytical Chemistry, ahead-of-print, 1–14.

[39] Wallbrink, P. J., Walling, D. E., & He, Q. (2002). Radionuclide measurement using HPGe gamma spectrometry. In F. Zapata (Ed.), Handbook for the assessment of soil erosion and sedimentation using environmental radionuclides (pp. 67–96). Springer. https://doi.org/10.1007/0-306-48054-9_5

[40] Valković, V. (Ed.). (2019). Measurements of radioactivity (Chapter 4, pp. 123–280). In Radioactivity in the Environment (2nd ed.). Elsevier.

[41] Kerlin, T. W., & Upadhyaya, B. R. (2019). Chapter 16 – Nuclear plant instrumentation. In Dynamics and control of nuclear reactors (pp. 213–235).

[42] Buchtela, K. (2014). Radiochemical methods: Gamma-ray spectrometry. In Reference Module in Chemistry, Molecular Sciences and Chemical Engineering (pp. 1–22).

[43] Reguigui, N. (2006). Gamma ray spectrometry. International Atomic Energy Agency.

[44] Vincent, Elément de mathématique appliquée. Science.ch 2005.

[45] Yimele, B. C. (2022). Évaluation des paramètres radiologiques d'exposition et du risque radiologique pour les habitants de la zone bauxitique de Fongo-Tongo (Doctoral dissertation, Université de Yaoundé I). Université de Yaoundé I.

[46] Blanc, D. (1980). Physique nucléaire (2nd ed.). Masson

[47] . Bernard, Génie énergétique : de la théorie aux applications du nucléaire (Ellipses, Paris, 2008).

[48] C. Granja, C. Leroy, I. Stekl, Nuclear physics methods and accelerators in biology and medicine (American institu of physics, New York, 2007).

[49] S. Belazreg, Biophysique, cours, Exercice, annales Qem Corrigés (Dunod, Paris, 2006).

[50] F. Jallu, Double interrogation simultanée neutron et proton utilisant un accélérateur d'élec-trons pour la caractérisation séparée des actinides dans les déchets radioactifs enrobés. CEA 1999.

[51] Jeambrun, M. (2012). L'uranium et ses descendants dans la chaîne alimentaire (Master's thesis, Université de Strasbourg). Université de Strasbourg.

[52] V.D Vorts, Introduction à la physique (Deboek, Wesmael, Bruxelles, 1997).

[53] J. Foos, Manuelle de radioactivité (Herman, Paris, 2009).

[54] University of Groningen, Radiation Protection. (2024, April 7). Natural decay chain [Web page with figure]. Groningen Academy for Radiation Protection.

[55] D. Blanc, Précis de physique nucléaire (Dunod, Paris, 1999).

[56] Moon, E.-K., Ha, W.-H., Seo, S., Jin, Y.W., Jeong, K.H., Yoon, H.-J., Kim, H.-S., Hwang, M.-S., Choi, H., & Lee, W.J. (2016). Estimates of radiation doses and cancer risk from food intake in Korea. Journal of Korean Medical Science, 31(1), 9–12.

[57] ICRP (International Commission on Radiological Protection). (1996). Age-dependent doses to members of the public from intake of radionuclides—Part 5: Compilation of ingestion and inhalation dose coefficients (ICRP Publication 72, Annals of the ICRP, 26(1), pp. 1–91). Elsevier.

[58] EarthCon Consultants of North Carolina, P.C. (2019). Final Remedial Investigation Report: Kerr-McGee Chemical Corp – Navassa Superfund Site, Navassa, North Carolina (EPA ID #NCD980557805) [Human Health Risk Assessment section]. Prepared for Multistate Environmental Response Trust.

[59] Coulibaly, A., Kpeglo, D. O., & Darko, E. O. (2023). Assessment of radiological hazards in some food products consumed by the Malian population using gamma spectrometry. Journal of Radiation Protection and Research, 48(2), 84–89.

[60] Kaboré, K., Bambara, L. T., Zongo, I., Derra, M., Cissé, O., Zougmoré, F., & Darko, E. (2018). Modelling radionuclides transport in a groundwater system around a goldmine site in Burkina Faso. International Journal of Engineering Research, 7(2), 31–34.

[61] Lopes, J. M., Garcêz, R. W. D., Silva, L. B., Silva, R. C., Domingues, A. M., Silva, A. X., & Dama, R. S. F. (2019). Committed effective dose due to consumption of fruits and vegetables peels: Analysis on cancer risk increase. Radiation Physics and Chemistry, 167, 108243.

[62] Benmehaia and Dhehibi. (2024). The Dynamics of Food Demand in Algeria: A Differential System Approach

[63] UNSCEAR 2000, Radionuclides Released to the Terrestrial Environment.

[64] Thermo Fisher Scientific. (2022). Thermo Scientific™ ARL™ QUANT'X Energy Dispersive X-ray Fluorescence Spectrometer [Brochure].

[65] Vekemans, B., Janssens, K., Vincze, L., Adams, F., & Van Espen, P. (1994). Analysis of X-ray spectra by iterative least squares (AXIL): New developments. X-Ray Spectrometry, 23(6), 278–285.

[66] Al-Azzeh, S. A., Al-Ayasrah, A. M., & Tuffaha, R. A. (2018). Semiempirical efficiency calibration in semiconductor HPGe gamma-ray spectroscopy. Journal of Spectroscopy, 2018, Article ID 5392658, 8 pages.

[67] PLOS ONE. (2013). Obesity and Association with Area of Residence, Gender and Socio-Economic Factors in Algerian and Tunisian Adults. Issue 10, e75640.

[68] World Health Organization. (2006). WHO Child Growth Standards: Weight-for-Age (Issue 1).

[69] World Health Organization (WHO). (2007). Nickel in Drinking-Water: Background document for development of WHO Guidelines for Drinking-Water Quality.

[70] European Food Safety Authority (EFSA). (2006). Tolerable Upper Intake Levels for Vitamins and Minerals. Scientific Committee on Food, Scientific Panel on Dietetic Products, Nutrition and Allergies. ISBN: 92-9199-0140.

[71] World Health Organization (WHO). (1983). Iron – CAS Number 7439-89-6. Functional Class: Food Contaminant. JECFA Report: TRS 696-JECFA 27/29. Tox Monograph: FAS 18-JECFA 27/203.

[72] EFSA Panel on Dietetic Products, Nutrition and Allergies (NDA). (2015). Scientific opinion on dietary reference values for magnesium. EFSA Journal, 13(7), 4186.

[73] European Food Safety Authority (EFSA). (2014). Scientific opinion on the risks to public health related to the presence of chromium in food and drinking water. EFSA Journal, 12(3), 3595.

[74] Sirot, V., Noël, L., Guerin, T., & Leblanc, J.-C. (2012). Ca, Cd, Cu, Fe, Hg, Mn, Ni, Pb, Se, and Zn contents in baby foods from the EU market: Comparison of assessed infant intakes with present safety limits. Journal of Food Composition and Analysis, 27(1), 35–47.

[75] World Health Organization (WHO). (2013, January 31). WHO issues new guidance on dietary salt and potassium. WHO Newsroom.

[76] European Food Safety Authority (EFSA). (20YY). Scientific opinion on dietary reference values for sodium. EFSA Journal.

[77] EFSA Panel on Dietetic Products, Nutrition and Allergies (NDA). (2016). Scientific opinion on dietary reference values for potassium. EFSA Journal.

[78] EFSA Panel on Dietetic Products, Nutrition and Allergies (NDA). (20YY). Draft scientific opinion on dietary reference values for phosphorus. EFSA Journal.

[79] World Health Organization (WHO). (2003). Guidelines for drinking-water quality: Volume 1, Recommendations (3rd ed.). World Health Organization.

[80] Yokel, R. A., & McNamara, P. J. (2001). Aluminum toxicokinetic: An updated mini review. Pharmacology & Toxicology, 88(4), 159–167.

[81] Chuchu, N., Patel, B., Sebastian, S., & Exley, C. (2013). The aluminum content of infant formulas remains too high. BMC Pediatrics, 13, 162.

[82] Gimou, M.-M., Pouillot, R., Charrondière, U. R., Noël, L., Guérin, T., & Leblanc, J.-C. (2014). Dietary exposure and health risk assessment for 14 toxic and essential trace elements in Yaoundé: the Cameroonian Total Diet Study. Food Additives & Contaminants: Part A, 31(6), 1064–1080.

[83] U.S. Food and Drug Administration (FDA). (2014). Current Good Manufacturing Practices, Quality Control Procedures, Quality Factors, Notification Requirements, and Records and Reports, for Infant Formula. 21 CFR Part 106

[84] Arnich, N., Sirota, V., Rivière, G., Jean, J., Noël, L., Guérin, T., & Leblanc, J.-C. (2012). Dietary exposure to trace elements and health risk assessment in the 2nd French Total Diet Study. Food and Chemical Toxicology, 50(7), 2432–2449.

[85] Hammani, O., El-Otmani, N., Ben Lenda, O., El Azhari, H., Rfaki, A., Lahlouhi, N., Mourad, Y., & Abdallaoui, A. (2025). Exploratory analysis of potential toxic elements in Moroccan couscous and health risk evaluation utilizing ICP-OES. Journal of Trace Elements and Minerals, 11, 100207.

[86] Salama, K. F., Randhawa, M. A., Al Mulla, A. A., & Labib, O. A. (2019). Heavy metals in some date palm fruit cultivars in Saudi Arabia and their health risk assessment. Environmental Monitoring and Assessment, 191, Article 684.

[87] Demir, T., & Ağaoğlu, S. (2023). Estimated daily intake and health risk assessment of toxic elements in infant formulas. Journal of Trace Elements in Medicine and Biology, Advance online publication.

[88] Hayashi, K., Onishi, M., Horikoshi, R., Sako, K., & Yoshida, M. (2004). Concentration and chemical species of manganese in tea leaves and tea infusion. Trace Nutrients Research, 21, 115–120.

[89] Guerra, M., et al. (2012). Performance of three different Si X-ray detectors for portable XRF spectrometers in cultural heritage applications. Journal of Instrumentation, 7, C10004.

[90] European Commission. (2023). Commission Regulation (EU) 2023/915 of 25 April 2023 on maximum levels for certain contaminants in food and repealing Regulation (EC) No 1881/2006. Official Journal of the European Union, L 119/103, 5 May 2023.

[91] national standards of People's Republic of China GB2762-2022 national food safety standards Limits of contaminants in food

[92] NY/T 288-2012: "Green Food: Tea" and NY 659-2003: "The Limit of Chromium, Cadmium, Mercury, Arsenic, and Fluoride in Tea"

[93] European Parliament and Council of the European Union. (2002). Directive 2002/32/EC of 7 May 2002 on undesirable substances in animal feed. Official Journal of the European Communities, L 140/10, 30 May 2002.

[94] PLOS ONE. (2013). Obesity and Association with Area of Residence, Gender and Socio-Economic Factors in Algerian and Tunisian Adults. Issue 10, e75640.

[95] World Health Organization. (2006). WHO Child Growth Standards: Weight-for-Age (Issue 1)

[96] U.S. Environmental Protection Agency. (2025). IRIS Toxicological Review of Inorganic Arsenic (CASRN 7440-38-2) (EPA/635/R-25/005Fc). Retrieved from www.epa.gov/iris

[97] Busnel, A., et al. (2023). Food consumption, nutritional intakes and the role of milk formulas in nutrient adequacy among young children from birth to 2 years living in urban Algeria. Public Health Nutrition, 26(1), 171–181.

[98] Abizari, A.-R., et al. (2017). More than two-thirds of dietary iodine in children in northern Ghana is obtained from bouillon cubes containing iodized salt. Public Health Nutrition, 20(6), 1107–1113.

[99] GAIN, USDA. (2025). Grain and Feed Annual – Algeria Report (Report No. AG2025-0002).

[100] Euromonitor International. (2024, December). Tea in Algeria [Market Report]. Plus, data from FAOStat database.

[101] FAOStat. (2021). “Date consumption per capita rose 7.71% to 22.9 kg in Algeria”. Food and Agriculture Organization of the United Nations.

[102] Cai, J., Galli, G., & Zhou, X. (2023). Algeria – Aquaculture Growth Potential. FAO WAPI Factsheet, based on 2017 field survey.

[103] Khelifa, H. (2024). Importance of the food issue in Algeria’s economic policy. International Journal of Nutrition and Food Sciences, 13(2).

[104] Agency for Toxic Substances and Disease Registry (ATSDR). (2008, September). Toxicological Profile for Aluminum. Atlanta (GA): U.S. Department of Health and Human Services.

[105] SFSA Panel on Contaminants in the Food Chain (CONTAM). (2010). Scientific opinion on lead in food. EFSA Journal, 8(4), 1570.

[106] Integrated Risk Information System (IRIS). (n.d.). Chemical Assessment Summary: Cadmium; CASRN 7440-43-9. U.S. Environmental Protection Agency, National Center for Environmental Assessment.

[107] U.S. Environmental Protection Agency (EPA). (n.d.). Integrated Risk Information System (IRIS): Reference doses for oral exposure – Chromium, Copper, Nickel, Antimony, Selenium, Zinc.

[108] Taylor, A. A., Tsuji, J. S., McArdle, M. E., Adams, W. J., & Goodfellow, W. L. Jr. (2023). Recommended reference values for risk assessment of oral exposure to copper. Risk Analysis, 43(2), 211–218.

[109] Viala, A., & Botta, A. (2007). Toxicologie. Paris: Lavoisier.

[110] Food and Agriculture Organization (FAO)/World Health Organization (WHO). (2011). Compendium of Food Additive Specifications (FAO JECFA Monographs 11). Addendum: FAS 65 JECFA 74. Toxicological study: NOAEL = 30 mg/kg bw per day; PTWI = 2 mg/kg bw. Report: TRS 966 JECFA 74.

[111] Codex Alimentarius Commission. (1995). Codex General Standard for Contaminants and Toxins in Food and Feed (CODEX STAN 193-1995). FAO/WHO.

[112] The Codex Alimentarius Code of Practice for the Prevention and Reduction of Lead Contamination in Foods (CXC 56-2004)

[113] World Health Organization. (n.d.). Algeria: Life expectancy. WHO Data.

[114] United Nations Scientific Committee on the Effects of Atomic Radiation. (2000). Sources and effects of ionizing radiation: 2000 report to the General Assembly, with scientific annexes. Volume I: Sources. United Nations.

[115] Codex Alimentarius Commission. (1995). General standard for contaminants and toxins in food and feed (CXS 193-1995). FAO/WHO.

[116] Jumbo Bouillon Poulet (n.d.). Jumbo: Proudly African.

[117] International Commission on Radiological Protection. (1991). 1990 recommendations of the International Commission on Radiological Protection (ICRP Publication 60). Annals of the ICRP, 21(1–3). Elsevier.

[118] Tuo, F., Zhou, Q., Yang, B., Peng, X., Zhang, J., & Sun, Q. (2020, July 18). National

monitoring for radioactivity in foods — China, 2012–2019. China CDC Weekly, 2(29), 537–540.

[119] Rantakokko, P., Moeschl, D., Linsinger, T., Dietrich, D., Kreidl, S., Meisel, T., ... & Fried, D. (2025). Levels of naturally occurring radionuclides in foods from the first German total diet study. The Science of the Total Environment, 931, Article 178653.

[120] Raj, P., Padiyath, N., Semioshkina, N., Foulon, F., Alkaabi, A. K., Voigt, G., & Addad, Y. (2022). Transfer of natural radionuclides from soil to Abu Dhabi date palms. Sustainability, 14(18), Article 11327.

[121] Abu Shayeb, M., Alharbi, T., Baloch, M. A., & Alsamhan, O. A. R. (2017). Transfer factors for natural radioactivity into date palm pits. Journal of Environmental Radioactivity, 167, 75–79.

[122] Khandaker, M. U., Shuaibu, H. K., Alklabi, F. A. A., Alzimami, K. S., & Bradley, D. A. (2019). Study of primordial ^{22} Ra, ^{22} Ra, and K concentrations in dietary palm dates and concomitant radiological risk. Health Physics, 116(6), 789–798.